GREAT SALT LAKE SHORELANDS PRESERVE WATER BUDGET, STREAM MONITORING, VEGETATION MAPPING, AND REMOTE SENSING ANALYSIS

by Claire Spangenberg Kellner, Rebecca Molinari, Diane Menuz, Peter Goodwin, and Hugh Hurlow

UTAH DNR GEOLOGICAL SURVEY

REPORT OF INVESTIGATION 289
UTAH GEOLOGICAL SURVEY
UTAH DEPARTMENT OF NATURAL RESOURCES
2025

Blank pages are intentional for printing purposes.

GREAT SALT LAKE SHORELANDS PRESERVE WATER BUDGET, STREAM MONITORING, VEGETATION MAPPING, AND REMOTE SENSING ANALYSIS

by Claire Spangenberg Kellner, Rebecca Molinari, Diane Menuz, Peter Goodwin, and Hugh Hurlow

Cover photo: *Miller Pond situated on the eastern shore of the Great Salt Lake within the Great Salt Lake Shorelands Preserve, with Antelope Island visible across Farmington Bay to the west.*

Suggested citation:

Kellner, C.S., Molinari, R., Menuz, D., Goodwin, P., and Hurlow, H., 2025, Great Salt Lake Shorelands Preserve water budget, stream monitoring, vegetation mapping, and remote sensing analysis, Utah Geological Survey Report of Investigation 289, 52 p., 3 appendices, https://doi.org/10.34191/RI-289.

REPORT OF INVESTIGATION 289
UTAH GEOLOGICAL SURVEY
UTAH DEPARTMENT OF NATURAL RESOURCES
2025

STATE OF UTAH
Spencer J. Cox, Governor

DEPARTMENT OF NATURAL RESOURCES
Joel Ferry, Executive Director

UTAH GEOLOGICAL SURVEY
Darlene Batatian, Director

PUBLICATIONS
contact
Natural Resources Map & Bookstore
1594 W. North Temple
Salt Lake City, UT 84116
telephone: 801-537-3320
toll-free: 1-888-UTAH MAP
website: utahmapstore.com
email: geostore@utah.gov

UTAH GEOLOGICAL SURVEY
contact
1594 W. North Temple, Suite 3110
Salt Lake City, UT 84116
telephone: 801-537-3300
website: geology.utah.gov

CONTENTS

FIGURES

TABLES

GREAT SALT LAKE SHORELANDS PRESERVE WATER BUDGET, STREAM MONITORING, VEGETATION MAPPING, AND REMOTE SENSING ANALYSIS

by Claire Spangenberg Kellner, Rebecca Molinari, Diane Menuz, Peter Goodwin, and Hugh Hurlow

ABSTRACT

The Great Salt Lake Shorelands Preserve ("Preserve" hereafter) includes nearly 5000 acres of wetlands, interspersed ponds and ditches, and uplands on the eastern margin of Great Salt Lake (GSL) in Davis County, Utah. The wetlands provide critical habitat for local and migratory birds on the North American Flyway and a wide range of other species, and important ecological functions including water-quality improvement and flood control. Changes in invasive vegetation, drought conditions, and land-use practices threaten the long-term water supply, water quality, and ecological health of the Preserve wetlands, requiring new management strategies. The goal of this project was to collect and analyze hydrologic and vegetation data to provide a basis for planning and evaluating the effectiveness of restoration efforts.

Methods included manual measurements of surface-water flows and groundwater levels during synoptic measurement events ("flow runs") (2021-2023), continuous streamflow monitoring of major inflows, development of an annual water budget, vegetation mapping, and calculation and analysis of 30-year and 10-year vegetation trends using Normalized Difference Vegetation Index (NDVI).

For water years 2022 and 2023 combined, surface inflows averaged about 17,000 acre-feet annually, with Kays Creek, Freeport Drain, Syracuse Drain, and the B5 drain as the largest contributors. These features have peak flows at distinctly different times of year. We observed an increase in surface water inflows of 8000 acre-ft from the extreme drought conditions of water year 2022 to a historically wet water year in 2023. Shallow groundwater inflow was estimated at 2400 acre-feet annually, with an additional 1400 acre-feet from the deeper confined aquifer. Groundwater flow estimates are highly uncertain because they are based on measurements in a small part of the Preserve and extrapolated to the entire area. Water leaves the Preserve primarily through evapotranspiration (ET) and surface-water flow.

Our estimates of total annual water inflow to the Preserve for water years 2022 and 2023 are 22,150 acre-feet and 32,750 acre-feet, respectively, with an average value of 27,450 acre-feet. We estimated surface water outflows using two approaches: option A (using only the outflows that were physically measured) and option B (calculating outflows by estimating ET from the Outflow Area and assuming that *Phragmites* in the Outflow Area consume all available surface water outflow, in situ precipitation and groundwater outflow). Our estimates of total annual water outflows using option A for water years 2022 and 2023 are 21,000 acre-feet and 22,700 acre-feet, respectively, with an average value of 21,300 acre-feet. Our estimates of total water outflows using option B for water years 2022 and 2023 are 25,600 acre-feet and 23,600 acre-feet, respectively, with an average value of 24,600 acre-feet. Combined standard uncertainties of the water budget ranged from 12-15%.

Vegetation mapping revealed Mesic Meadow and Phragmites as the dominant classes within the Preserve. Mesic Grasses and Dense Phragmites were the dominant subclasses, respectively. In the Outflow Area, Phragmites and Wet Meadow were the most extensively mapped vegetation classes. Dense Phragmites and Dense Saltgrass were the dominant subclasses, respectively.

Comparison to previous vegetation mapping showed that in the Preserve, both water and shore declined from 1981 to 1997 but have since recovered to 1981-level coverage. The predominant location of open water has moved from the northwestern part of the Preserve to the southeastern part. The amount of dry emergent vegetation has increased approximately linearly. In the Outflow Area, the amount of water and shore decreased substantially between 1981 and 2020 and was replaced primarily by wet emergent vegetation. Wet emergent vegetation, predominantly *Phragmites*, increased dramatically between 1997 and 2014 at the expense of open water and other vegetation.

To evaluate and map changes in vegetation health over time, we used satellite imagery to calculate and analyze spatial and temporal trends in NDVI for each year spanning 1992 to 2021 for 19 hydrology-delineated subdivisions of the Preserve. Most of the hydrology units in the Preserve had no significant temporal trend in NDVI, whereas those in the Outflow Area had significant increasing trends. Some small patches of upland areas in the northern part of the Preserve, about 8% of the total Preserve area, showed negative trends in NDVI that could not be attributed to *Phragmites* removal. Positive NDVI trends in the Outflow Area represent rapid expansion of *Phragmites* that occurred as Great Salt Lake levels declined.

Statistical analysis and modeling of NDVI trends indicated that Summer Palmer Drought Severity Index (PDSI), GSL

water levels, impermeable surface area in adjacent land, and management practices appear to have measurable effects on vegetation over time. Impoundments and *Phragmites* treatments can offset potential drying from drought. Vegetation expanded dramatically onto the GSL playa as lake levels and groundwater levels declined.

This research provides critical data for water management planning, including timing and quantities of surface inflows that can benefit specific habitats. Although the flow rates of artesian wells is small, the collective water rights are greater and these rights could be aggregated and new flowing wells installed that sustain local habitat or dilute surface inflows having poor water quality. The vegetation analyses establish baselines for evaluating future conditions and management effectiveness. The fact that the wetlands water budget can be balanced within uncertainty by assuming that the *Phragmites* in the Outflow Area consumes effectively all of the surface water and shallow groundwater outflow from the Preserve indicates that this invasive plant consumes a significant amount of water that could otherwise support more beneficial habitat as well as GSL water levels. Our vegetation change, NDVI analyses, and driver variable modeling collectively suggest that *Phragmites* treatment can produce measurable changes in the overall vegetation composition of this area, lending support to current efforts for large-scale *Phragmites* treatments.

INTRODUCTION

The Great Salt Lake Shorelands Preserve ("Preserve" hereafter) occupies 4966 acres on the east shore of Great Salt Lake (GSL) in Layton, Davis County, Utah, about 25 miles north of Salt Lake City between the Farmington Bay Waterfowl Management Area and the Antelope Island State Park Causeway (Figures 1 and 2). The Preserve is owned and managed by The Nature Conservancy as a wildlife refuge and open space, primarily for migratory birds. Preserve wetlands are part of the 351,000 acres of wetlands along Great Salt Lake's eastern margin that provide essential ecological functions including mitigating water quality issues and providing critical habitat for migratory birds (Utah Division of Forestry, Fire and State Lands, 2013).

The Preserve was established because of the important role that Great Salt Lake plays in providing stopover, nesting, and foraging habitat for millions of birds each year. The region has been designated a globally important bird area by the National Audubon Society and serves as a critical link on the Pacific Flyway for birds migrating between northern breeding grounds and winter locations. Wetlands around the lake play a critical role in providing the food and shelter these birds need. Emergent wetland plants are an important source of seeds and vegetative parts that are consumed by many bird species and provide habitat for insects, fish, reptiles, and birds (Roberts, 2013; Downard et al., 2017).

Almost all surface water entering GSL flows through the surrounding wetlands first. As the lake level rises or falls, these areas shrink or expand accordingly, creating a dynamic boundary between the wetlands and the lake. The Preserve consists mainly of fringe wetlands, with some areas of impounded wetlands and playa mudflats providing a mix of wetland and upland habitat types (Downard, 2024). This mix of habitats provides refuge for over 250 species of birds. A recent study by The Nature Conservancy (2023) found over 108 species of birds using the Preserve in the spring, including 93 for nesting.

Phragmites australis, a nonnative plant that reproduces both sexually and asexually, has rapidly invaded wetlands throughout the region and become the dominant *Phragmites* species around GSL (Kettenring et al., 2020). While a native species of *Phragmites* is found occasionally in Utah wetlands, the invasive variety threatens the habitat diversity that supports the Preserve's rich avian community. Its dense, monotypic stands outcompete native vegetation, reducing habitat availability for shorebirds, while its substantial water demand contributes to decreased water availability for Great Salt Lake.

The Preserve depends on both surface water and groundwater to sustain its wetland and upland habitats. Surface water sources include perennial and ephemeral streams, agricultural drains, and stormwater drains and runoff. Understanding the availability and dynamics of water resources in the face of changing land use patterns is essential for effective conservation and management efforts. The Preserve faces rapidly changing hydrologic conditions, including the conversion of agricultural lands into residential and industrial areas and construction of the West Davis Corridor freeway along its northeastern boundary.

Considering these ongoing changes in the Preserve's hydrology, the objectives of this project were to (1) create a comprehensive water budget for the Preserve by quantifying surface water and groundwater inflows and outflows, changes in groundwater storage, and evapotranspiration (ET); (2) characterize current vegetation distribution by vegetation mapping; and (3) assess historical changes in vegetation health by analyzing NDVI (Normalized Difference Vegetation Index) from remotely sensed imagery. Beyond providing specific data for the Preserve, this research aims to create a template that can be applied to other wetland preserves along the east shore that will contribute to data-based decision-making and the long-term management of GSL.

By quantifying each component of the water budget equation, we can assess the overall water balance and gain

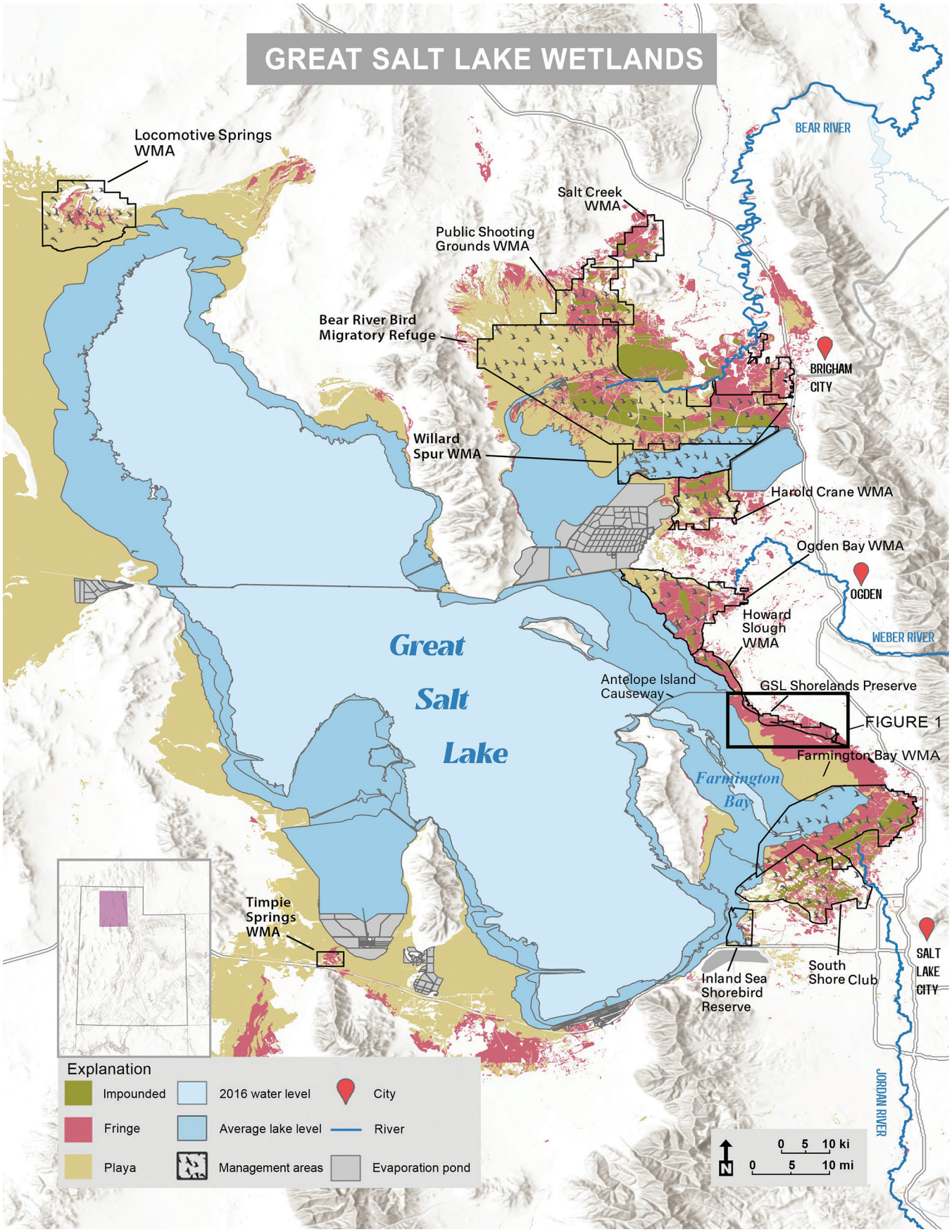

Figure 1. *Great Salt Lake and adjacent wetland/waterfowl preserves and wetland types.*

insights into water availability and utilization within the Preserve. This information will enable the Preserve managers to develop science-based strategies to ensure sustainable use and conservation of water resources, while also considering the impacts of ongoing projects and the Preserve's role within the larger context of the Great Salt Lake ecosystem. By understanding the intricate relationships between water inputs, outputs, and storage changes within the Preserve, we hope to provide data to effectively manage and conserve the vital water resources necessary for sustaining the unique wetland habitats and associated wildlife populations in this ecologically significant area.

Our data collection during 2021 and 2022 occurred during record-setting drought conditions. Flows and groundwater levels from that time period do not, therefore, represent long-term averages. We extended surface-flow data collection through November 2023 to include conditions following record-high snowfall and snow water content in the Wasatch Range. These two data represent extremes, and we expect that most water years will fall within the range we were able to capture within our study period. We report some groundwater levels through September 2024 for the purpose of calculating horizontal flow of shallow groundwater as part of the water budget.

GEOGRAPHIC SETTING

Physiography and Land Use

The Preserve is in western Davis County, Utah, along the eastern shoreline of GSL on the northeastern margin of Farmington Bay, between the Farmington Bay Waterfowl Management Area to the southeast and the Howard Slough Waterfowl Management Area to the northwest (Figure 1). These and other specially designated and managed wetland areas create a near-continuous corridor of wetland habitat along GSL's eastern shore from Farmington Bay to Bear River Bay. Their importance will only increase with continued population increase and land development along the Wasatch Front.

Davis County's population increased by about 20% between 2010 and 2022 (U.S. Census Bureau, 2023). Once a largely agricultural area, the county has experienced dramatic land use changes in the past few decades, converting agricultural land into numerous housing developments and industrial use. Some farm and grazing land still exist in proximity to the Preserve, but the dramatic decrease in agricultural runoff has led to decreased amounts of surface water inflows (Mike Kolendrianos and Chris Brown, Preserve Managers, verbal communications during 2022 and 2023).

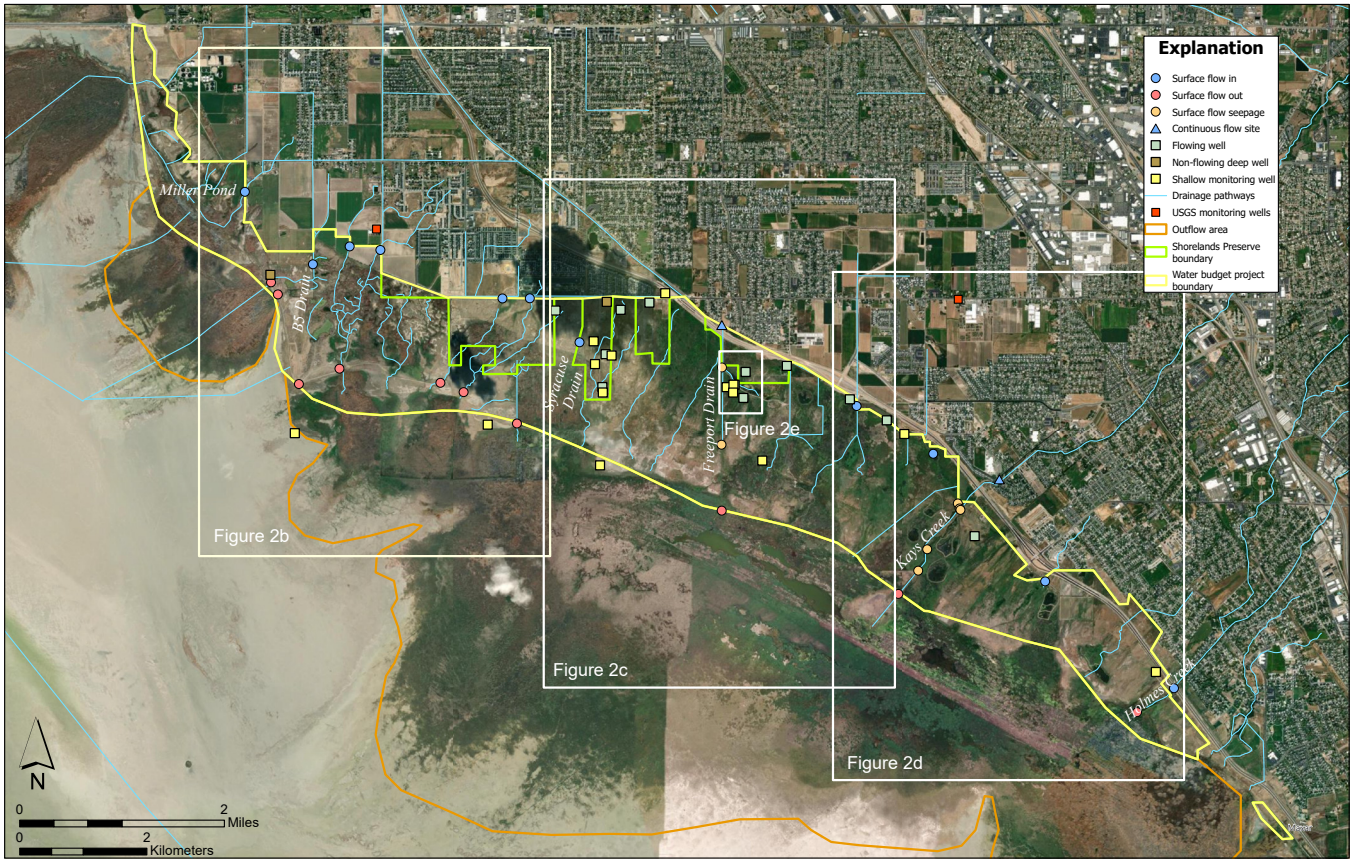

Figure 2. *Great Salt Lake Shorelands Preserve showing measurement sites for this study.* ***B)*** *Northeastern part of study area.* ***C)*** *Central part of study area.* ***D)*** *Southwestern part of study area.* ***E)*** *Freeport Pond area detail.*

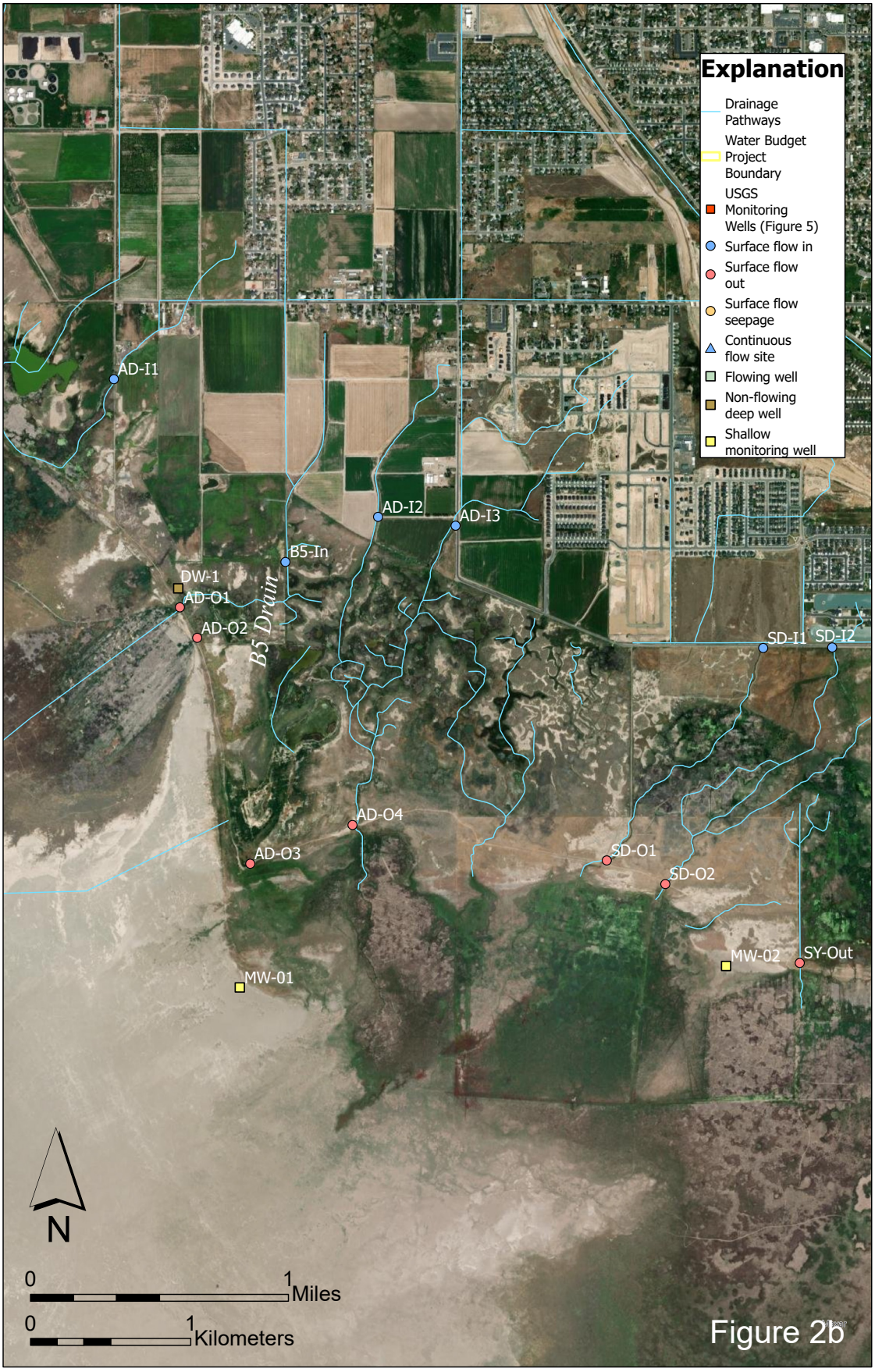

Figure 2 Continued. *Great Salt Lake Shorelands Preserve showing measurement sites for this study.* ***B)*** *Northeastern part of study area.* ***C)*** *Central part of study area.* ***D)*** *Southwestern part of study area.* ***E)*** *Freeport Pond area detail.*

Figure 2 Continued. *Great Salt Lake Shorelands Preserve showing measurement sites for this study.* ***B)*** *Northeastern part of study area.* ***C)*** *Central part of study area.* ***D)*** *Southwestern part of study area.* ***E)*** *Freeport Pond area detail.*

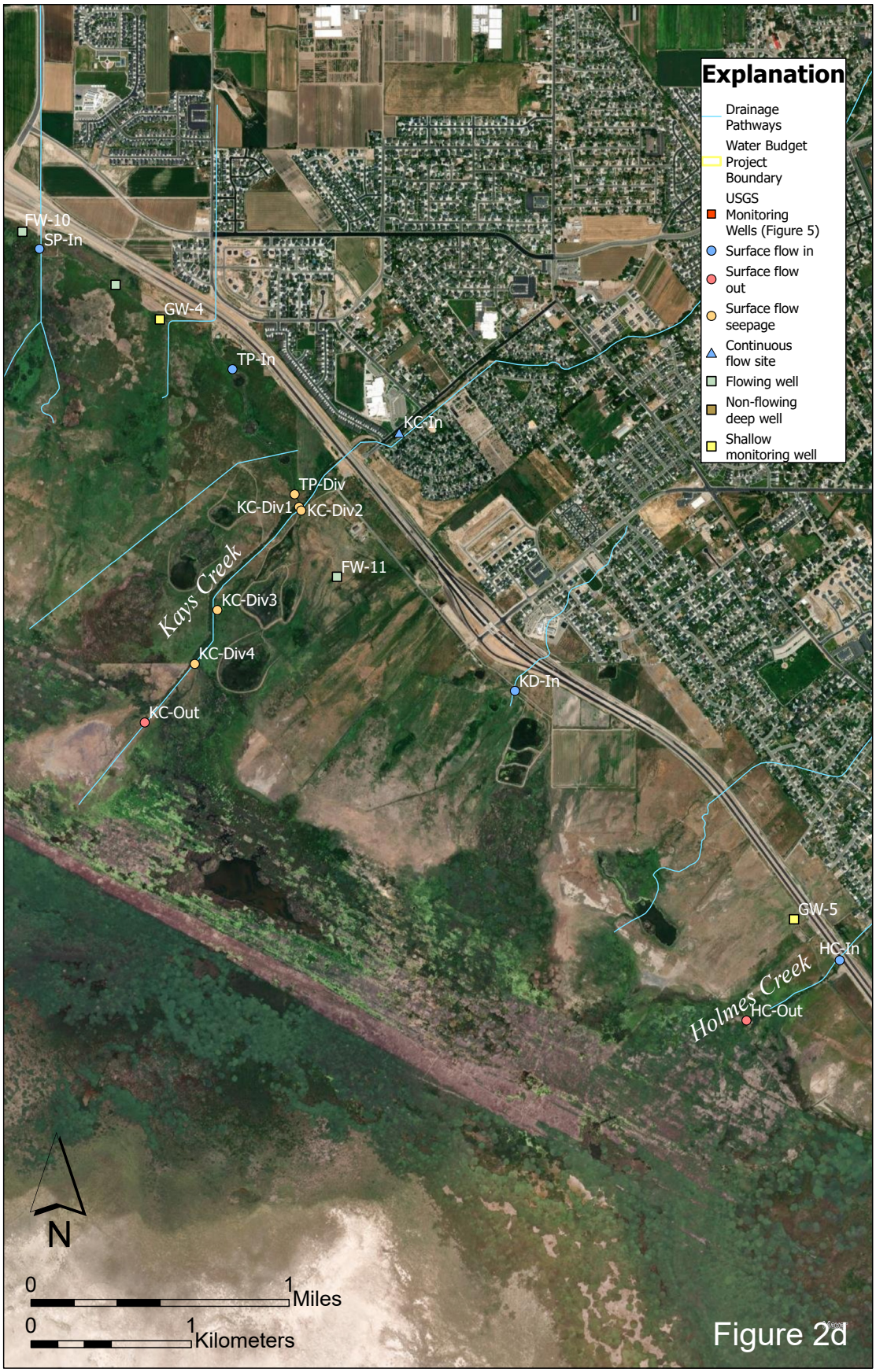

Figure 2 Continued. *Great Salt Lake Shorelands Preserve showing measurement sites for this study.* ***B)*** *Northeastern part of study area.* ***C)*** *Central part of study area.* ***D)*** *Southwestern part of study area.* ***E)*** *Freeport Pond area detail.*

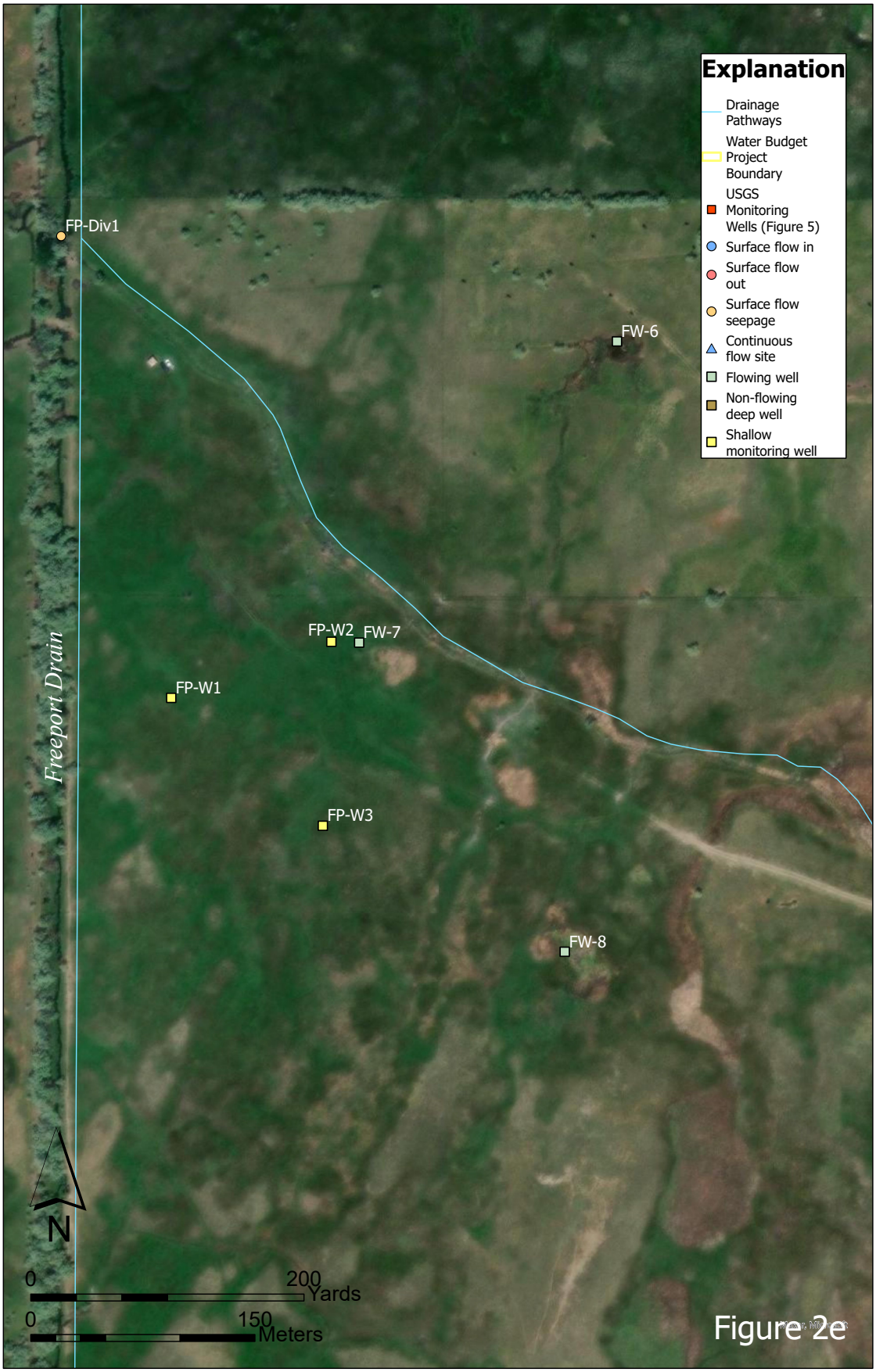

Figure 2 Continued. *Great Salt Lake Shorelands Preserve showing measurement sites for this study.* ***B)*** *Northeastern part of study area.* ***C)*** *Central part of study area.* ***D)*** *Southwestern part of study area.* ***E)*** *Freeport Pond area detail.*

The Utah Department of Transportation (UDOT) broke ground in 2021 on the West Davis Corridor Project (WDCP). Completed in summer 2024, this four-lane divided highway adjoins the Preserve along its northeastern boundary for nearly 6 miles (5.6 mi). Mitigation measures included small basins to contain storm water runoff on the margin of the Shorelands Preserve.

Precipitation

Annual precipitation at the Hill Air Force Base/Ogden climate station (about 7 miles northeast of the Preserve) for water years 2013 through 2023 varied from 7.01 to 23.31 inches and averaged 15.47 inches, whereas the average precipitation for water years 2021 and 2022 was 12.50 inches (Figure 3A; Utah Climate Center, 2024), reflecting the drought conditions throughout the western U.S. intermontane region as measured by the Palmer Drought Severity Index (PDSI) (Figure 3B; Alley, 1984; Desert Research Institute, 2024). Annual precipitation for water year 2023 was 12.20 inches.

Surface Water

Surface water flows into the Preserve from three main sources: perennial streams, agricultural runoff, and stormwater

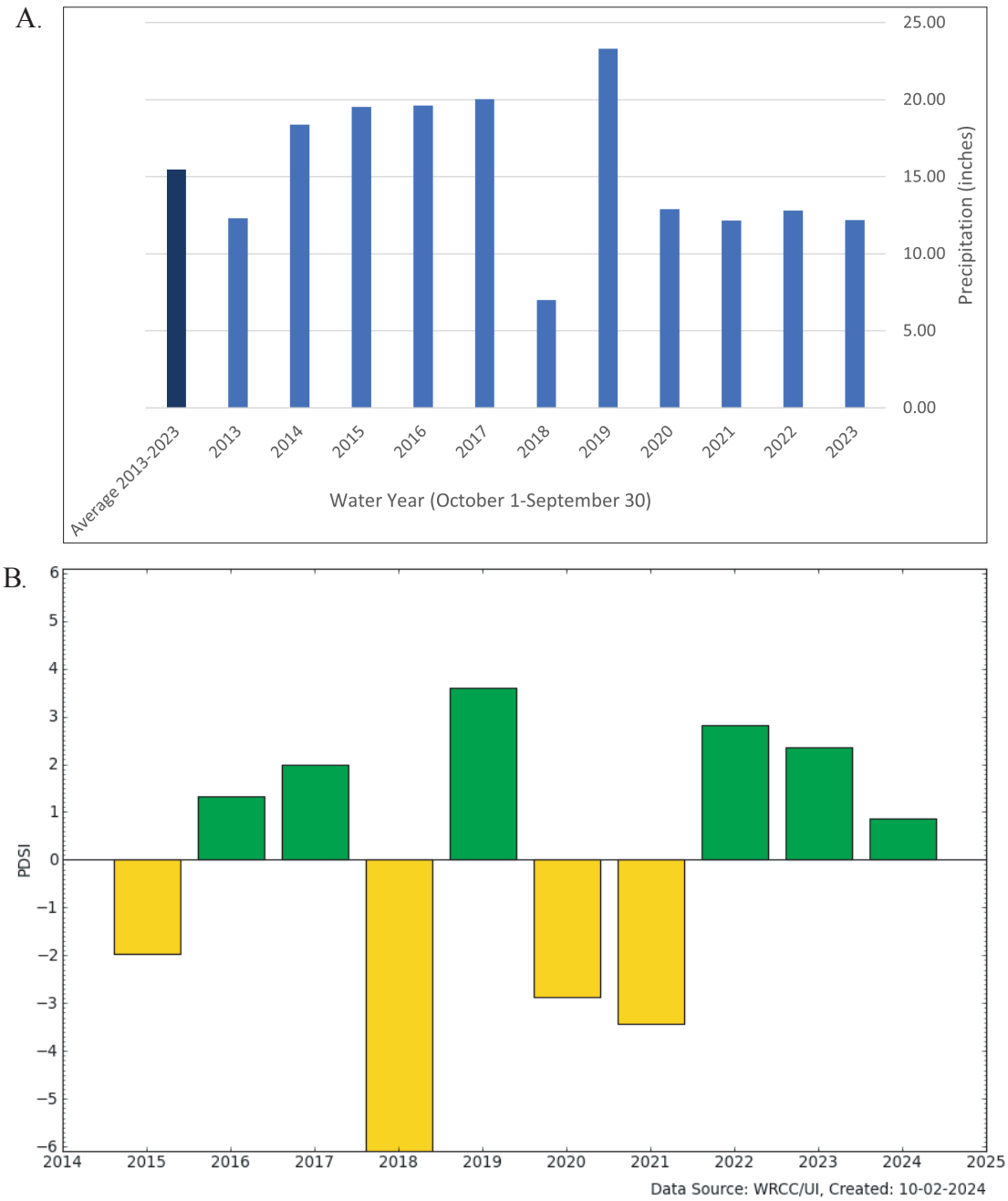

Figure 3. *Climate data for the study area.* ***A)*** *Records of precipitation at the Hill Air Force Base climate station (Utah Climate Center, 2024). WY = water year.* ***B)*** *Palmer Drought Severity Index (PDSI) for calendar years 2015 through 2024 (incomplete) at the Preserve (Desert Research Institute, 2024). Negative PDSI values indicate drought conditions.*

drains. Flow from artesian wells is a fourth, relatively minor source of surface water. Two perennial streams, Kays Creek and Holmes Creek, are the greatest source of surface water to the southeastern part of the Preserve. Both streams originate in the Wasatch Range northeast of the study area, flow southwest through the town of Layton before entering the Preserve and terminate in impounded ponds and as diffuse flow along the northeastern shore of Farmington Bay.

Several other features contribute surface water to the Preserve. The largest of these is the Freeport Drain, a French drain that collects stormwater from an industrial area and parts of Clearfield about two and a half miles north of the Preserve. Freeport Drain flows in a straight man-made ditch south to the southwestern edge of the Preserve wetlands. Beginning April 2023, in the north-central part of the Preserve north of the visitors center, Freeport Drain was partly diverted to the southeast to fill the newly constructed Freeport Ponds that provide habitat, reduce contaminants, filter garbage, and contribute to local groundwater recharge. The two other relatively large surface water sources are the Syracuse Drain and the B5 Drain agricultural runoff ditches extending from farms near the northwestern end of the Preserve. Numerous smaller stormwater drains and culverts deliver water to the Preserve after rainfall and during spring runoff.

As water availability changes with land use, The Nature Conservancy (TNC) managers have worked diligently to make good use of the water that enters the Preserve. The Preserve has impounded wetland areas, most of which are sourced by Kays Creek, the B5 Drain, and the Freeport Drain. These impoundments create habitat, filter contaminants, and catch debris before water flows out toward GSL. Additional future impoundments using water from surface flow sources are planned in the northwestern and central parts of the Preserve.

HYDROGEOLOGIC SETTING

The Wasatch Front is underlain by a complex system of sedimentary ("basin fill") and bedrock aquifers that produce the region's groundwater supply (Anderson et al., 1994; Gates, 1995). The basin-fill aquifer consists of unconsolidated sediments including clay, sand, and gravel that are predominantly coarse grained along the mountain front and are progressively finer grained to the west where they are interbedded with fine-grained lacustrine deposits (Clyde et al., 1984; Gates, 1995). The sand and gravel deposits have a relatively high porosity and hydraulic conductivity, allowing them to store and transmit significant amounts of groundwater (Duffield, 2023), whereas the clay-rich deposits can store groundwater but movement through them is very slow. The basin-fill aquifer is a critical source of groundwater for municipal, agricultural, and industrial needs in the region, as well as groundwater flow to GSL (Gates, 1995; Zamora and Inkenbrandt, 2024).

Bedrock aquifers include fractured-rock formations that are exposed in the mountain blocks and underlie the basin-fill sediments. The principal bedrock aquifers along the Wasatch Front are Paleozoic-age limestone and sandstone and fractured Paleozoic- to Precambrian-age quartzite. Joints and faults enhance the hydraulic conductivity of bedrock, allowing water to flow through the system (Fetter, 2001, p. 327–359). Wells completed in bedrock aquifers near the Wasatch Range front provide water for both domestic and agricultural uses.

The land that is now the Preserve was inundated by Lake Bonneville during Late Pleistocene time, by the earliest manifestation of GSL during latest Pleistocene or Early Holocene time, and in the mid-1980s (Sack, 2005; Solomon, 2007; Oviatt, 2014). Surficial and shallow-subsurface (≤ 3–5 ft below land surface) sediments are Holocene to Late Pleistocene, and deeper sediments are Late Pleistocene and older; all were deposited mainly in alluvial-fan and lacustrine environments (Sack, 2005; Solomon, 2007). Surficial and shallow-subsurface sediments are predominantly alluvial and lacustrine sand and clay in the northwestern two-thirds of the Preserve, and fine-grained lacustrine deposits and marsh deposits (fine-grained, organic-rich sediment in wetlands and impounded ponds) in the southeastern one-third (Sack, 2005; Solomon, 2007). The shoreline marking the Gilbert highstand (renamed the Currey cycle of Great Salt Lake by Oviatt et al, 2024) of GSL occurs along the northeastern Preserve boundary, and a potential Holocene-age shoreline occurs in places about halfway between the northwestern and southeastern boundaries (Sack, 2005; Solomon, 2007). According to Preserve managers, the surficial deposits are typically saturated within a few feet of the land surface and overlie a hardpan layer. Sediments below the hardpan layer consist of interbedded sand, clay, and rare gravel deposited in lacustrine and alluvial-fan environments during the regressive phase of Lake Bonneville, and older, similar Pleistocene to Pliocene sediments (McKean and Hylland, 2019; McKean, verbal communication, July 7, 2023).

The surficial and shallow subsurface deposits comprise the shallow unconfined aquifer, and the deposits at depths greater than about 30 feet comprise the uppermost part of the regional confined basin-fill aquifer. Gates (1995, Figure 4) presented a conceptual hydrogeologic model for groundwater discharge areas along the Wasatch Front, including the eastern GSL margin, which we have adapted to the Preserve study area (Figure 4). The hydraulic head in the confined aquifer has an upward vertical component that drives water to or above the land surface in cased wells. Slow, diffuse flow may occur from the confined basin-fill aquifer to the shallow unconfined aquifer. At the beginning of this study we anticipated that groundwater below the hardpan layer is confined, however, that is not the case (see "Groundwater Levels" section) and the confined conditions are likely caused by laterally extensive clay-rich zones. The horizontal component of groundwater flow in both aquifers is generally to the southwest toward GSL (Feth et al., 1966; Gates, 1995, Figure 7).

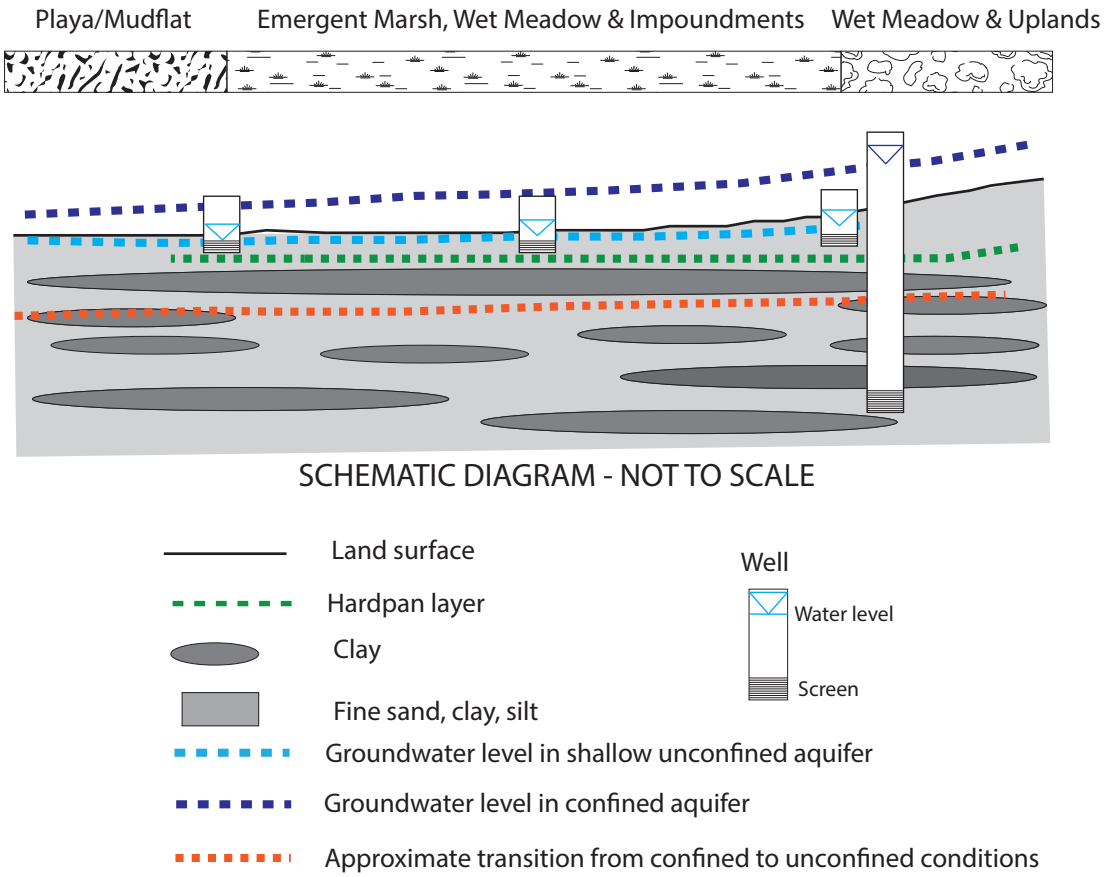

Figure 4. *Conceptual model of groundwater conditions at the Great Salt Lake Shorelands Preserve, modified from Gates (1995, Figure 4), and generalized vegetation communities based on the vegetation map produced for this study.*

From a regional perspective, stream flow and groundwater recharge are derived from infiltration of precipitation and snowmelt on the Wasatch Range, along the mountain front, and on the valley floor, in order of decreasing importance (Gates, 1995; Thiros, 1995). Stream water originates in the Wasatch Range and may receive inputs from shallow groundwater and tributary streams on the valley floor. Drain water is derived from shallow groundwater, agricultural water, and from infiltration of precipitation on the valley floor. Shallow groundwater is recharged by infiltration of precipitation along the mountain front and on the valley floor, and by infiltration of stream water along the mountain front and eastern part of the valley floor where surficial deposits are generally coarse grained. Groundwater in the confined basin-fill aquifer below the Preserve is recharged predominantly along the mountain front where sedimentary deposits of the Weber River delta are coarse grained. The groundwater then flows downward into the deeper (> 30 feet below land surface) aquifers and toward Great Salt Lake (Clyde et al., 1984).

Ten older water wells on the Preserve, along with their water rights, were purchased with the land by The Nature Conservancy. These wells are more than 100 feet deep, are completed in the confined basin-fill aquifer, and are artesian. In 2019 as part of its water quality monitoring associated with the WDCP, the Utah Department of Transportation (UDOT) contracted to install 14 groundwater monitoring wells, 7 of which are adjacent to or within the Preserve and which we refer to as the WDCP monitor wells. HDR Engineering manages, measures water levels, and samples the wells. They kindly provided us access to the wells for sampling in September 2021. HDR Engineering publishes annual reports on their monitoring including minimum and maximum measured depth to water and a hydrograph for each well (HDR Engineering, 2021, 2022, 2023, 2024). For the seven wells of interest in this study, depths to water vary from 9 to 20 feet. In the three wells having geologic logs, strata included clay, silty clay, silty sand, and sand to at least 20 feet below land surface (HDR Engineering, written communication, July 31, 2023).

The U.S. Geological Survey has measured groundwater levels annually (or more frequently) since as early as 1980 in two wells along the northwestern boundary of the Preserve. Groundwater levels in well 410410112050001, completed in the confined basin-fill aquifer, declined by 21.15 feet from March 1984 to March 2024, a long-term average rate of decline of 0.58 feet per year (Figure 5A; U.S. Geological Survey, 2024). Groundwater levels in well 410337112000501, completed in the confined basin-fill aquifer, declined by 18.77 feet from March 1984 to March 2024, a long-term average rate of decline of 0.69 feet per year (Figure 5B; U.S. Geological Survey, 2024). The U.S. Geological Survey has measured groundwater levels

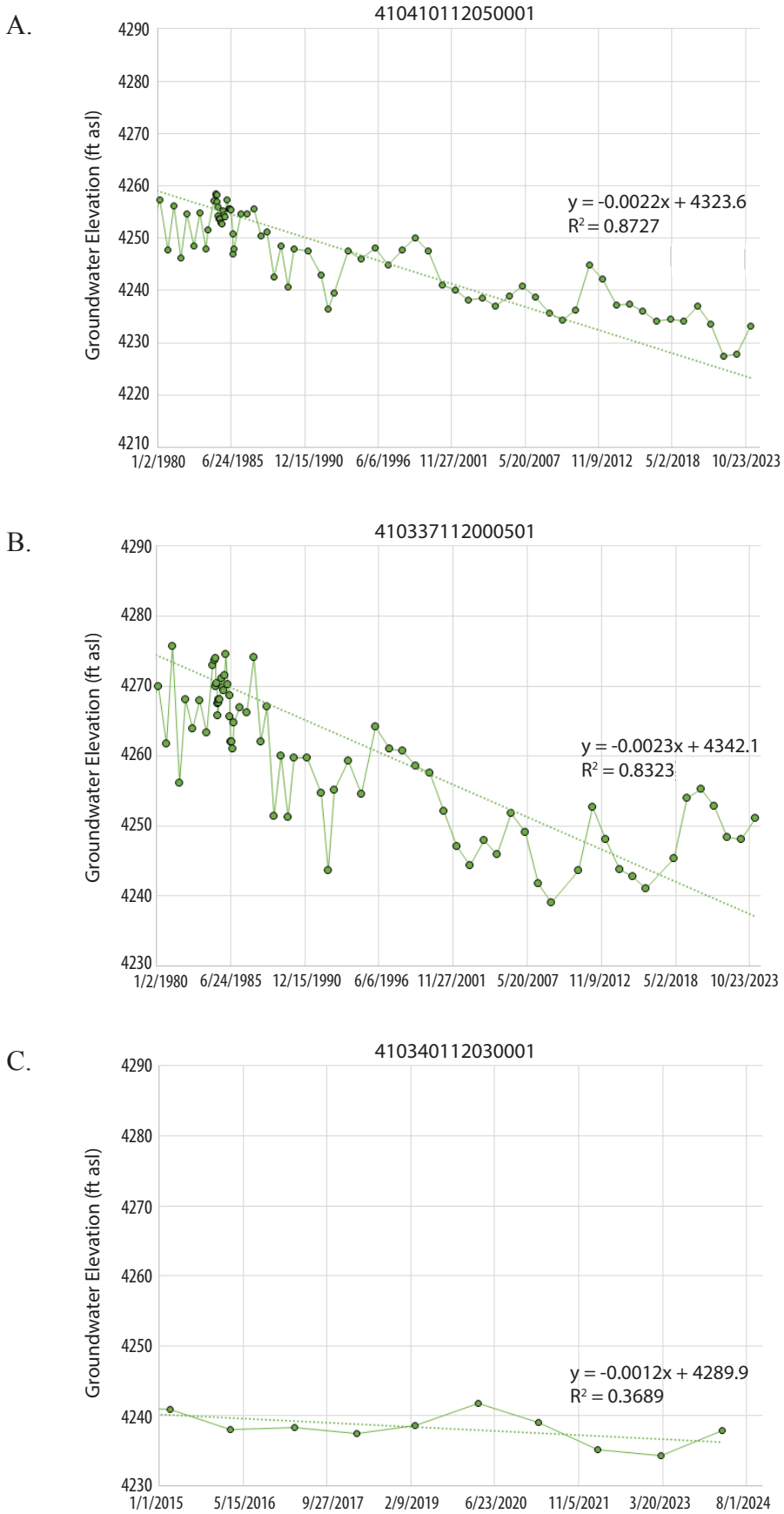

Figure 5. *Water-level hydrographs for three wells monitored by the U.S. Geological Survey. Locations are shown on Figure 2. The data can be found by entering the well ID numbers in the NWIS website (U.S. Geological Survey, 2024).* ***A)*** *Well 410410112050001.* ***B)*** *Well 410337112000501.* ***C)*** *Well 410340112030001.*

annually since 2014 in a third well along the northern Preserve boundary, 410340112030001, also completed in the confined basin-fill aquifer, in which water levels declined by 3.51 feet from March 2014 to March 2024, a ten-year average rate of decline of 0.44 feet per year (Figure 5C). During the same time period, groundwater levels in well 410410112050001 declined at a rate of 0.51 feet per year whereas groundwater levels in well 410340112030001 increased at a rate of 1.28 feet per year. This increase may be due to local conditions such as conversion of land use from agricultural to residential. Groundwater-level declines ranging from 51.52 to 33.83 feet occurred throughout the Weber delta from 1984 to 2024 (NWIS data, retrieved July 25, 2023). The Great Salt Lake Strike Team (2023) attributed declines in Great Salt Lake levels as follows: "human water use comprises 67% to 73%, natural variability 15% to 23%, and climate warming 8% to 11% of Great Salt Lake's low elevation." The causes of groundwater-level declines in and near the Preserve are likely similar.

SURFACE WATER

Introduction

We conducted seven seasonal flow runs (synoptic measurements of flow rates at key locations within a three-day period) to capture quantities and seasonal variations in surface water flows into and out of the Preserve. The flow runs occurred during spring runoff, irrigation season, and fall/winter base flow, to coincide with different surface water flow regimes. Our objective was to measure all significant surface water sources, to characterize peak and minimum flow periods, and integrate the data to produce annual flow rates in acre-feet per year.

Preserve managers identified Kays Creek and the Freeport Drain as the primary sources of surface water. To quantify the water contributions from these sites throughout our study period, we established stream stage and flow monitoring sites at both locations to collect continuous water level (stage) measurements and made periodic (bi-weekly to monthly) manual flow measurements to develop ratings curves (quantitative relationship between stage and flow rate) for the sites. In addition to conducting seasonal measurements during our larger flow run campaigns, these continuous stage measurements enabled us to more accurately determine the total volume of water contributed by these sites. Given that Kays Creek and the Freeport Drain originate from distinct sources, we anticipated observing varying responses to climatic factors such as precipitation and spring runoff.

Methods

Flow Runs

We measured surface flow at 11 inflow sites, 11 outflow sites, and points of diversion (surface-flow seepage points in Figure 2D) along Kays Creek (Figure 2D) using a Hach FH950 Portable Velocity System. In channels having suitable geometry, we applied the 0.6 depth method to calculate discharge, whereas certain measurement points at culverts and pipes necessitated the use of the 0.9*Vmax method to capture velocity. To measure the flow rates of artesian wells, we used a stopwatch and graduated bucket and repeated the measurements three times at each site.

To illustrate how we extrapolated our flow run data to estimate total volumetric flow, consider the B5 Drain where it enters the Preserve. On May 15, 2023, the instantaneous flow rate at this location was 3.64 cubic feet per second (cfs) (station B5-In, Table 1). Using this measurement, we estimated the total inflow at this site for the 2023 spring runoff period as follows:

3.64 cfs/4359.9 cubic feet per acre-foot*86,400 seconds/day*30 days = 216.58 acre-feet

To estimate the annual water volume from flow run data, we divided the year into three time periods: spring runoff (spring), irrigation season (summer), and base flow (fall and winter combined). Dates vary from year to year but the period of peak spring runoff spans approximately 30 days from mid-April to mid-May. Irrigation season occurs during the warmer summer months for about 150 days from mid-May to mid-October. Base flow period includes the remaining 185 days from mid-October to mid-April. We conducted flow runs during each of these time periods from October 2021 through November 2023. For each time period, we assumed that the flow rates measured at each site during the corresponding flow run could be extrapolated over the entire period to estimate the total volumetric flow for that site.

Flow measurements across the outflow boundary of the Preserve provided insights into the surface water–groundwater water dynamics by comparing inflows and outflows during each flow run, and extrapolating the instantaneous values to the appropriate time periods. These values cannot, however, lead directly to estimates of groundwater storage change due to ET from vegetation lining the streams.

Continuous Monitoring

We installed continuous stream gages at the inflow points of Kays Creek and the Freeport Drain. We deployed Heron dipperLoggers, housed in 2-inch diameter PVC casings, to collect water depth measurements every 30 minutes, and we installed staff gages at each site. Erica Rau (U.S. Geological Survey) aided in the development of the ratings curves for these sites by establishing correlations between water depths and manually measured discharges. The ratings curves can be applied to transducer data to calculate discharges at frequent intervals. Calculating the area under the curve for calculated discharges enabled us to determine the total volume of water passing through these sites over the course of a year.

Table 1. *Summary of flow data and values used to calculate the water budget. Streams are highlighted in blue, agricultural drains in green, and storm drains in orange.*

INFLOWS

Site	Site Name	Major/Minor Inflow	Discharge Measurements (cfs)							Water Year 2022 Flow Volume (acre-feet)				Water Year 2023 Volume (acre-feet)				2022–2023 Average Volume (acre-feet)			
			October 28 2021	*April 27 2022*	*August 27 2022*[1]	*November 17 2022*	*May 15 2023*	*August 29 2023*	*November 20 2023*[3]	*2021/2022 Base Flow*	*2022 Spring Runoff*	*2022 Irrigation/Summer*[1]	*WY 2022 Total*	*2022/2023 Base Flow*	*2023 Spring Runoff*	*2023 Irrigation/Summer*	*WY 2023 Total*	*Base Flow*	*Spring Runoff*	*Irrigation/ Summer*	*Annual Volume*
KC-In	**Kays Creek**	Major	7.88	19.10	0.90	2.91	38.95	10.19	4.67	2892	1137	269	4297	1068	2318	3032	6418	1980	1727	1650	**5357**
HC-In	**Holmes Creek**	Major	2.50	0.73	0.69	0.97	37.69	0.53	0.09	917	43	204	1165	357	2243	158	2758	637	1143	181	1961
B5-In	**B5 Drain**	Major	0.62	0.59	1.24	0.73	3.64	2.25	0.78	227	35	369	632	269	217	670	1156	248	126	520	**894**
AD-I1	**Agricultural Drain 1**	Minor	0.74	0.00	0.24	0.05	3.91	0.30	0.05	272	0	70	342	18	233	89	340	145	116	80	341
AD-I3	**Agricultural Drain 2**	Minor	0.13	0.96	0.09	0.15	0.00	0.63	0.20	46	57	26	129	55	0	188	243	50	29	107	186
FP-In	**Freeport Drain**	Major	3.62	1.82	8.43	1.77	1.51	7.82[4]	2.30	1330	108	2508	3946	650	90	2327	3067	990	99	2417	**3506**
SY-In	**Syracuse Drain**	Major	1.41	0.98	0.31	4.16	5.26	6.06	0.55	518	58	92	668	1528	313	1803	3644	1023	186	947	**2156**
SD-I1	**Storm Drain 1**	Minor	0.65	0.36	0.55	0.67	1.01	1.02	0.20	237	21	164	422	247	60	303	610	242	41	233	516
SD-I2	**Storm Drain 2**	Minor	0.24	0.33	0.31	0.00	1.60	0.38	0.40	88	20	93	201	0	95	112	207	44	57	103	204
KD-I1	**Kaysville Drain 1**	Minor	0.00	0.30	0.36	0.19	0.26	0.43	0.25	0	18	106	123	71	16	127	213	35	17	116	168
KD-I2	**Kaysville Drain 2**	Minor	0.00	0.32	0.32	0.21	0.62	0.46	0.40	0	19	95	114	79	37	137	252	39	28	116	183
SP-In	**Spiral Pond**	Minor	0.00	0.66	0.54	0.00	2.02	3.95	0.95	0	39	161	201	0	120	1174	1294	0	80	668	748
	Sum of Inflows		17.79	26.14	13.98	11.84	96.47	34.01	10.84	**6526**	**1556**	**4158**	**12,240**	**4343**	**5740**	**10,119**	**20,201**	**5435**	**3648**	**7138**	**16,221**
												Value used in Water Budget:[2]	**13,000**			**Value used in Water Budget:**[2]	**21,000**			**Value used in Water Budget:**[2]	**17,000**

OUTFLOWS

KC-3	**Kays Creek 3**	Major	8.22	7.39	*1.07*	1.13	15.06	5.65	2.99	3015	439	*324*	3778	413	896	1681	2990	1714	668	1002	**3384**
KC-Div4	**Kays Creek Diversion 4**	Minor	0.52	1.27	*0.33*	0.19	2.58	1.72	0.63	192	75	*99*	366	71	154	511	736	131	114	305	551
HC-O1	**Holmes Creek Out 1**	Major	0.91	0.27	*0.06*	0.36	13.74	0.33	0.05	334	16	*19*	369	130	817	97	1045	232	417	58	707
HC-O2	**Holmes Creek Out 2**	Major	2.36	0.69	*0.01*	0.92	35.51	0.03	0.03	864	41	*2*	907	337	2113	10	2460	601	1077	6	1684
AD-O5	**Ag Drain Out 5**	Minor	0.00	0.00	*0.00*	0.00	0.00	0.00	0.00	1	0	*0*	1	0	0	0	0	0	0	0	0
AD-O6	**Ag Drain Out 6**	Minor	0.00	0.00	*0.00*	0.00	0.00	0.00	0.00	0	0	*0*	0	0	0	0	0	0	0	0	0
AD-O1	**Ag Drain Out 1**	Minor	0.20	0.00	*0.07*	0.00	0.00	0.38	0.10	72	0	*22*	94	0	0	114	114	36	0	68	104
AD-O2	**Ag Drain Out 2**	Minor	0.34	0.04	*0.00*	0.12	0.00	0.00	0.00	125	2	*0*	127	43	0	0	43	84	1	0	85
AD-O3	**Ag Drain Out 3**	Minor	0.18	0.20	*0.00*	0.00	0.11	0.00	0.00	66	12	*0*	78	0	7	0	7	33	9	0	43
AD-O4	**Ag Drain Out 4**	Minor	0.85	0.00	*0.00*	0.00	0.29	0.00	0.00	311	0	*0*	311	0	17	0	17	155	9	0	164
FP-Out	**Freeport Out**	Major	2.76	2.10	*0.28*	1.35	0.55	1.45	2.06	1013	125	*83*	1222	495	33	432	960	754	79	258	**1091**
SY-Out	**Syracuse Drain Out**	Major	2.19	1.05	*0.41*	0.00	1.25	2.17	0.74	803	62	*125*	990	0	74	646	721	401	68	385	**855**
SD-O1	**Storm Drain Out 1**	Minor	0.15	0.00	*0.00*	0.00	0.00	0.00	0.11	55	0	*0*	55	0	0	0	0	28	0	0	28
SD-O2	**Storm Drain Out 2**	Minor	0.66	0.46	*0.09*	0.00	0.63	0.49	0.43	243	28	*28*	299	0	38	145	183	121	33	87	241
	Sum of Outflows		19.33	13.45	0.00	4.06	69.73	12.22	7.14	**7094**	**800**	***701***	**8595**	**1489**	**4149**	**3637**	**9276**	**4291**	**2475**	**2169**	**8935**
												Value used in Water Budget:[2]	**8600**			**Value used in Water Budget:**[2]	**9300**			**Value used in Water Budget:**[2]	**8900**

WELLS

FW-2	**Flowing Well 2**	Minor	0.006	0.001	0.001	0.001	0.001	0.001	0.001	2.10	0.49	0.46	3.06	0.41	0.41	0.37	1.19	0.98	0.23	0.21	1.41
FW-3	**Flowing Well 3**	Minor	0.005	0.006	0.004	0.004	0.005	0.005	0.005	1.68	2.05	1.38	5.11	1.27	1.89	1.64	4.80	1.55	0.99	0.75	3.29
FW-4	**Flowing Well 4**	Minor	0.006	0.009	0.009	0.009	0.009	0.000	0.009	2.27	3.27	3.16	8.70	3.11	3.28	0.00	6.39	2.85	1.64	0.79	5.28
FW-6	**Flowing Well 6**	Minor	0.000	0.023	0.020	0.019	0.022	0.019	0.026	0.00	8.31	7.14	15.44	7.02	7.92	7.04	21.97	5.46	4.06	3.54	13.06
FW-7	**Flowing Well 7**	Minor	0.000	0.001	0.000	0.000	0.001	0.000	0.001	0.00	0.39	0.00	0.39	0.00	0.37	0.00	0.37	0.16	0.19	0.00	0.35
FW-8	**Flowing Well 8**	Minor	0.005	0.007	0.007	0.007	0.008	0.006	0.008	1.65	2.42	2.52	6.59	2.60	2.76	2.33	7.69	2.36	1.30	1.21	4.87
FW-9	**Flowing Well 9**	Minor	0.024	0.032	0.034	0.015	0.021	0.020	0.021	8.69	11.67	12.29	32.64	5.35	7.78	7.10	20.23	7.25	4.86	4.85	16.95
FW-10	**Flowing Well 10**	Minor	0.000	0.005	0.004	0.000	0.004	0.000	0.000	0.00	1.92	1.39	3.31	0.00	1.54	0.00	1.54	0.00	0.87	0.35	1.21
FW-11	**Flowing Well 11**	Minor	0.000	0.011	0.011	0.011	0.012	0.012	0.011	0.00	4.02	4.02	8.04	3.97	4.21	4.40	12.58	2.59	2.06	2.11	6.76
																			Sum of Inflows		**53**
																			Value used in Water Budget:[5]		**50**

Notes:
[1] Outflow values for August 27, 2022, shown in italics, are estimated as 19% of the outflow values measured on August 29, 2023, based on the ratio of values measured on May 15, 2023, and April 27, 2022.
[2] To estimate the water budget, we used the results of continuous flow monitoring of Kays Creek instead of the extrapolated flow run results. These values are rounded to the nearest 100 acre-feet.
[3] Not used in water budget calculations.
[4] Value is not a direct measurement, it was extracted from stream gage data at that site.
[5] Value rounded to the nearest 10 acre-feet in water budget calculation.

Results

Flow Runs

Inflows: Over the seven flow runs conducted at the Preserve, the flow rates and relative proportions of the various sources of surface-water inflow to the Preserve varied significantly by season (Tables 1–3; Figures 6 and 7). Inflow from all sources combined measured during flow runs ranged from 10.84 to 96.47 cfs (Table 1; Figures 6 and 7).

Manually measured inflow in Kays Creek ranged from 0.90 cfs in August 2022 to 38.95 cfs in May 2023 (Table 1; Figure 6). Inflow in the Freeport Drain ranged from 8.43 cfs in August 2022 to 1.51 cfs in May 2023, and inflow in the Syracuse Drain ranged from 0.31 cfs in August 2022 to 6.06 cfs in August 2023 (Table 1; Figure 6).

The greatest overall flow rates were measured during the spring runoff periods of both 2022 and 2023 (Table 1; Figure 6). During the spring of 2022, a year characterized by severe

Table 2. *Flow run results in acre-feet grouped by source type.*

Source Type	Base Flow	Percent	Spring Runoff	Percent	Irrigation Season	Percent	Water Year	Percent
INFLOWS								
Water Year 2022								
Streams	3809	58%	1180	76%	473	11%	5462	45%
Agricultural Drains	545	8%	92	6%	466	11%	1102	9%
Storm Drains	2173	33%	284	18%	3219	77%	5676	46%
Total	6526		1556		4158		12,240	
Water Year 2023								
Streams	1426	33%	4560	79%	3189	32%	9175	45%
Agricultural Drains	343	8%	449	8%	947	9%	1739	9%
Storm Drains	2574	59%	731	13%	5982	59%	9287	46%
Total	4343		5740		10,119		20,201	
2022–2023 Average								
Streams	2617	48%	2870	79%	1831	26%	7319	45%
Agricultural Drains	444	8%	271	7%	706	10%	1421	9%
Storm Drains	2374	44%	507	14%	4601	64%	7482	46%
Total	5435		3648		7138		16,221	
OUTFLOWS								
Water Year 2022								
Streams	4405	62%	571	71%	443	n/a	5420	63%
Agricultural Drains	575	8%	14	2%	22	n/a	610	7%
Storm Drains	2114	30%	215	27%	236	n/a	2565	30%
Total	7094		800		701		8595	
Water Year 2023								
Streams	951	64%	3980	96%	2299	63%	7230	78%
Agricultural Drains	43	3%	24	1%	114	3%	181	2%
Storm Drains	495	33%	145	3%	1224	34%	1864	20%
Total	1489		4149		3637		9276	
2022–2023 Average								
Streams	2678	62%	2276	92%	1371	63%	6325	71%
Agricultural Drains	309	7%	19	1%	68	3%	396	4%
Storm Drains	1305	30%	180	7%	730	34%	2214	25%
Total	4291		2475		2169		8935	

Table 3. *Flow run results in cubic feet per second for the primary features in each source type category.*

Source Type	Base Flow	Percent	Spring Runoff	Percent	Irrigation Season	Percent	Water Year	Percent
INFLOWS								
Water Year 2022								
Kays Creek	7.88	44%	19.10	73%	0.90	6%	27.88	48%
Syracuse Drain	1.41	8%	0.98	4%	0.31	2%	2.70	5%
Freeport Drain	3.62	20%	1.82	7%	8.43	60%	13.87	24%
Total Inflows	17.79		26.14		13.98		57.90	
Water Year 2023								
Kays Creek	2.91	25%	38.95	40%	10.19	30%	52.05	37%
Syracuse Drain	4.16	35%	5.26	5%	6.06	18%	15.48	11%
Freeport Drain	1.77	15%	1.51	2%	7.82	23%	11.10	8%
Total Inflows	11.84		96.47		34.01		142.31	
OUTFLOWS								
Water Year 2022								
Kays Creek	8.22	43%	7.39	55%	n/a	n/a	16.67	51%
Syracuse Drain	2.19	11%	1.05	8%	n/a	n/a	3.65	11%
Freeport Drain	2.76	14%	2.10	16%	n/a	n/a	5.14	16%
Total Outflows	19.33		13.45				32.78	
Water Year 2023								
Kays Creek	1.13	28%	15.06	22%	5.65	46%	21.83	25%
Syracuse Drain	0.00	0%	1.25	2%	2.17	18%	3.42	4%
Freeport Drain	1.35	33%	0.55	1%	1.45	12%	3.35	4%
Total Outflows	4.06		69.73		12.22		86.02	

drought conditions, surface water inflow to the Preserve was 26.14 cfs. In contrast, the subsequent spring of 2023 marked a historically significant runoff event, contributing 96.47 cfs. The irrigation season and base flow time periods of 2023 received instantaneous inflows of 34.01 and 11.84 cfs, respectively. The base flow periods of 2022 and 2023, following the irrigation season when agricultural water usage tapered off, had the lowest inflows to the Preserve of 11.84 and 10.84, respectively (Table 1; Figure 6).

Streams were the greatest source of surface water inflow during the water year 2022 base flow season, providing 58% of total inflows, whereas storm drains provided 59% of total surface inflows during the 2023 base flow season (Table 2; Figure 7D). Streams were the dominant source of surface inflow in the spring runoff time period, accounting for 76% of total surface inflow in April 2022 and 79% in May 2023 (Table 2). Storm drains were the greatest source of surface water inflow during the water year 2022 irrigation season, accounting for 77% of total surface inflow in August 2022, and 59% of total surface inflow in August 2023 (Table 2; Figure 7D). Kays Creek and Freeport Drain were the dominant individual sources of inflow except for the base flow period in water year 2023 in which Syracuse Drain was the dominant source (Table 3; Figure 6).

Flow rates from artesian wells ranged from 0.004 to 0.02 cubic feet per second (Table A1). We estimated an average annual flow rate of 53 acre-feet per year from the artesian wells for 2022 and 2023 (Table 1).

Outflows: Like the surface inflows, the flow rates and relative proportions of the various sources of surface-water outflow from the Preserve varied significantly by season (Tables 1–3; Figures 6 and 7). During the seven flow runs, the total instantaneous outflow from all sources ranged from 4.06 to 69.33 cfs, discounting the August 27, 2022, flow run when no outflow sources were measurable (Table 1, Figures 6 and 7).

Manually measured outflow in Kays Creek ranged from 1.13 cfs in November 2022 to 15.06 cfs in May 2023. Outflow in the Syracuse Drain ranged from 0 cfs in November 2022 to 2.19 cfs in October 2021. Outflow in Freeport Drain ranged from 0.55 cfs in May 2022 to 2.76 cfs in October 2021 (Table 1; Figure 6).

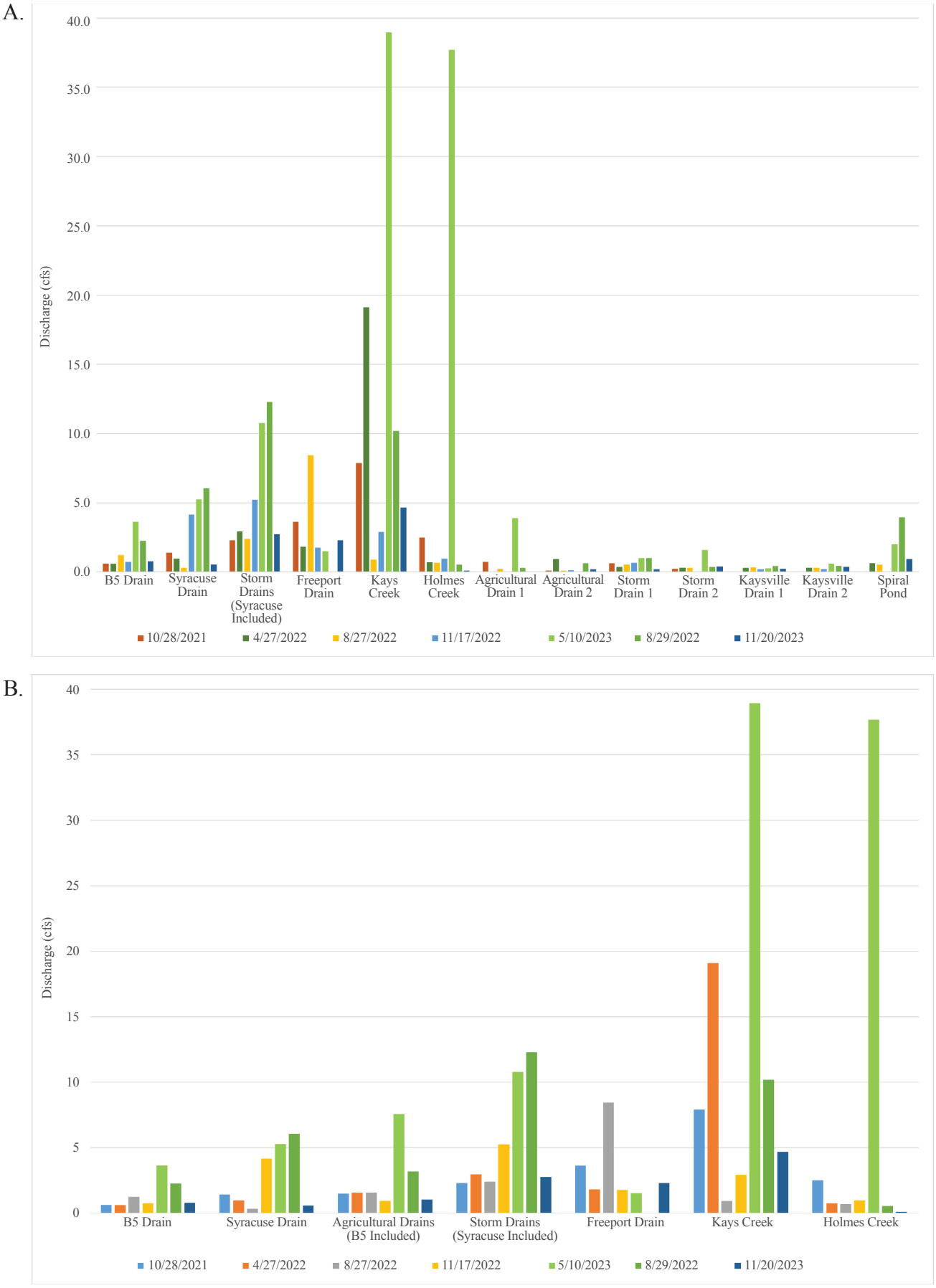

Figure 6. *Flow run results for surface water inflow.* ***A)*** *All sources.* ***B)*** *Major inputs. Outflow values are shown as negative numbers.*

C.

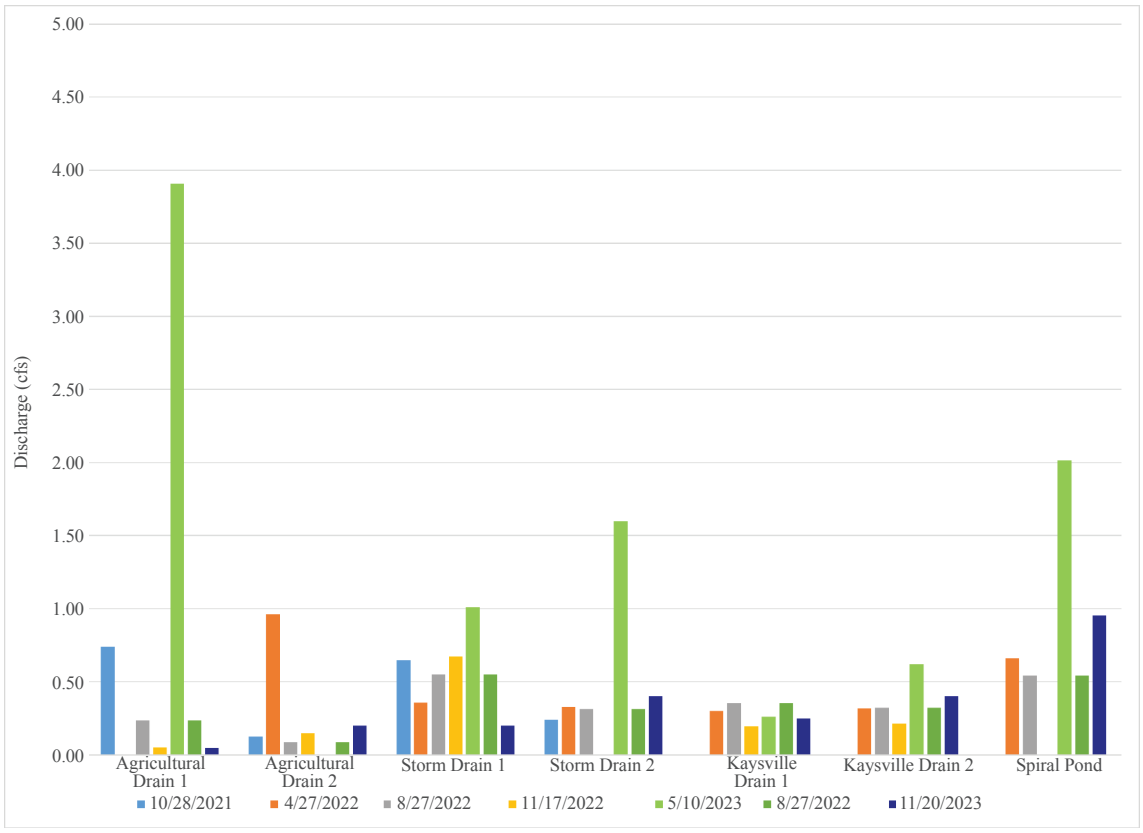

D.

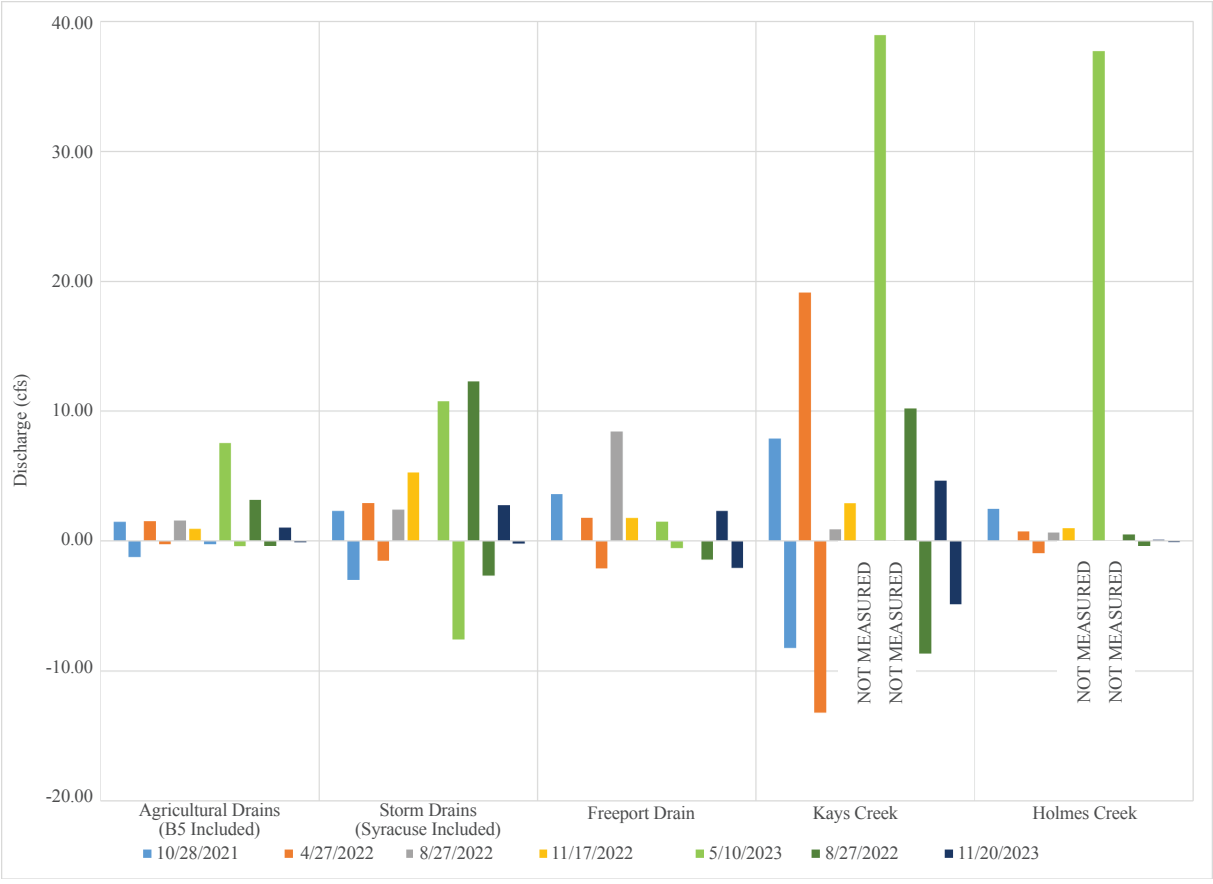

Figure 6 (continued). *Flow run results for surface water inflow.* ***C)*** *Minor inputs.* ***D)*** *Inflows and outflows. Outflow values are shown as negative numbers.*

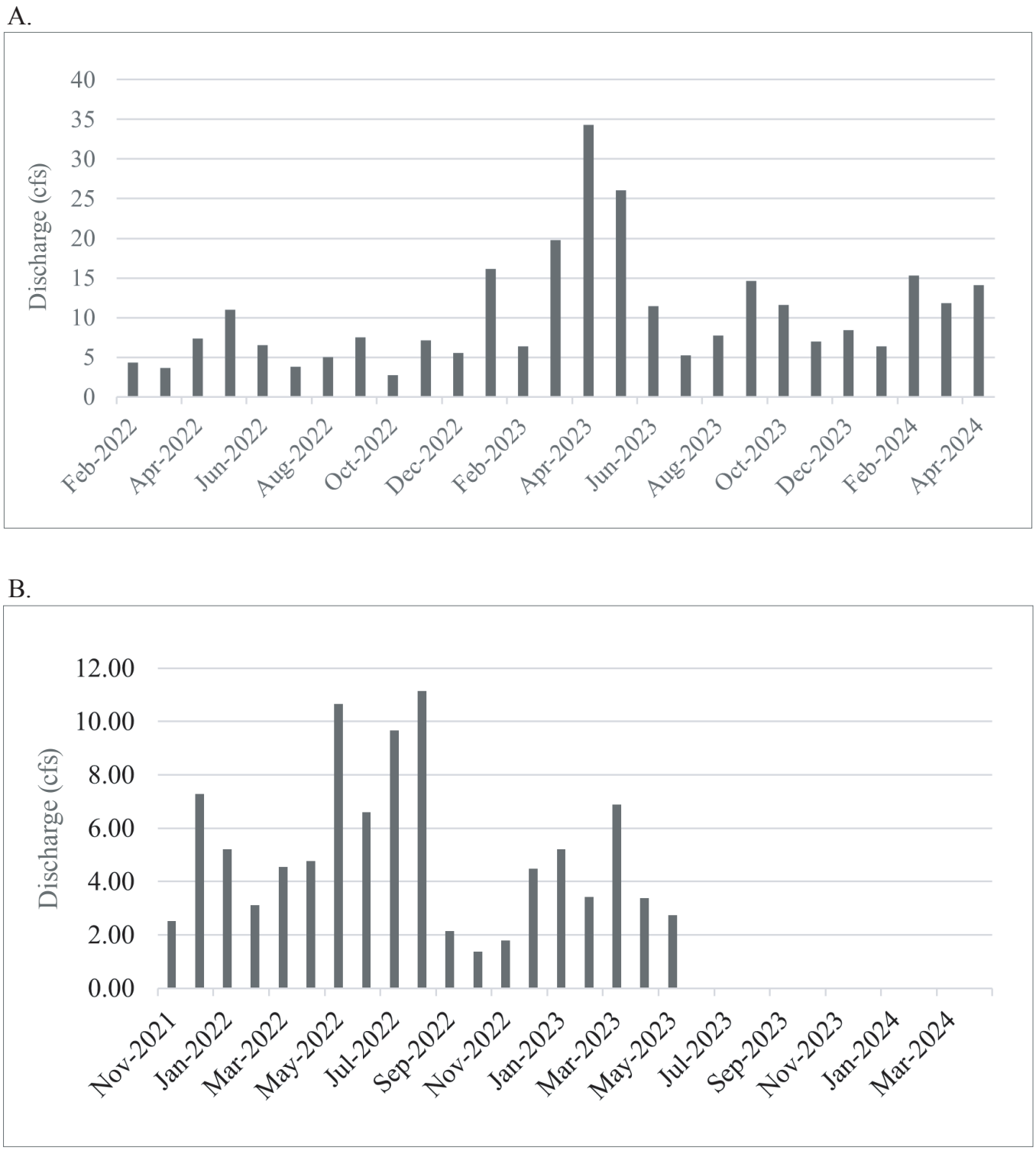

Figure 7. *Average monthly and annual inflows based on extrapolated flow run results.* ***A)*** *Average monthly inflows for Kays Creek.* ***B)*** *Average monthly inflows for Freeport Drain.*

C.

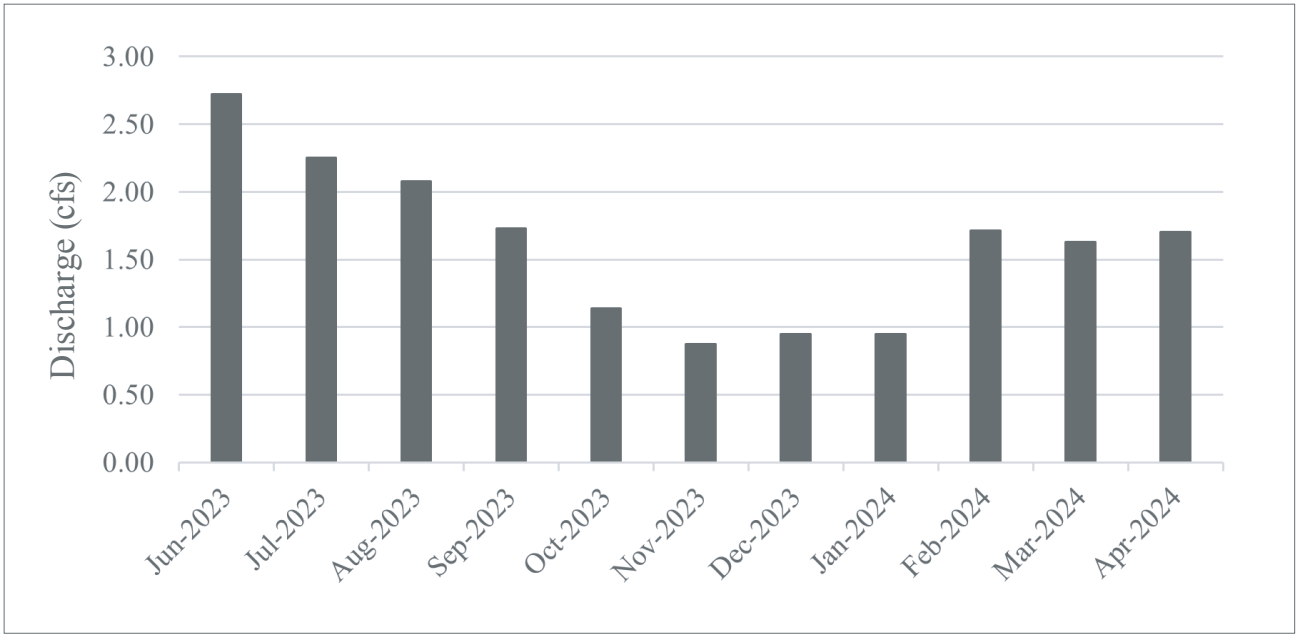

D.

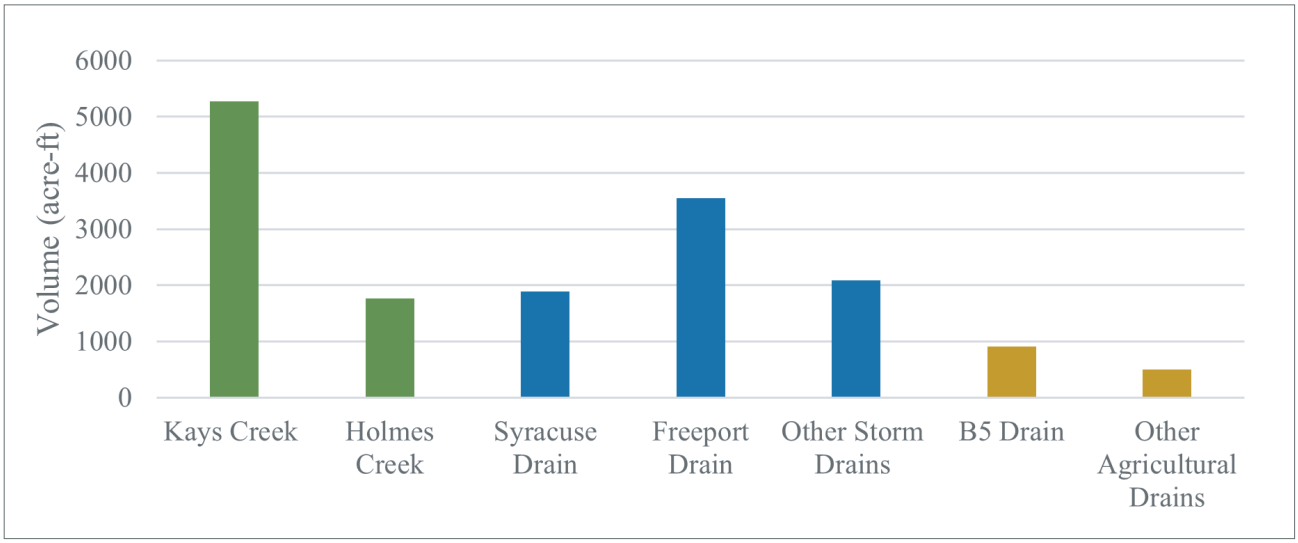

Figure 7 (continued). *Average monthly and annual inflows based on extrapolated flow run results.* ***C)*** *Average monthly inflows for B5 drain.* ***D)*** *Average annual inflows to the Preserve.*

Streams were the dominant source of surface outflow in the 2022 and 2023 base-flow time periods, accounting for 62% and 64% of total surface outflows in November 2022 and 2023, respectively (Table 2; Figure 7D). Streams were the dominant source of surface water outflow in the spring runoff time periods of water years 2022 and 2023, accounting for 71% and 96% of total surface outflows, respectively (Table 2; Figure 7D). Unfortunately, we were unable to collect surface outflow measurements during the 2022 irrigation season. To fill this data gap, we estimated outflows for this time period by multiplying the 2023 irrigation season measurements by the ratio of the spring runoff measurements for 2022 versus 2023 (19%). For example, the estimate for the Kays Creek 3 station for August 27, 2022, is 1.07 cfs, 19% of the measured flow for this station on August 29, 2023 (5.65 cfs). Streams were the greatest source of surface water outflow during the 2023 irrigation season, providing 63% of total outflows (Table 2). Kays Creek was the greatest individual source of surface outflow, except for the base flow time period of water year 2023 during which Freeport Drain provided 33% of total outflows (Table 3; Figure 7).

Net Gains and Losses: The lower outflows compared to inflows can be attributed to numerous man-made diversions and impoundment structures, such as ditches and ponds, which decelerate water flow to increase open water and wetland

vegetation coverage and local shallow groundwater recharge. When comparing surface water inflows and outflows in the western part of the Preserve, we consistently observed a net loss of water. This area includes numerous ditch diversions and impoundments. Conversely, in the central part of the Preserve we typically observed nearly equal outflows and inflows. This area features more channelized flow patterns and fewer impoundments, providing fewer opportunities for direct groundwater recharge.

At the Freeport Drain, we measured greater outflow than inflow during the 2022 spring runoff, indicating groundwater flow to the drain channel. However, following the installation of the Freeport Ponds in the spring of 2023, we measured significantly less outflow than inflow due to the diversion of water from the drain into these new ponds near the northern Preserve boundary.

Measuring Kays Creek and Holmes Creek regularly during flow runs presented safety challenges, especially during peak spring runoff in 2023 when accessing lower reaches was problematic. In the spring of 2022, during a smaller runoff year, Kays Creek exhibited a net loss of 6.1 cubic feet per second (cfs) between the inflow and outflow measurement points. In contrast, Holmes Creek experienced a net gain of 0.22 cfs along its course during the same period.

Continuous Monitoring

Continuous monitoring data and rating curves for Kays Creek, Freeport Drain and B5 Drain are shown in Figures 8A, 8B, and 8C, respectively. The rating curve for Kays Creek (formulated by E. Rau, U.S. Geological Survey, written communication, July 2023) is well constrained and integration of the flow-rate curve yielded total inflow estimates of 4890 acre-feet for 2022 and 6780 acre-feet for 2023. Monthly average discharges at Kays Creek were higher for every month of 2023 compared to 2022 (Figure 8A). Average discharge peaked in May 2022 at 11.0 cfs and in April 2023 at 34.3 cfs. The mean monthly discharge at Kays Creek varied between 2022 and 2023 (Figure 7A). Kays Creek had higher monthly averages throughout all months in 2023 compared to the previous year. The difference is most dramatic during spring runoff in April and May of 2023 where discharge averaged 34.31 cfs and 26.03 respectively in contrast to 7.35 cfs and 11.00 cfs observed in April and May of 2022.

Comparing the total annual inflow estimates from Kays Creek using the ratings curve, which we consider more accurate, with those derived from the extrapolated flow run data provides a check on the validity of the latter method. Total annual inflow in Kays Creek during water year 2022 was 4890 acre-feet using the ratings curve and 4300 acre-feet using the extrapolated flow run measurements, a difference of 13%. Total annual inflow in Kays Creek during water year 2023 was 6780 acre-feet using the ratings curve and 6420 acre-feet using the extrapolated flow run measurements, a difference of 6%. The average annual inflow for water years 2022 and 2023 was 5830 acre-feet using the ratings curve and 5360 acre-feet using the extrapolated flow run measurements, a difference of 10%. Extrapolating the flow run values likely did not account for high flow time periods that were captured by the continuous monitoring, explaining the lower estimates using that method.

The Freeport Drain ratings curve was poor quality, likely due to a low ratio of stage to flow rate and changes in channel morphology during the project period. The ratings curve yielded total inflow estimates of 3940 acre-feet for water year 2022 and 4740 acre-feet for water year 2023. Freeport Drain inflows using the extrapolated flow run data were 3950 acre-feet for water year 2022 and 3070 acre-feet for water year 2023. Like the Kays Creek data, the flow run values likely did not account for high flow time periods, however, the ratings curve for these higher flow rates is suspect.

The gauge at the B5 drain was installed in June 2023 and showed a clear trend of decreasing discharge throughout the irrigation season and then increasing during the base flow and spring runoff time periods (Figure 8C).

Summary

Estimated annual surface water inflows to the Preserve based on the results from the flow runs are 12,240 acre-feet for water year 2022, 20,200 for water year 2023, and averaged 16,220 acre-feet for the two water years. Estimated annual surface water outflows are 7890 acre-feet for water year 2022, 9280 for water year 2023, and averaged 8935 acre-feet for the two water years. Surface water inflows in 2023 were about 7960 acre-feet greater than in 2022, whereas outflows were only about 1380 acre-feet more in 2023 than in 2022. This suggests that surface water storage, ET, and soil moisture increased substantially during 2023, taking up a large proportion of the increased inflows. Surface water storage and soil moisture were likely much lower than typical by the end of water year 2022.

GROUNDWATER LEVELS

Introduction

We measured groundwater levels in wells on the Preserve to characterize the hydraulic head of both the shallow unconfined and confined aquifers and estimate groundwater flow directions and rates. Hydraulic head is "an indicator of the total energy available to move groundwater through an aquifer," and "is measured by the height to which a column of water will stand above a reference elevation (or 'datum'), such as mean sea level. A water-level measurement made under static

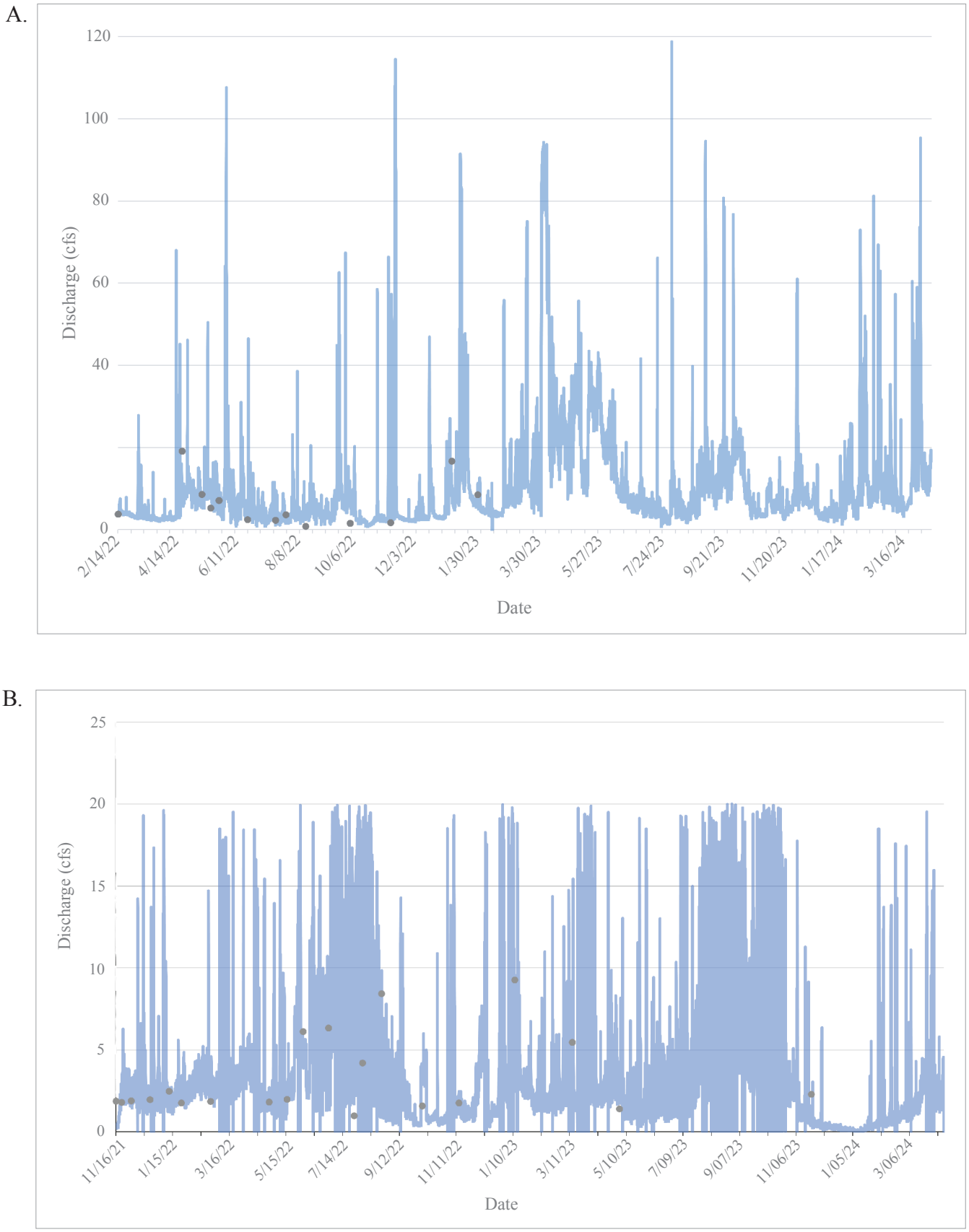

Figure 8. *Results of continuous monitoring of stream flow.* ***A)*** *Kays Creek discharge calculated from water levels and ratings curve, manual flow data, and precipitation. Black dots are manual flow data.* ***B)*** *Freeport Drain water levels. Black dots are manual flow data.*

C.

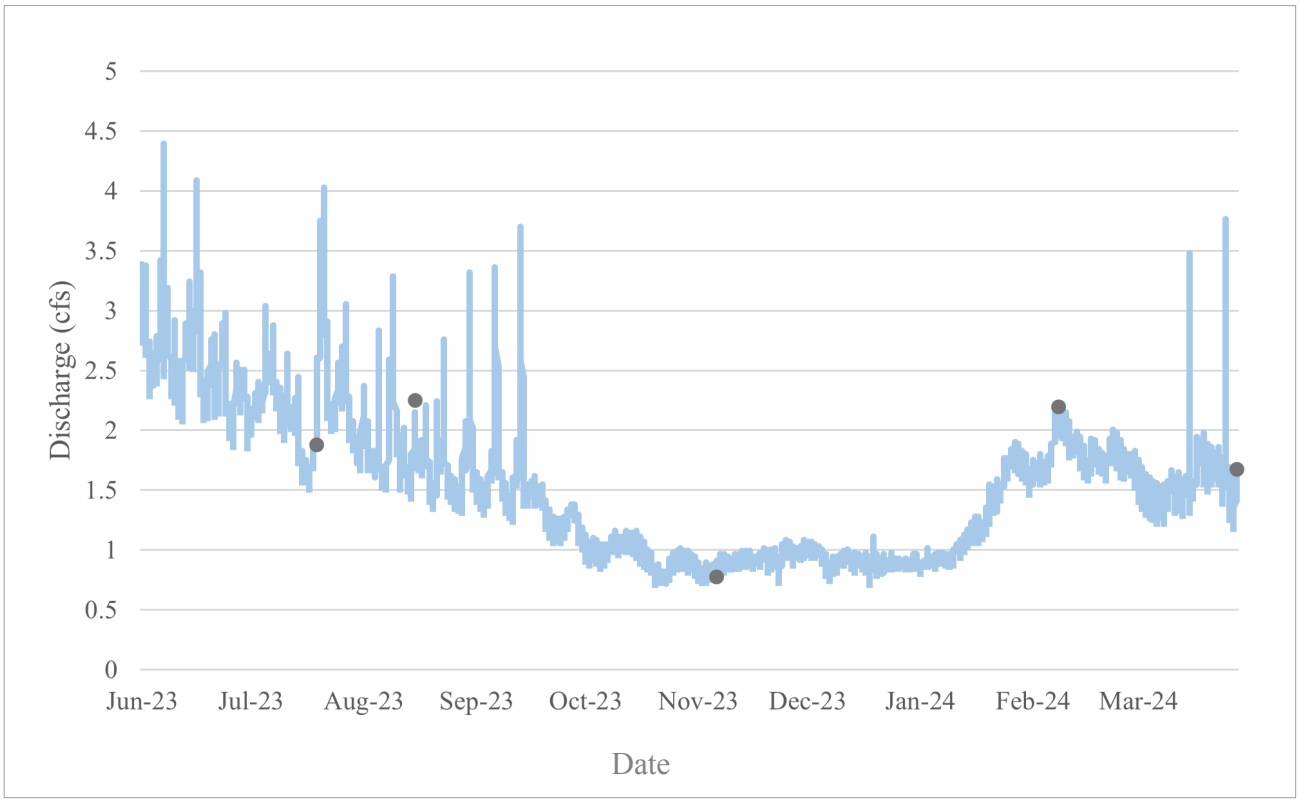

Figure 8 (continued). *Results of continuous monitoring of stream flow.* ***C)*** *B5 drain discharge calculated from water levels and ratings curve. Black dots are manual flow data.*

(non-pumping) conditions is a measurement of the hydraulic head in the aquifer at the depth of the screened or open interval of a well." (Taylor and Alley, 2013). Groundwater flows from areas of higher to lower hydraulic head, approximately normal to contours of equal head value except under special conditions such as anisotropic aquifer properties. For our purposes, groundwater-level elevations in well-sealed wells are equivalent to hydraulic heads and provide information about aquifer conditions and groundwater flow directions. Records of wells measured in this study are in Appendix A, Table A2.

Methods

We measured groundwater levels during the spring and fall of 2022 and spring of 2023 flow runs. For the artesian wells, we either (1) sealed the well heads, attached pressure gauges, allowed the reading to stabilize, and converted the pressure to height above the gauge using the conversion factor 1 pound per square inch of pressure = 2.31 feet of head; or (2) extended the well head upward by attaching PVC, allowing the water level to stabilize, and measuring depth to groundwater from the top of the extension using an electronic sounding tape. For all wells, we measured the land-surface elevation using high-precision differential GPS, and recorded the height of the measuring point above or below the land surface where the GPS reading was obtained ("stickup") using a steel tape graduated in hundredths of feet. From these measurements we calculated groundwater-level elevations as: (land-surface elevation) - (height of measuring point above land surface) - (depth to water below measuring point) (all units in feet).

We installed four piezometers (FP-W1, FP-W2S, FP-W2D, and FP-W3; Table A2; Figure 2E) south of the proposed Freeport Pond impounded wetlands in April 2022 to measure possible aquifer recharge associated with the new impoundment. During summer 2023 we installed four piezometers along the southwestern boundary of the Preserve and used data from two of these piezometers (MW-03 and MW-04; Table A2; Figure 2C) to calculate groundwater flow in the shallow unconfined aquifer. During summer 2024 we installed two additional wells near Freeport Drain (FP-W3S and FP-W3D; Table A2; Figure 2E). We used data from our piezometers and select wells from the WDCP to calculate groundwater flow in the shallow unconfined aquifer.

Results

Groundwater levels in wells completed in the confined aquifer ranged from 2.39 feet below the land surface to 23.56 feet above land surface (Table A3). Groundwater levels in these wells fluctuated by about 0.5 to 3 feet over the period of record (Figure 9). Groundwater-level elevations, averaged for

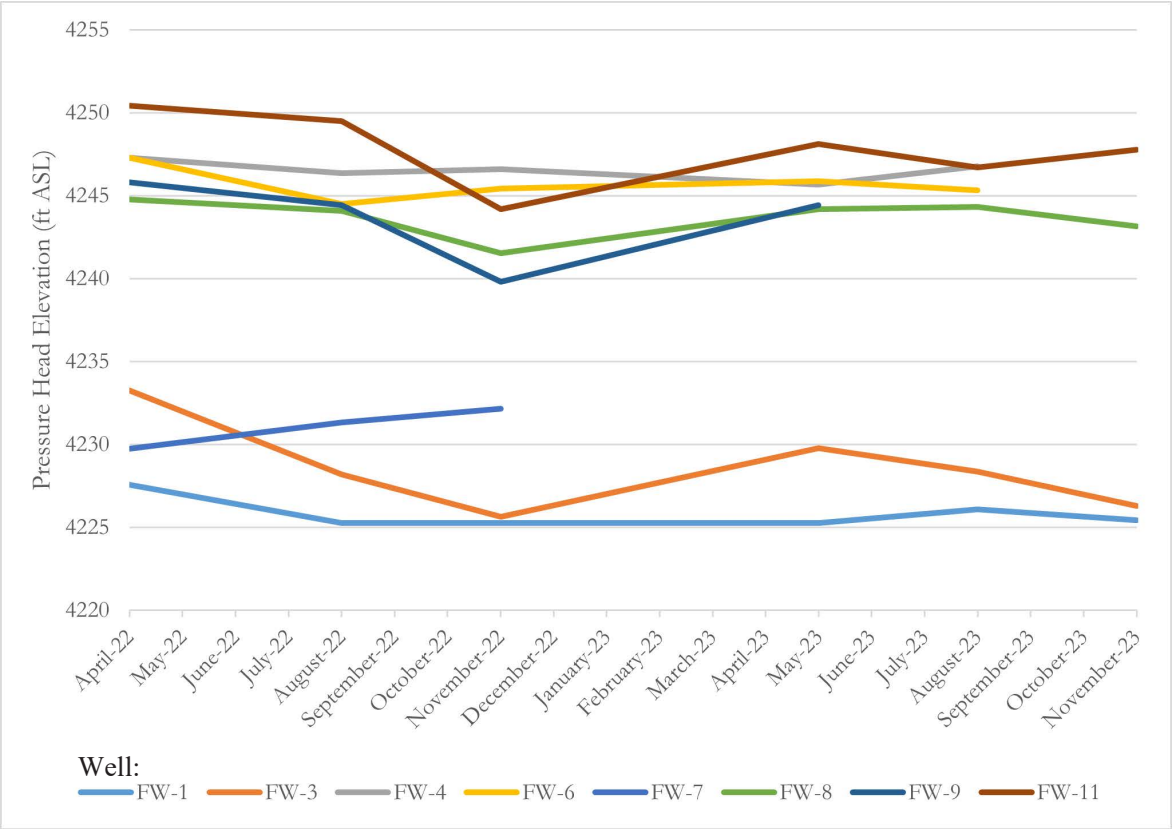

Figure 9. *Groundwater levels from flowing wells derived from pressure heads measured during flow runs.*

each well over all measurements from April 27, 2022, to May 17, 2023, ranged from 4225.8 to 4248.0 feet. The distribution of these wells throughout the Preserve is insufficient to draw potentiometric-surface contours.

The potentiometric elevations measured in the artesian wells are as much as 21 feet higher than the groundwater-level elevations in nearby wells completed in the shallow unconfined aquifer. This relation indicates the potential for groundwater to flow upward from the confined aquifer into the unconfined aquifer. The presence and depth below land surface of the hardpan layer throughout the Preserve is variable based on augering by B. Downard (verbal communication, September 27, 2023), conducted during her Ph.D. research at Utah State University.

Groundwater levels in the piezometers near the Freeport Pond ranged from 0 to 6.05 feet below land surface and from 4222.67 to 4227.07 feet elevation. The three shallowest wells, ranging from 3.8 to 5.1 feet deep (FP-W1, FP-W2S, and FP-W3), were dry from June through November 2022. The deeper well (FP-W2D, 10.8 feet deep) did not go dry.

We were unable to access water-level data from the WDCP monitoring wells and, therefore, relied on the hydrographs and basic statistics in the annual reports for three of the seven wells near or in the Preserve (HDR Engineering, 2021, 2022, 2023, 2024). In 2022, average depth to water over the entire year in the three WDCP wells along the northeastern Preserve boundary ranged from 0.7 to 4.6 feet below land surface, and hydrographs indicate groundwater-level declines of between 0.5 and 6.5 feet from March to late September.

CHEMISTRY AND ENVIRONMENTAL TRACERS

Introduction

Because the Preserve receives water from different sources (stream, drains, and groundwater), we hypothesized that these different sources of groundwater may have different compositions of major-solute and stable isotopes (concentrations of the heavier isotopes of the water molecule, ^{2}H and ^{18}O). We were specifically interested in whether the deeper confined aquifer has a distinct chemical composition that reflects its recharge in the high Wasatch Range and flow through the confined basin-fill aquifer to the GSL margin. We also wanted to identify the source(s) of the groundwater in the shallow unconfined aquifer (potential sources include recharge of stream flow, direct infiltration of precipitation, and seepage from the confined aquifer).

Methods

Using sample bottles provided by the Utah Public Health Laboratory, we collected water samples from flowing wells,

shallow groundwater monitoring wells, streams, and drains (Figure 10A; Table A4) for analyses of major solute (Ca, Mg, Na, K, Cl, SO_4, HCO_3) and total-dissolved-solids concentrations. We filtered the samples for cation analyses using 45 micrometer (µm) disc filters attached to a syringe or 45 µm paper filters in a cartridge attached to the outflow tubing of a peristaltic pump. We refrigerated the samples and submitted them to the Utah Public Health Laboratory within the prescribed holding times. We collected samples for stable-isotope concentration measurement in 3 milliliter (mL) plastic vials using 45 µm disc filters attached to a syringe and crimped the metal caps to seal the samples. Samples were then refrigerated and submitted to the University of Utah's SIRFER Laboratory for analyses. Stable-isotope compositions are reported in the "delta" notation as δ^2H and $\delta^{18}O$, reflecting the concentrations of these isotopes relative to the more common isotopes of hydrogen and oxygen (^1H and ^{16}O, respectively) (Clark and Fritz, 1997). We calculated a local meteoric water line (LMWL) (Friedman et al., 2002) to represent the stable-isotopic composition of precipitation in the region and to provide a reference for sample interpretation from data from the Quail Point Station in North Salt Lake (Bowen, 2023).

Results

Shallow groundwater from the WDCP monitoring wells includes Ca-, Na-, Mg-HCO_3 and Na-Cl water types (representing general compositional ranges) (Figure 10B; Table A4). Groundwater from the flowing wells is Na-HCO_3 type, and its major-ion composition is more uniform than, and clearly distinct from, that of the WDCP monitoring wells. We did not collect cation samples from surface water so are not able to compare their major-solute compositions to those of the groundwater samples. Total-dissolved-solids concentrations in five of the six groundwater samples ranged from 480 to 578 milligrams per liter (mg/L); the sample from well H-2 had a distinctly greater TDS value of 1380 mg/L (Figure 10C). Concentrations of chloride and bicarbonate were greater in this sample than in the others, accounting for the elevated TDS value.

Stable isotope compositions are offset from the LMWL and are dispersed away from that reference line toward greater (i.e., less negative) δ^2H and $\delta^{18}O$ values (Figure 11). The three main water sources—surface water (streams and drains combined), shallow groundwater, and deep groundwater—show distinct compositions and trends. Surface water samples are

A.

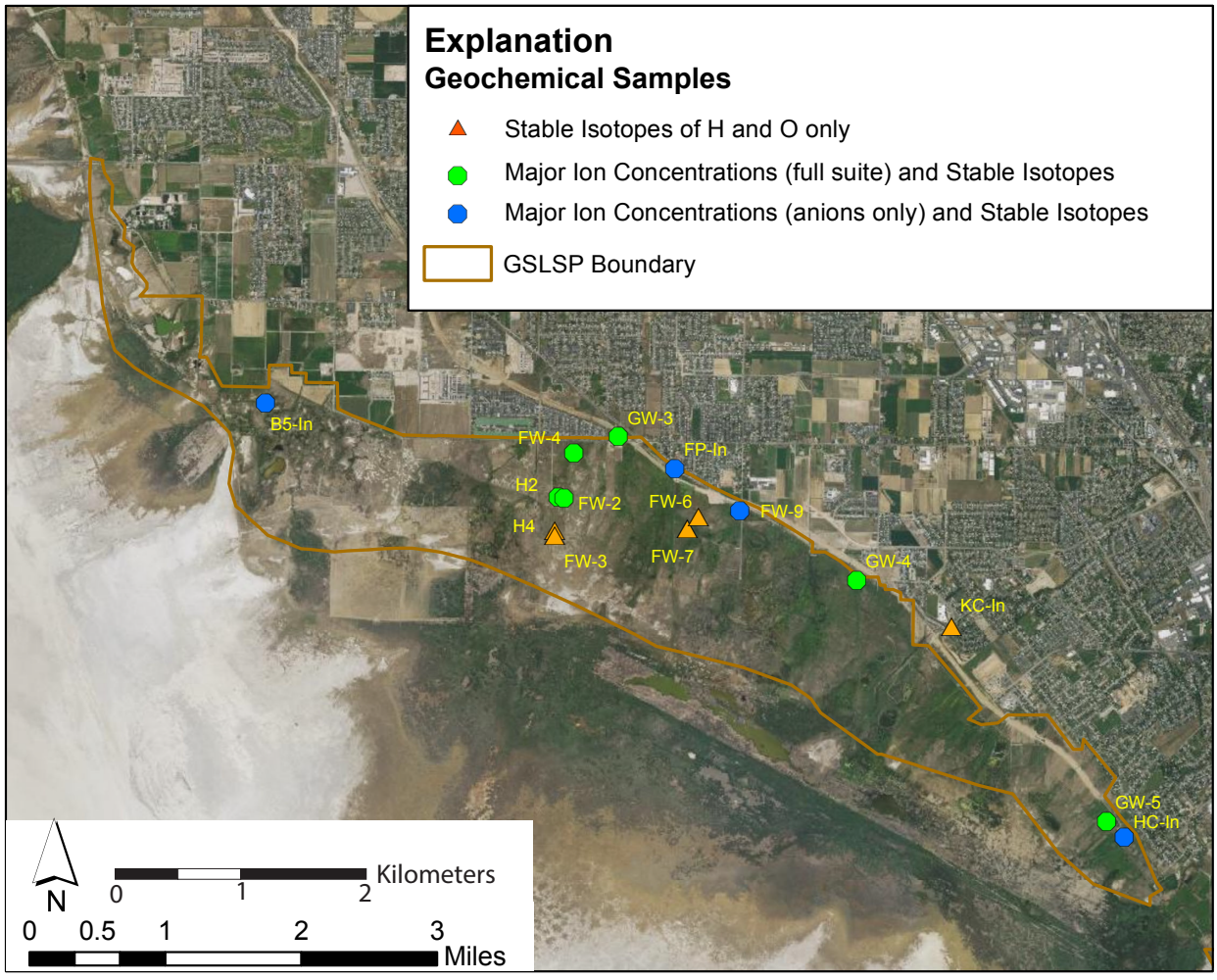

Figure 10. *Groundwater and surface water chemistry.* ***A)*** *Location of samples collected for chemical analyses. See Table A4 for sample information and results, and Figure 2 for locations. GSLSP = Great Salt Lake Shoreland Preserve.*

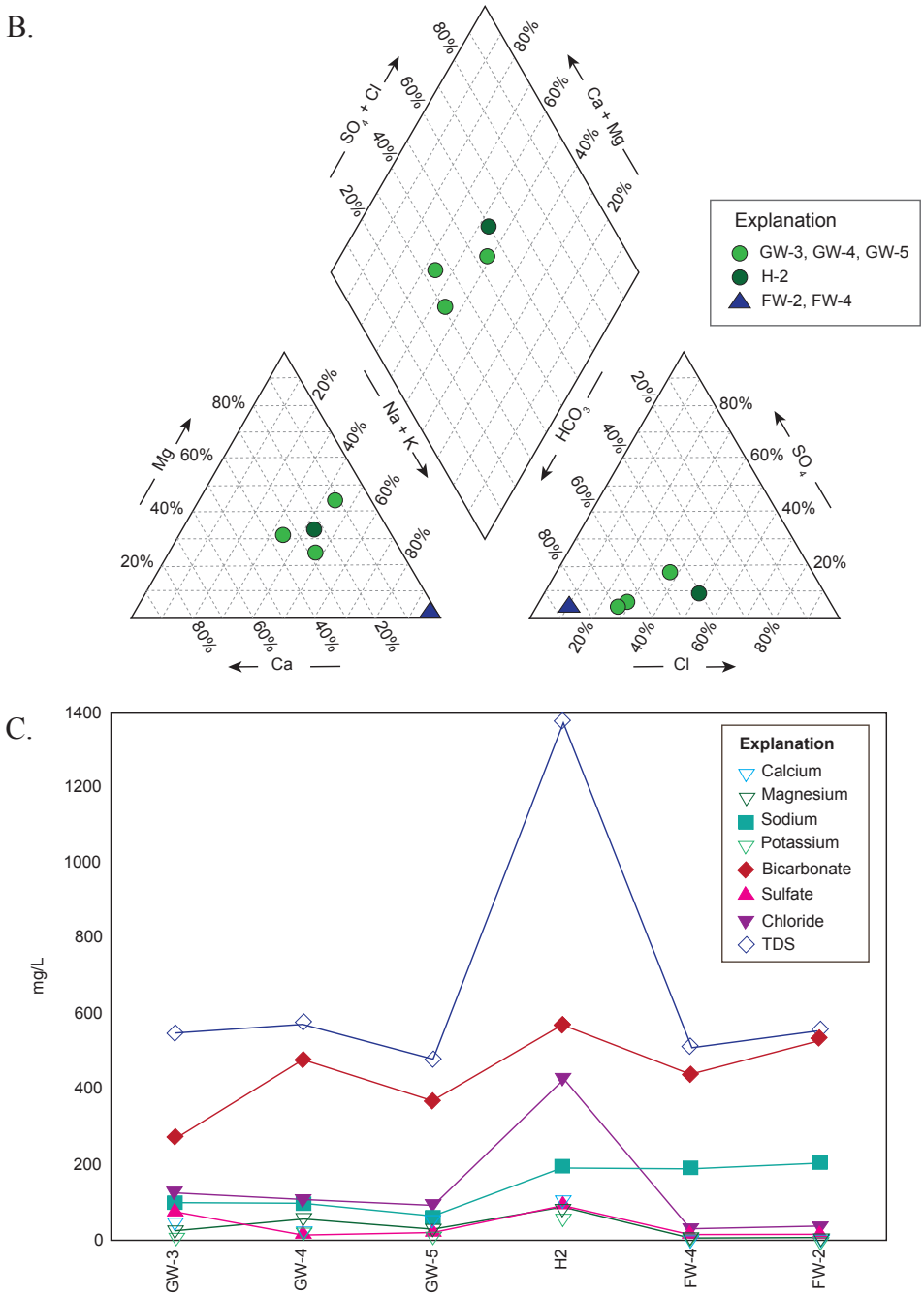

Figure 10 (continued). *Groundwater and surface water chemistry.* ***B)*** *Piper diagram showing variation of sample compositions. Results from WDCP monitoring wells are in green, and results from flowing wells are in blue.* ***C)*** *Variations in concentrations of individual constituents. TDS is total dissolved solids concentration.*

dispersed away from the GMWL along a line having a slope of 3.4. Deep groundwater samples from the flowing wells have distinctly lower δ values than surface water and are dispersed along a line having a slope of 3.3. Shallow groundwater samples from the WDCP monitoring wells have δ values that show greater variation in δ^2H and less variation in $\delta^{18}O$ compared to the deep groundwater and surface water samples and are dispersed along a line having a slope of 5.5.

The slopes of the linear regression lines through the surface water and deep groundwater samples are consistent with fractionation of the stable-isotopic compositions of these waters by evaporation (Clark and Fritz, 1997). The distinctly different compositions of the intersections of the regression lines with the LMWL suggest that their source waters had different starting compositions. The more negative δ values of the flowing well samples suggest the groundwater from the deep confined aquifer was recharged under cooler conditions, either at greater elevations during modern time or during the Holocene or Pleistocene under generally cooler climates. The stable isotope compositions of groundwater sampled from the shallow monitoring wells varies; some samples are like those from the flowing wells, some are like those from the surface waters, and some lie between those two trends. A regression

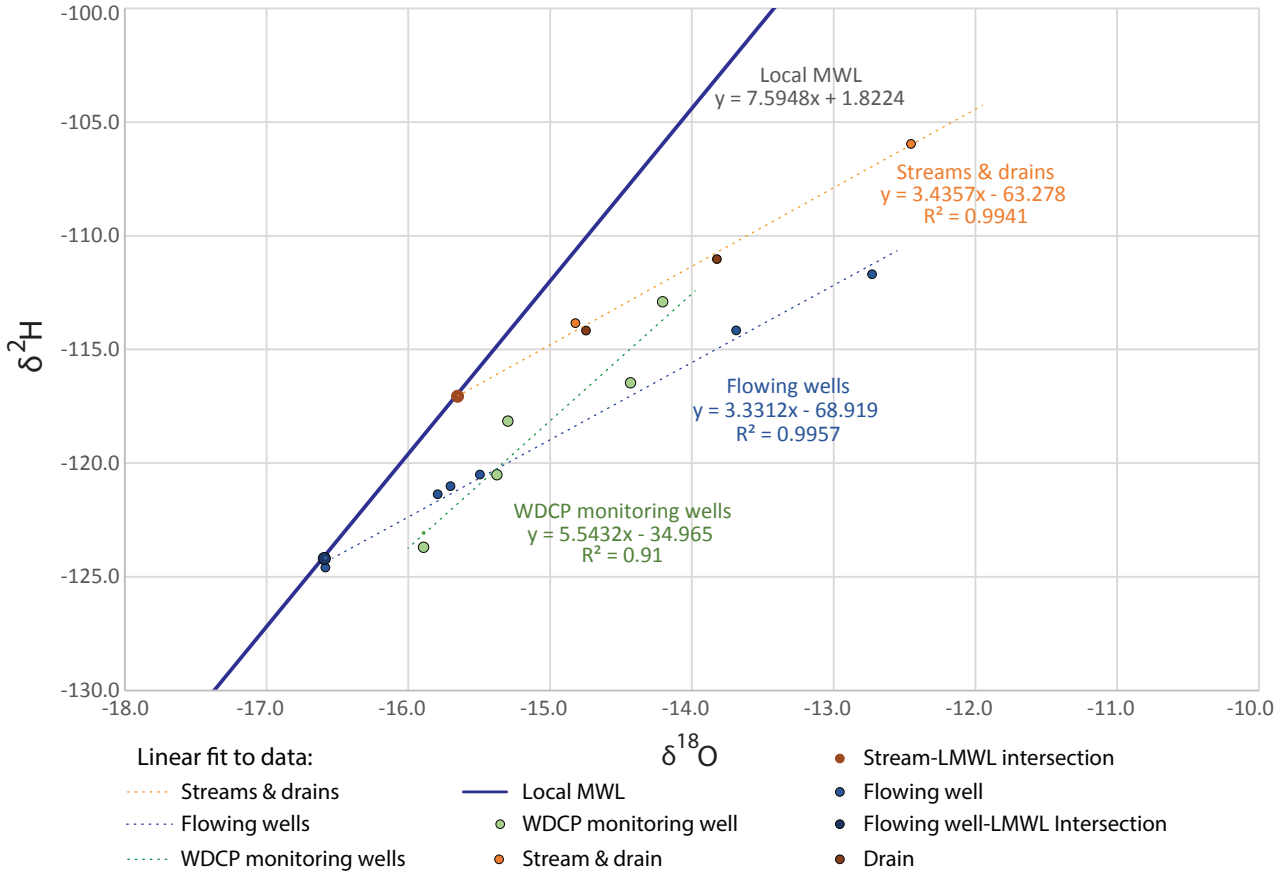

Figure 11. *Stable-isotope compositions of water samples, and regression lines and equations for each sample group. See Table 1 for sample information and results. Global MWL is the Global Mean Water Line.*

line through the shallow monitoring well samples has a slope of 5.5, distinct from the other two groups and similar but not identical to the slope of the LMWL. We interpret these results to indicate that the shallow groundwater is a mixture of waters from precipitation, surface water, and groundwater from the confined aquifer. The relative proportions of these waters may vary depending on location or depth, but we do not have sufficient data to test those interpretations.

WATER BUDGET

Introduction

A water budget provides a comprehensive framework to quantify the inputs, outputs, and storage changes of water within a specific area over a given time period. By evaluating the various components of the water budget, we can gain insights into the hydrological dynamics and make informed decisions regarding water management strategies. In the case of the Preserve, understanding the water budget is crucial for evaluating potential management changes and new structures to preserve the integrity of wetlands, provide open water for migratory birds, sustain water-dependent ecosystems, and address potential impacts from ongoing projects such as the West Davis Corridor and continued urbanization of farmland.

Our water budget encompasses surface water, groundwater, and precipitation sources, and losses from ET and outflows. Surface water inputs include contributions from two perennial streams, agricultural drains, and stormwater runoff. These inputs are subject to changes as land use transitions occur within the surrounding areas. On the other hand, groundwater serves as a vital component, with both shallow and deep aquifer systems contributing to the overall water availability.

Methods

Water Budget Formulation and Boundaries

The annual water budget equation for the Preserve can be represented as:

$$Precip_{SP} + SW_{in} + GW_{in} = ET_{SP} + SW_{out} + GW_{out} + \Delta S \quad (1)$$

where:

$Precip_{SP}$ = total precipitation on the Preserve

SW_{in} = surface water inflow

GW_{in} = groundwater inflow

ET_{SP} = evapotranspiration from within the Preserve boundary

SW_{out} = surface water outflow

GW_{out} = groundwater outflow

ΔS = change in storage

All quantities are expressed in acre-feet per water year. We calculated water budgets for water years 2022, 2023, and the average of the two years.

Precipitation ($Precip_{SP}$) represents the input of water from rainfall and snowfall on the Preserve land surface, surface water inflow (SW_{in}) is the flow measured in channels along the northeastern boundary, and groundwater inflow (GW_{in}) includes flow within the shallow unconfined aquifer across the northeastern boundary and from the confined aquifer into the shallow unconfined aquifer within the Preserve. On the outflow side, evapotranspiration (ET_{SP}) is the combined processes of water loss through evaporation from the land surface and transpiration from plants. Surface water outflow (SW_{out}) accounts for the water leaving through surface water channels and dispersed flow. Groundwater outflow (GW_{out}) represents the flow of groundwater in the shallow unconfined aquifer across the southwestern Preserve boundary. The change in storage (*ΔS*) refers to the net change in groundwater storage within the Preserve. It accounts for changes in groundwater levels, but does not include surface water volumes or soil moisture content over the specified time period.

For the delineation of our project boundaries, we encompassed all land parcels under the ownership or management of TNC and some inset and adjacent parcels. The northeastern Preserve boundary serves as the inflow boundary, where all surface water and groundwater contributions flow into the Preserve. The southwestern boundary of the Preserve is the outflow boundary for the water budget, where surface water and groundwater outflow crosses the southern property line.

We defined the area southwest of the Preserve, where vegetation cover is predominantly *Phragmites australis*, as the Outflow Area for the following reasons. Near the Preserve's southwestern boundary, much of the surface flow is dispersed by multiple branching ditches, diffuse flow through dense *Phragmites*, or is impounded. Due to this configuration we were unable to confidently capture all surface flow out of the Preserve boundary by manual measurements. To address this data gap we applied two approaches to estimating surface water outflow. In outflow option A, we assumed that total outflow could be calculated according to equation 1. This approach underestimates total surface water outflow. In option B, we judged that the great majority of surface water and shallow groundwater departing the Preserve is consumed by the extensive *Phragmites australis* in the Outflow Area, intercepting most flow into Farmington Bay. We also assumed the *Phragmites* consumes all precipitation onto the Outflow Area. With this approach we estimated surface water outflow in option B as:

$$SW_{out} = ET_{OA} - Precip_{OA} - GW_{out} \quad (2)$$

where:

SW_{out} = total surface water outflow including both channelized and dispersed flows

ET_{OA} = evapotranspiration from the Outflow Area

$Precip_{OA}$ = precipitation on the outflow area

GW_{out} = groundwater outflow in the shallow unconfined aquifer

The water budget equation for the Preserve in option B is:

$$Precip_{SP} + SW_{in} + GW_{in} = ET_{SP} + ET_{OA} - Precip_{OA} - GW_{out} + \Delta S \quad (3)$$

Uncertainty Analysis

Evaluating the uncertainty of our water budget is not straightforward because it includes several different data sets having different collection methods and uncertainties. We chose to use the combined standard uncertainty (JCGM, 2008, p. 8–15) to estimate uncertainties of inflow and outflow water budgets as well as the total water budget.

Recharge/Inflow

Precipitation: We estimated precipitation for the purposes of the water budget using data obtained from gridMET (2023), a meteorological data set that interpolates between climate stations at high resolution. From these data we calculated the total annual precipitation on the Preserve and on the Outflow Area for water years 2022 and 2023.

Surface water: We used the total annual inflow estimates derived from the extrapolated flow runs (Table 1), but for Kays Creek we used the total annual inflow from the continuous monitoring instead of the flow run values.

Groundwater: We estimated groundwater flow in the shallow unconfined aquifer through the northeastern boundary of the Preserve and vertical flow from the confined aquifer to the unconfined aquifer within the Preserve using groundwater levels in select wells and Darcy's Law (e.g., Fetter, 2001, p. 142–145). Darcy's Law describes fluid flow through porous media, in this case groundwater flow in an aquifer:

$$Q = -KIA \quad (4)$$

where:

Q = groundwater flux (acre-feet per year)

K = hydraulic conductivity (feet per day) * 365 days/yr

I = hydraulic gradient (feet per feet)

A = area ($feet^2$) * 0.000023 $acres/ft^2$

We assumed a range of likely hydraulic conductivity values for fine-grained sand listed by Fetter (2001, p. 103), based on our examination of lithologic logs of wells in and adjacent to the Preserve and observations from our hand augering to a depth of 12 to 15 feet.

We estimated the horizontal hydraulic gradient in the upper 20 feet of the unconfined aquifer as the difference in water-level elevation divided by the length between the wells, choosing well pairs that form a line approximately perpendicular to the generalized local potentiometric-surface contours which trend northwest-southeast (Gates, 1995, Figure 7) (i.e., parallel to the horizontal component of the hydraulic gradient). We chose a depth of 20 feet based on depths, lithologic logs, and groundwater-level records from WDCP monitoring wells, which indicate unconfined conditions (HDR Engineering, 2024). To extrapolate flow rates derived from the linear traverses to the entire Preserve, we defined the vertical plane through which we calculated the flux to span the entire length of the Preserve. This approach necessarily involves substantial simplification of the hydrogeology of the study area.

Only two pairs of wells (WDCP monitoring wells GW-3 and H-2 [HDR Engineering, 2021, 2022, 2023, 2024] and UGS piezometers FP-W2D and FP-W3D; Table A2; Figures 2C and 2E) were appropriate to estimate groundwater flow into the Preserve. Neither well pair is ideal for these calculations. We do not have consistent access to the WDCP wells, whereas the UGS piezometers are both within the Preserve boundary and are closer together than preferable.

We estimated the vertical hydraulic gradient in the confined aquifer using two closely spaced wells (FW-1 and FW-4; Figure 2C) that have screened intervals noted on their logs. The vertical hydraulic gradient is the ratio of the difference between the water-level elevations to the difference between the elevations of the screen midpoints. Using Darcy's Law we calculated the vertical groundwater flow through a hypothetical one-foot-square horizontal plane. We then multiplied the resulting flow by the total land surface area of the Preserve to estimate vertical groundwater flow from the confined aquifer to the shallow unconfined aquifer throughout the study area. This value represents the vertical flow from the confined aquifer that does not reach the land surface through the flowing wells, but may sustain groundwater levels in the lower part of the shallow unconfined aquifer.

Discharge/Outflow

Evapotranspiration: Evapotranspiration (ET) refers to the combined processes of evaporation and transpiration, where water is transferred from the earth's surface (such as soil, vegetation, and water bodies) into the atmosphere in the form of water vapor (Allen et al., 1998; Roderick et al., 2019). Evaporation occurs when water changes from a liquid state to a gaseous state directly from surfaces (Jensen et al., 1990). Transpiration, on the other hand, is the process by which plants absorb water through their roots and release it as vapor through their leaves (Monteith and Unsworth, 2013).

In the context of a water budget, ET represents a significant loss of water from the study area. By quantifying ET, researchers and water managers can better understand the water balance within a system and make informed decisions regarding water allocation and management strategies (Jensen et al., 1990; Roderick et al., 2019). Including ET in a water budget allows for a more comprehensive assessment of water availability and usage. It helps estimate the total water inputs (such as precipitation and surface water inflows), outputs (such as surface water outflows and groundwater recharge), and losses (primarily through ET) within a given area over a specific time period (Allen et al., 1998; Monteith and Unsworth, 2013).

We conducted two separate ET calculations (vegetation-based and using OpenET) for both the Preserve and the Outflow Area to account for different components of the water budget. In the first method, we used the vegetation map of the Preserve and Outflow Area generated during this study, using remote sensing data, aerial imagery, and our expertise in vegetation mapping, to classify and map vegetation units (see Vegetation Mapping section). We assigned ET rates to each vegetation unit based on the results of Bright et al. (2007), who provided ranges of ET rates for vegetation units within our region of interest. We derived ET rates for each vegetation map unit by multiplying each map-unit area by its appropriate ET rate. To determine cumulative ET volumes over a one-year period, we summed the individual ET volumes of all vegetation units within the Preserve and Outflow Area boundaries. Using this method results in one ET value for water years 2022 and 2023.

As an alternate approach to estimating ET, we obtained remotely sensed evapotranspiration estimates for the study area from OpenET, available through Google Earth Engine or through the public Application Programming Interface (API) (https://openetdata.org/) and uses multiple models that leverage 30-meter Landsat imagery and gridded weather data to estimate actual evapotranspiration (Gorelick et al., 2017; Melton et al., 2022). OpenET provides an ensemble model, which is an average of all models, as well as the minimum and maximum values of those models. Using the public API to get the most recent data, we took the monthly mean values of the ensemble model for each vegetation unit for the period of interest as well as the maximum and minimum range and multiplied them by the area. This method results in separate ET values for water years 2022 and 2023.

Surface Water: For outflow option A, we estimated surface water outflow using only our extrapolated flow run values. For outflow option B, we estimated surface water outflow by subtracting the Outflow Area precipitation and groundwater outflow estimates from the Outflow Area ET, based on the knowledge that we did not capture all surface water outflow by direct measurements and on the assumption that total ET in the outflow area includes all precipitation, shallow groundwater, and surface outflow.

Groundwater: We estimated groundwater flow in the shallow unconfined aquifer out of the Preserve using two pairs of wells near the northeastern and southwestern Preserve boundaries (FP-W2D and MW-04, and GW-3 and MW-03, respectively) (Figures 2C and 2E), using the same methods described in the Recharge/Inflow section.

Change in Groundwater Storage

We estimated change in storage in the shallow unconfined aquifer using depth to groundwater reported by HDR Engineering (2021, 2022, 2023, 2024) for the WDCP monitoring wells and for the piezometers we installed. We calculated storage changes for two time periods: (1) within a water year using the minimum and maximum depths to water from land surface, and (2) year to year by comparing observed depths to water between the two years. We estimated the specific yield of the predominantly fine-grained sand of the shallow aquifer as 0.22 (Duffield, 2023). We estimated the groundwater storage change during a water year as the difference between minimum (spring) and maximum (fall) measured depth to water multiplied by the specific yield. We calculated year-to-year groundwater storage changes using the difference in the minimum depth to water and the difference in the maximum depth to water, then taking the average of the two. We multiplied the storage changes by the surface area of the Preserve to very roughly estimate total within-year and year-to-year changes in groundwater storage.

Results

Uncertainty Analysis

Uncertainties of the individual components of the water budgets varied from 10% to 67%. The combined standard uncertainties for the water budgets as a whole are 12% using outflow option A and 15% using outflow option B. Based on these uncertainties, we report individual components of the water budget to two significant figures to align with the precision of the data. This ensures the reported values do not imply greater accuracy than the uncertainty allows while also allowing us to build our water budget.

Recharge/Inflow

Precipitation: Our annual precipitation estimates derived from gridMET for the Preserve are 5300 acre-feet for water year 2022 and 7900 acre-feet for water year 2023. The average precipitation for water years 2022 and 2023 is 6600 acre-feet. Our annual precipitation estimates for the Outflow Area are 12,000 acre-feet for water year 2022 and 17,000 acre-feet for water year 2023. The average precipitation on the Outflow Area for water years 2022 and 2023 is 14,000 acre-feet.

Surface Water: Based on the flow run results for all features except Kays Creek, for which we used the continuous monitoring results, our estimates of surface water inflow were 13,000 acre-feet for 2022 and 21,000 acre-feet for 2023, with an average value of 17,000 acre-feet (Table 1). Of this, 5800 acre-ft (35% of total surface water inflows) was from Kays Creek, 3500 ac-ft (21%) from Freeport Drain, 2150 ac-ft (13%) from Syracuse Drain, and 1960 ac-ft (12%) from Holmes Creek. We included the estimated flow rate of artesian wells of 50 acre-feet per year in the water budget.

Groundwater: We estimated horizontal groundwater flow rates into the Preserve of 1260 and 3540 acre-feet per year along the two traverses (Table 4). Our preferred estimate is 2400 acre-feet per year, the average of these two estimates.

We estimated an average vertical flow rate in the confined aquifer, in the vicinity of wells FW-1 and FW-4 of 0.29 acre-feet (Table 4). Extrapolation over the entire Preserve area is highly speculative but yields our preferred estimate of 1400 acre-feet per year.

Discharge/Outflow

Evapotranspiration: Using the vegetation-based rates, we estimated an average value of 12,550 acre-feet per year of ET from within the Preserve boundary and an average value of 19,450 acre-feet per year of ET from the Outflow Area (Table 5a). Using the OpenET ensemble model for the Preserve, we estimated total annual ET of 11,700 acre-feet for water year 2022 and 12,400 acre-feet for water year 2023, and an average value of 12,000 acre-feet (Tables 5b and 6). Using the OpenET ensemble model for the Outflow Area, we estimated total annual ET of 26,000 acre-feet for water year 2022 and 28,000 acre-feet for water year 2023, and an average value of 27,000 acre-feet (Table 6).

Surface water: From our surface outflow measurements we estimated 8600 acre-feet for 2022 and 9300 acre-feet for 2023, with an average value of 8900 acre-feet (Table 6). We used this value for surface water outflow in outflow option A. Similarly to inflows, the largest outflows were observed at Kays Creek, Holmes Creek, Freeport Drain, and the Syracuse Drain (Table 2). Outflow option B yielded surface water outflow estimates of 13,600 acre-feet for water year 2022 and 10,600 acre-feet for water year 2023, with an average of 12,600 acre-feet (Table 6).

Groundwater: Our estimated shallow groundwater flow rate into the Preserve is 2400 acre-feet per year, and our estimated flow rate out of Preserve is 400 acre-feet per year. Our estimate of vertical groundwater flow from the confined aquifer to the shallow unconfined aquifer is 1400 acre-feet per year (Table 6).

Significant additional uncertainties accompany these calculations. If more measurements were available, the estimated flow rate would likely vary seasonally and year-to-year. Well coverage in the Preserve is sparse compared to the land area, so extrapolating the results for the well pairs is highly speculative. We do not have direct estimates of hydraulic

Table 4. *Estimates of groundwater flow in confined and unconfined aquifers using groundwater levels collected during this study and Darcy's Law.*

Wells		Hydraulic Gradient			Flow Area			Hydraulic Conductivity[6]			Flows[7]					
Well	Water Level Date	Water Level Elevation (ft)	X[1] (ft)	Grad[2] (ft/ft)	Depth[3] (ft)	Length[4] (ft)	Area[5] (ft2)	K1 (ft/d)	K2 (ft/d)	K3 (ft/d)	Q1 (ft^3/d)	Q1 (afy)	Q2 (ft^3/d)	Q2 (afy)	Q3 (ft^3/d)	Q3 (afy)
Horizontal flow in shallow unconfined aquifer																
Into Shorelands Preserve																
GW-3	9/21/21	4236.5	4220	-0.0062	20	42,400	848,000	3	28	283	-14993	-126	-149930.2479	-1256	-1499302.479	-12565
H-2	9/13/21	4210.2														
FP-W2D	7/2/24	4224.9	268	-0.0176	20	42,400	848,000	3	28	283	-42248	-354	-422476	-3541	-4224759	-35405
FP-W3D	7/3/24	4220.2														
													Average	**-2398**		
Through & Out of Shorelands Preserve																
FP-W2D	9/26/24	4230.24	3445	-0.0039	10	42,400	424,000	3	28	283	-4696	-39	-46961	-394	-469615	-3936
MW-04	9/26/24	4216.78														
GW-3	2/15/23	4237.7	9670	-0.004	10	42,400	424,000	3	28	283	-4818	-40	-48177	-404	-481774	-4037
MW-03	2/6/24	4198.9														
													Average	**-399**		
Vertical flow in confined aquifer[8]																
FW-1	5/17/23	4225.26	170.5	0.1196	1	1	1	3	28	283	0.34	0.003	3.39	0.028	33.92	0.28
FW-4	5/17/23	4245.66									**Study Area:**	**14**		**141**		**1412**
FW-1	11/15/22	4225.26	170.5	0.125	1	1	1	3	28	283	0.35	0.003	3.54	0.03	35.45	0.3
FW-4	11/16/22	4246.58									**Study Area:**	**15**		**148**		**1475**
FW-1	8/24/22	4225.26	170.5	0.1237	1	1	1	3	28	283	0.35	0.003	3.51	0.029	35.06	0.29
FW-4	8/24/22	4246.35									**Study Area:**	**15**		**146**		**1459**
FW-1	4/27/22	4227.56	170.5	0.1157	1	1	1	3	28	283	0.33	0.003	3.279	0.027	32.787	0.275
FW-4	4/27/22	4247.28									**Study Area:**	**14**		**136**		**1365**
															Average for Entire Study Area:	**1428**

Notes:

[1]Horizontal distance between the two wells. For vertical flow, this value is the vertical distance between screen midpoints.

[2]Horizontal hydraulic gradient between the two wells. For vertical flow, this value is the vertical hydraulic gradient. The sign of the hydraulic gradient is based on Darcy's Law which defines the volumetric flow rate, Q, as positive in the direction of flow under a negative change in head (i.e., head decreases in the direction of flow). Thus, both horizontal and vertical flow into and out of the Shorelands Preserve is shown as having negtive values.

[3]Depth of cross section through which flow is calculated.

[4]Length of cross section through which flow is calculated.

[5]Cross section area through which flow is calculated.

[6]We used the minimum, and maximum hydraulic conductivity values for fine sand reported by Fetter (2001), and the midpoint of that range.

[7]We calculated a range of possible groundwater flow rates using the same hydraulic gradient and cross sectional area, and the three values of hydraulic conductivity. The middle value is our preferred estimate.

[8]We calculated flow through a horizontal plane, one-foot-square, around the well, then extrapolated to the entire study area by multiplying the flow rate by the Shorelands Preserve surface area. We calculated flow rates from water levels in nearby wells whose screen depths are known and assumed this flow rate occurs at the base of the transition of confined to unconfined groundwater conditions. These are the only two wells in the study area that are suitable for this calculation.

Table 5a. *Evapotranspiration calculations based on vegetation ET rates and vegetation map.*

ENTIRE PROJECT AREA		ET rates (all values in feet)			Annual ET Volume (all values in acre-feet)		
ET UNIT	**Acreage**	**low**	**average**	**high**	**low**	**average**	**high**
Dense Desert Shrubland	70.88	1.00	1.24	1.80	70.88	87.89	127.58
Dry Playa	5720.35	0.40	0.71	1.10	2288.14	4061.45	6292.39
Grassland	613.21	1.60	2.14	2.70	981.14	1312.28	1655.68
Marshland	3582.86	3.60	4.07	4.60	12,898.29	14,582.23	16,481.15
Meadowland	3037.74	2.20	2.59	3.30	6683.03	7867.75	10,024.55
Open Water	200.72	4.60	5.10	5.60	923.32	1023.68	1124.04
Recently irrigated cropland	1408.40	1.60	2.14	2.70	2253.44	3013.98	3802.68
Sparse Desert Shrubland	60.97	0.50	0.90	1.10	30.49	54.88	67.07
Xerophytic	76.11	0.00	0.00	0.00	0.00	0.00	0.00
TOTAL	**14,771.25**				**26,128.74**	**32,004.14**	**39,575.14**

SHORELANDS BOUNDARY		ET rates (all values in feet)			Annual ET Volume (all values in acre-feet)		
ET UNIT	**Acreage**	**low**	**average**	**high**	**low**	**average**	**high**
Dense Desert Shrubland	70.76	1.00	1.24	1.80	70.76	87.75	127.37
Dry Playa	763.42	0.40	0.71	1.10	305.37	542.03	839.76
Grassland	131.82	1.60	2.14	2.70	210.92	282.10	355.92
Marshland	1033.91	3.60	4.07	4.60	3722.09	4208.03	4756.00
Meadowland	2429.22	2.20	2.59	3.30	5344.29	6291.69	8016.44
Open Water	92.23	4.60	5.10	5.60	424.25	470.36	516.47
Recently irrigated cropland	285.04	1.60	2.14	2.70	456.06	609.98	769.60
Sparse Desert Shrubland	60.85	0.50	0.90	1.10	30.42	54.76	66.93
Xerophytic	74.67	0.00	0.00	0.00	0.00	0.00	0.00
TOTAL	**4941.92**				**10,564.16**	**12,546.70**	**15,448.50**

OUTFLOW AREA		ET rates (all values in acre-feet)			Annual ET Volume (all values in acre-feet)		
ET UNIT	**Acreage**	**low**	**average**	**high**	**low**	**average**	**high**
Dense Desert Shrubland	0.00	1.00	1.24	1.80	0.00	0.00	0.00
Dry Playa	4959.62	0.40	0.71	1.10	1983.85	3521.33	5455.58
Grassland	480.78	1.60	2.14	2.70	769.24	1028.86	1298.09
Marshland	2549.65	3.60	4.07	4.60	9178.75	10,377.09	11,728.40
Meadowland	605.36	2.20	2.59	3.30	1331.80	1567.89	1997.70
Open Water	108.39	4.60	5.10	5.60	498.60	552.80	606.99
Recently irrigated cropland	1123.13	1.60	2.14	2.70	1797.01	2403.50	3032.46
Sparse Desert Shrubland	0.00	0.50	0.90	1.10	0.00	0.00	0.00
Xerophytic	0.00	0.00	0.00	0.00	0.00	0.00	0.00
TOTAL	**9826.93**				**15,559.25**	**19,451.46**	**24,119.22**

Table 5b. *Evapotranspiration calculations using OpenET.*

OpenET Estimates

ENTIRE PROJECT AREA		WY22 ET Volume (acre-feet)			WY23 ET Volume (acre-feet)			Average Annual ET Volume (acre-feet)		
ET UNIT	**Acreage**	**min**	**ensemble**	**max**	**min**	**ensemble**	**max**	**min**	**ensemble**	**max**
Dense Desert Shrubland	70.88	60	111	168	21	40	58	41	76	113
Dry Playa	5720.35	1768	2998	4260	153	236	316	960	1617	2288
Grassland	613.21	2809	4260	5792	1929	3251	4545	2369	3755	5169
Marshland	3582.86	15,348	20,620	25,932	3196	4598	5954	9272	12,609	15,943
Meadowland	3037.74	5758	8478	11,189	16,846	22,015	27,412	11,302	15,246	19,300
Open Water	200.72	556	748	928	6261	8937	11,603	3408	4843	6265
Recently irrigated cropland	1408.40	364	500	636	221	300	379	293	400	507
Sparse Desert Shrubland	60.97	57	101	148	417	544	666	237	323	407
Xerophytic	76.11	82	136	195	79	119	160	80	127	177
TOTAL	**14,771.25**	**26,802**	**37,952**	**49,247**	**29,124**	**40,039**	**51,091**	**27,963**	**38,995**	**50,169**

SHORELANDS BOUNDARY		WY22 ET Volume (acre-feet)			WY23 ET Volume (acre-feet)			Average Annual ET Volume (acre-feet)		
ET UNIT	**Acreage**	**min**	**ensemble**	**max**	**min**	**ensemble**	**max**	**min**	**ensemble**	**max**
Dense Desert Shrubland	70.76	60	111	168	21	40	58	41	76	113
Dry Playa	763.42	183	326	478	82	129	174	133	227	326
Grassland	131.82	2712	4094	5555	224	365	511	1468	2229	3033
Marshland	1033.91	2644	3613	4629	3083	4418	5708	2863	4015	5169
Meadowland	2429.22	1828	2525	3259	2944	3911	4865	2386	3218	4062
Open Water	92.23	223	307	389	1903	2596	3265	1063	1452	1827
Recently irrigated cropland	285.04	364	500	636	221	300	379	293	400	507
Sparse Desert Shrubland	60.85	57	101	148	417	544	666	237	323	407
Xerophytic	74.67	82	136	195	79	119	160	80	127	177
TOTAL	**4941.92**	**8153**	**11,713**	**15,456**	**8975**	**12,421**	**15,785**	**8564**	**12,067**	**15,621**

OUTFLOW AREA		WY22 ET Volume (acre-feet)			WY23 ET Volume (acre-feet)			Average Annual ET Volume (acre-feet)		
ET UNIT	**Acreage**	**min**	**ensemble**	**max**	**min**	**ensemble**	**max**	**min**	**ensemble**	**max**
Dense Desert Shrubland	0.00	0	0	0	0	0	0	0	0	0
Dry Playa	4959.62	1585	2672	3781	71	106	142	828	1389	1961
Grassland	480.78	98	166	238	1706	2886	4034	902	1526	2136
Marshland	2549.65	12,705	17,007	21,303	113	180	246	6409	8594	10,774
Meadowland	605.36	3930	5953	7930	13,902	18,104	22,547	8916	12,028	15,239
Open Water	108.39	333	441	539	4359	6342	8338	2346	3391	4438
Recently irrigated cropland	0.00	0	0	0	0	0	0	0	0	0
Sparse Desert Shrubland	0.00	0	0	0	0	0	0	0	0	0
Xerophytic	0.00	0	0	0	0	0	0	0	0	0
TOTAL	**9826.93**	**18,650**	**26,239**	**33,791**	**20,150**	**27,618**	**35,306**	**19,400**	**26,928**	**34,549**

Table 6. *Water budgets for water years 2022 and 2023 and the averages of the two years.*

INFLOWS	**WY 2022**	**WY 2023**	**Average**	**Water Budget Term**
Precipitation[1]	5300	7900	6600	$Precip_{SP}$
Surface Water In[2]	13,000	21,000	17,000	SW_{in}
Flowing Wells In[3]	50	50	50	SW_{in}
Shallow Groundwater In[4]	2400	2400	2400	Gw_{in}
Confined Groundwater In[4]	1400	1400	1400	Gw_{in}
Total Inflows	1400	1400	1400	

OUTFLOW Option A				
Evapotranspiration from Shorelands Preserve[5]	12,000	13,000	12,000	ET_{SP}
Surface Water Out[6]	8600	9300	8900	SW_{out}
Groundwater Out[4]	400	400	400	GW_{out}
Total Outflows	**21,000**	**22,700**	**21,300**	

Inflows - Option A Outflows	**1150**	**10,050**	**6150**
Percent Difference	5%	36%	25%

OUTFLOW Option B				
Evapotranspiration from Shorelands Preserve[5]	12,000	13,000	12,000	ET_{SP}
Evapotranspiration from Outflow Area[5]	26,000	28,000	27,000	ET_{OA}
Precipitation on Outflow Area[1]	12,000	17,000	14,000	$Precip_{OA}$
Groundwater Out[4]	400	400	400	GW_{out}
Surface Water Out[7]	13,600	10,600	12,600	SW_{out}
Total Outflows	**25,600**	**23,600**	**24,600**	

Inflows - Option B Outflows	**-3450**	**9150**	**2850**
Percent Difference	14%	32%	11%

Comparing Outflow Options A & B			
Surface Water Out (proxy for dispersed flow)	5000	1300	3700
Percent Difference	45%	13%	34%

[1] Using gridMET (2023; statistical gridding of precipitation station data).

[2] Based on extrapolated flow run values for all features except Kays Creek, which is based on continuous monitoring values.

[3] From manual measurements.

[4] Using Darcy's law, middle value of range of hydraulic conductivity for fine sand, groundwater levels in shallow piezometers, and assuming flow depth of 20 feet.

[5] Using OpenET ensemble water use rate.

[6] Based on extrapolated flow run values.

[7] Estimated as Sw_{out} = [ET from Outflow Area (ET_{OA}) - Precipitation on Outflow Area ($Precip_{OA}$) - groundwater flow from Shorelands Preserve to Outflow Area (GW_{out})].

conductivity, therefore cited a range of three possible values and used the middle value as our preferred estimate. None of these uncertainties, however, would likely change the relative importance of surface flow and groundwater flow in the overall water budget of the Preserve.

Horizontal groundwater outflow in the confined aquifer through the southwestern Preserve boundary, not part of the water budget as formulated here, is likely in equilibrium with the inflow during the time frame of this study, but has likely decreased substantially over the >40-year time period shown in the hydrographs in Figure 5. The long-term groundwater-level decline illustrated by those graphs represents a decline in the potentiometric surface in the confined aquifer. The horizontal hydraulic gradient that drives groundwater flow toward Great Salt Lake has, therefore, also likely declined substantially.

Change in Storage

Based on water-level fluctuations in wells in the shallow unconfined aquifer and an assumed storage coefficient, we estimate that within-year storage loss, from April to November, was 0.68 acre-feet, and that storage loss from spring of 2022 to spring of 2023 was 0.17 acre-feet (Table A6). This change in storage is much less than the estimated annual evapotranspiration, suggesting that a substantial part of the water used by the wetland vegetation is derived from precipitation and surface water. For this reason, we do not include groundwater storage change in our water budget calculation.

Summary

The boundary of our water budget for the Preserve includes the property owned by The Nature Conservancy and inset properties among which several will be (or have been) transferred to the Preserve as part of the mitigation program for the West Davis Corridor Project. Water inflows include precipitation on the land surface within the water budget boundary, surface water flow and groundwater flow through the northeastern boundary, and discharge from flowing wells and upward groundwater flow from the confined aquifer to the shallow unconfined aquifer within the boundary. Outflows include ET from within the boundary, and surface water and groundwater flow through the southwestern boundary. We used two methods to estimate surface water outflow: option A using only extrapolated flow run measurements, understanding that this approach did not account for dispersed flow; and option B using a secondary water budget for the Outflow Area assuming that essentially all surface water and groundwater flows from the Preserve into the Outflow Area are consumed by *Phragmites australis* there, so that the surface water outflow can be estimated as the ET from the Outflow Area minus the precipitation on the Outflow Area minus the groundwater outflow. We constructed water budgets for water years 2022 and 2023 which represent extreme low and high water years, and assume that the average values of inflows and outflows of these two water years represents reasonable long-term values.

The water budget is summarized in Table 6 and Figure 12. Our estimates of total annual water inflow to the Preserve for water years 2022 and 2023 are 22,150 acre-feet and 32,750 acre-feet, respectively, with an average value of 27,450 acre-feet. Our estimates of total annual water outflows using option A for water years 2022 and 2023 are 21,000 acre-feet and 22,700 acre-feet, respectively, with an average value of 21,300 acre-feet. Our estimates of total water outflows using option B for water years 2022 and 2023 are 25,600 acre-feet and 23,600 acre-feet, respectively, with an average value of 24,600 acre-feet.

The difference between total inflows and total outflows varied between options A and B for each water year and for the average values of the two water years. For water year 2022, inflows and outflows were closely matched using option A and outflows were greater than inflows using option B, primarily due to the high value of ET from the Outflow Area which resulted in a higher surface water outflow estimate. For water year 2023, inflows were substantially greater than outflows estimated from both options. For the average water budget values, inflows and outflows were more closely matched using option B but both approaches yield water budgets that are balanced within the uncertainty range of the method (about 12% to 24%). Comparing surface water outflow estimates from the outflow options, option B provided greater values and the two options are most closely matched for water year 2023 (Table 6).

VEGETATION MAPPING

Introduction

We mapped vegetation communities to reflect current habitat and conditions and to support additional groundwater and remote sensing analyses. Mapping was conducted "wall to wall" across the study area which includes (1) the Preserve area defined as all parcels currently owned by TNC, (2) parcels likely to be transferred to TNC and added to the Preserve ("New Parcels"), and (3) adjacent outflow areas to the west and southwest considered important for understanding water budgets in the study area (Outflow Area) (Figure 13). Broadly, we identified distinct vegetation communities and supporting hydrology through a combination of field studies and GIS-based photo-interpretation to create a contiguous dataset describing the dominant vegetation, typical hydropatterns, and likely water sources for each polygon in the dataset. Previous studies have also mapped vegetation communities at the Preserve, with each study grouping vegetation communities by slightly different parameters. "Vegetation classes" refers to the distinct groupings made by this UGS study whereas "vegetation communities" refers either to a broader, more general interpretation

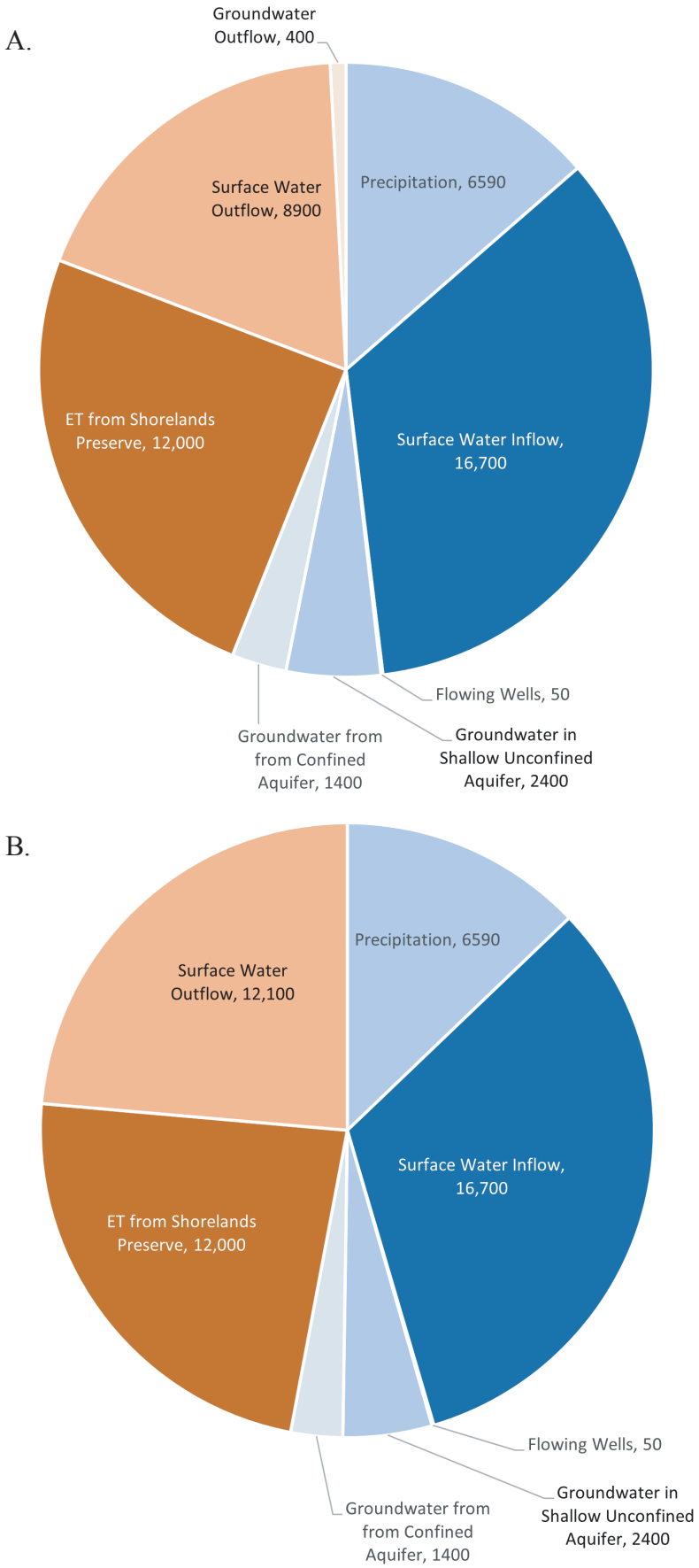

Figure 12. *Average water budgets for water years 2022 and 2023, using two options for calculating surface water outflows. Values are from Table 6. Inflows shown in blue; outflows shown in brown.* ***A)*** *Water budget using outflow option A.* ***B)*** *Water budget using outflow option B.*

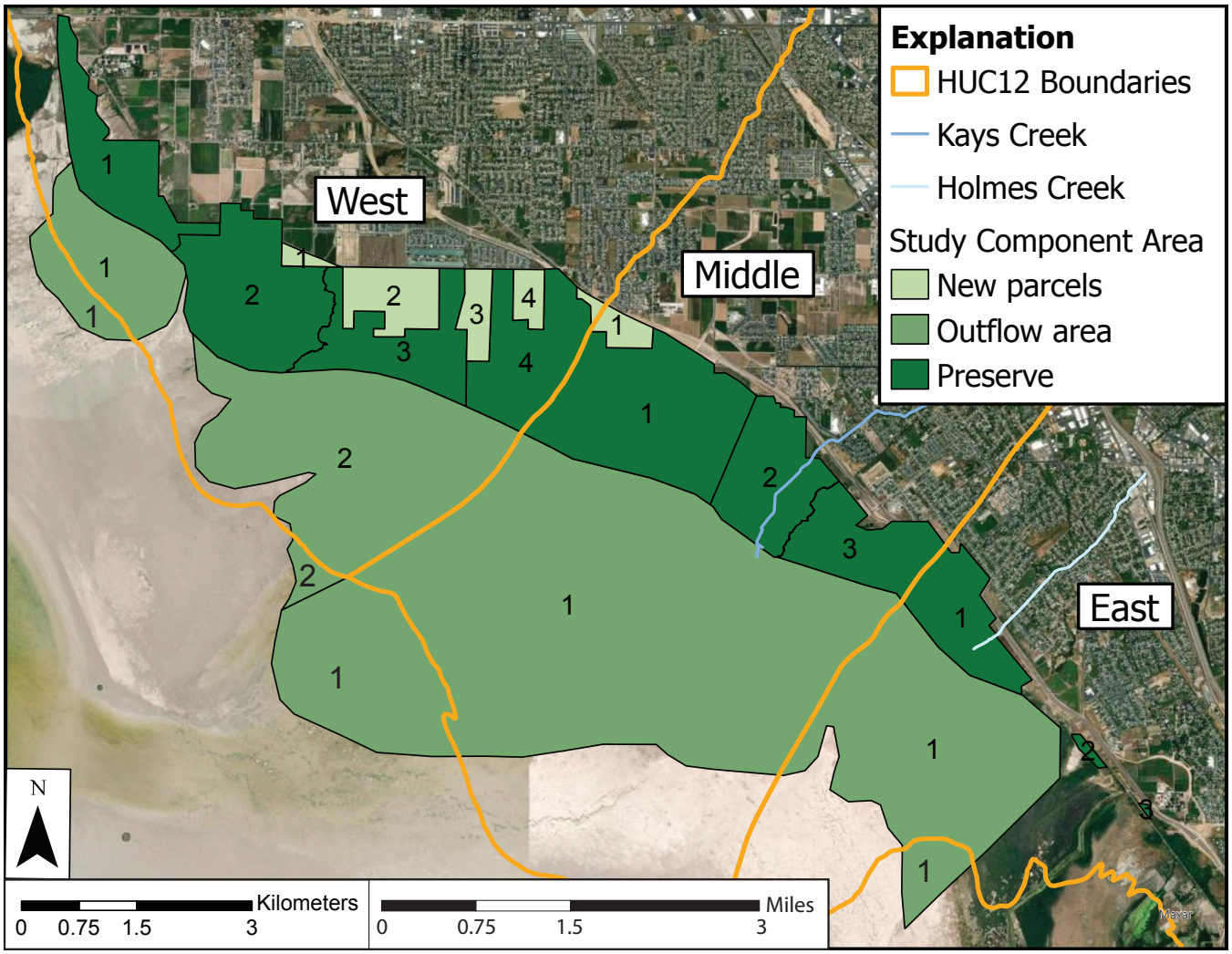

Figure 13. *Vegetation mapping component areas and hydrology units.*

or to groupings from previous studies (Ducks Unlimited, 2007; Long, 2014). For purposes of the water budget, the Preserve and New Parcels are combined as the Preserve, whereas they are separated in the vegetation and NDVI analyses to account for the possibility of different management strategies.

Methods

We identified vegetation communities, hydropatterns, and likely water sources present in the study area by reviewing existing vegetation mapping from Ducks Unlimited (2007), Long (2014), and the Natural Resources Conservation Service (2021). To verify existing mapping, Pete Goodwin, UGS wetland ecologist, conducted field surveys on July 28, 2021, August 11, 2021, August 26, 2021, and March 3, 2022. Vegetation communities were categorized into distinct vegetation classes that include two tiers: (1) a broad class generally distinguished by dominant hydrology or large vegetation differences, and (2) a more detailed subclass generally distinguished by relative cover of individual plant species (Table A7). We identified nine broad classes (Artificial, Marsh, Mesic Meadow, Phragmites [not italicized when referring to a mapped class or subclass], Playa, Upland, Water, Wet Meadow, and Woody Riparian) and eighteen subclasses; representative photos of each broad class and subclass are included in Appendix C. Subclasses were aligned to the ET units identified by Smith et al. (2007) for ET loss estimates. Hydropatterns and likely water sources were categorized into eight hydropatterns and seven water sources (Tables A8 and A9). Hydropatterns were based on Cowardin water regime classifications used by the National Wetland Inventory (NWI; Dahl et al., 2020). Features were assigned up to two likely water sources based primarily on sources identified through field surveys.

Identification and delineation of individual vegetation communities followed general UGS NWI mapping methods (Goodwin and Molinari, 2022). Polygons were hand-digitized through detailed review of the most recent National Agricultural Imagery Program (NAIP) aerial imagery collected August 12, 2021. We used a size threshold of 0.1 acres when identifying distinct polygons; features greater than 0.1 acres were mapped as distinct polygons and features below the threshold were merged into surrounding polygons. Polygon boundaries were largely drawn based on

vegetation, hydrology, and topographic differences readily visible in the 2021 NAIP imagery. Other imagery sources were also reviewed to better distinguish vegetation and hydrology including NAIP imagery collected in 2011, 2016, and 2018, fine-scale HEXAGON imagery from 2019, and historical aerial imagery freely available through Google Earth. Lidar datasets from 2016 and 2018 flights were also extremely useful for identifying distinct vegetation heights, topographic breaks, and small ditches and other irrigation features.

Results

Across the study area, Phragmites was the most extensively mapped vegetation class, followed by the Wet Meadow class (Table A10; Figure 14). In these two classes, roughly 90% and 80% were mapped as Dense Phragmites or Dense Saltgrass subclasses, respectively. Woody Riparian, Upland, and Artificial vegetation classes are the least extensive and Woody Riparian occupied only a fraction of a percent of the overall area. Permanent Water was mapped throughout the study area as small, isolated features occupying about 1% of the overall area.

Within the Preserve, Mesic Meadow was the most extensively mapped vegetation class (Table A10). Phragmites was the second-most extensive vegetation class but was much less common than in the Outflow Area. Mesic Grasses or Dense Phragmites accounted for about 89% and 75%, respectively, of the total Mesic Meadow and Phragmites vegetation class extents. The combined extents of Woody Riparian, Upland, and Artificial vegetation communities accounted for approximately 6% of the Preserve area. Playa vegetation communities were proportionally less extensive within the Preserve than within the Outflow Area or overall study area, whereas Permanent Water was proportionally more extensive.

The New Parcels showed generally similar trends to the Preserve. Mesic Meadow was the most extensively mapped vegetation class at 59% and Phragmites was the second at 11%

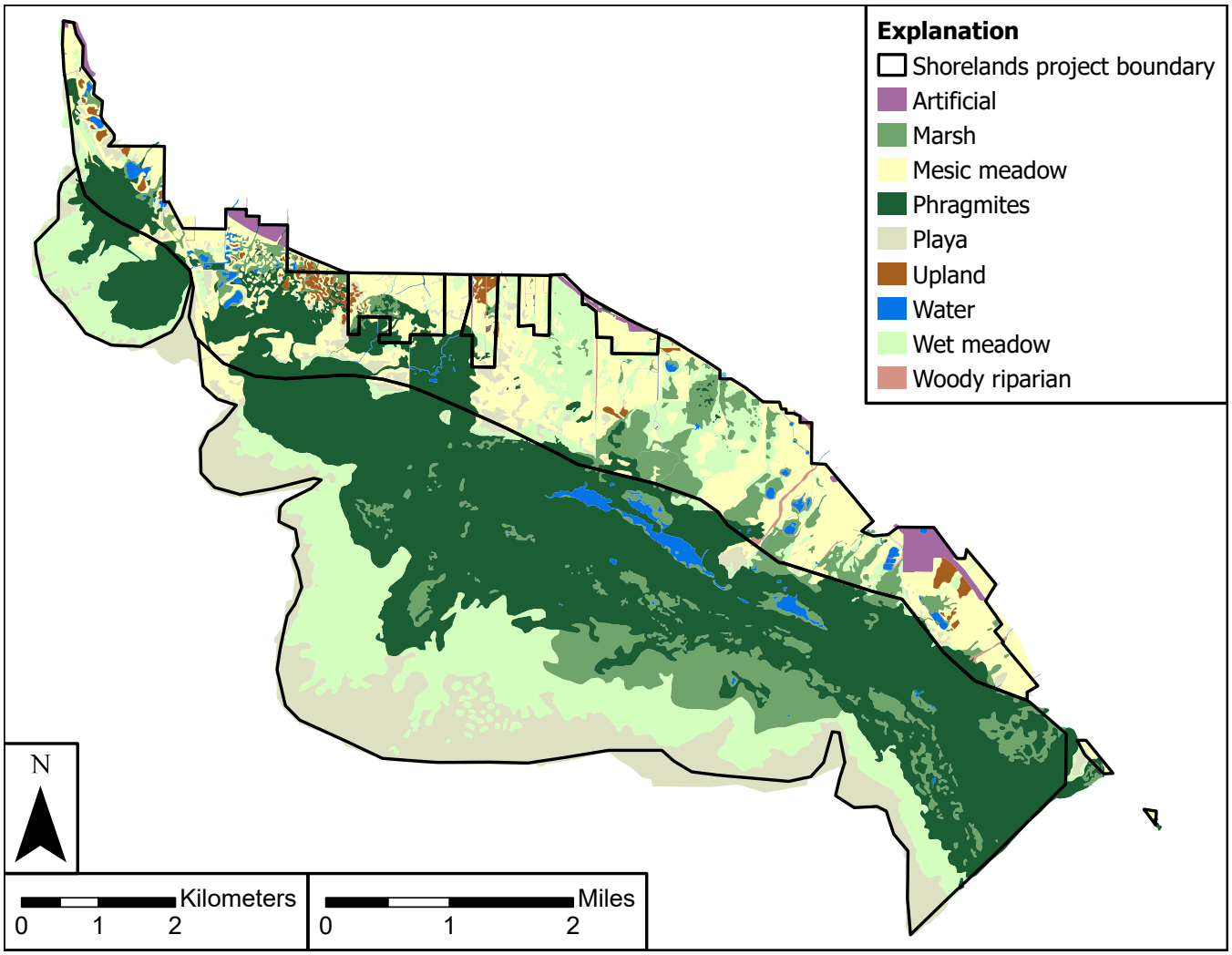

Figure 14. *Vegetation classes mapped using 2021 imagery.*

(Table A10). Woody Riparian was not mapped in the New Parcels component area and the other four classes of Playa, Marsh, Upland and Artificial each accounted for less than 10% of the New Parcels component area.

Vegetation class extents in the Outflow Area followed patterns similar to those in the overall study area (Table A10). Phragmites and Wet Meadow were the most extensively mapped vegetation classes but occupied a greater proportion of the Outflow Area than the study area as a whole. Subclasses mapped in these vegetation classes were primarily Dense Phragmites and Dense Saltgrass, accounting for 93% and 99% of their respective vegetation class extent. Vegetation classes uncommon across the study area were either absent (Artificial and Upland) or nearly absent (Woody Riparian) in the Outflow Area, and the Mesic Meadow class was nearly absent from the Outflow Area. Permanent water was mapped throughout the Outflow Area in proportions similar to the overall area.

We observed several areas in recent or historical imagery that appeared to have been treated to control invasive *Phragmites*. These treatment areas occurred throughout the study area but appeared concentrated in a few locations: along the southwestern and western boundaries of the Preserve, marshes along the boardwalk at the visitor's center, and near canal outflow areas. Most areas where treatments were observed were mapped as the Phragmites class, but roughly one-third of the treated areas had reverted to Marsh or Permanent Water classes. These reverted communities occurred at two locations within the study area: (1) along the boardwalk and (2) down-gradient of a series of newly constructed ponds. Of all the areas mapped as Phragmites, only a quarter appeared to have been treated; these treated Phragmites areas were similarly concentrated along the southwestern and western boundaries of the Preserve and canal outflow areas.

BROAD VEGETATION CHANGE

Introduction

We used data from three different NWI mapping projects and mapping data from this project to compare changes in land cover classes in the study area over time. The study area was mapped by NWI in 1981, 1997, and 2014, except for the far southeastern part of the Outflow Area, which was not mapped in 1997 and thus is excluded from this analysis. We created a new boundary file based on the area where the 1997 data was available and clipped each of the four layers by this new boundary (Figure 15).

Methods

We analyzed broad categories of cover across years because standards and methods for NWI mapping have changed and because of the high potential for variation in interpretation of small differences in water regimes across observers over time. Features were categorized as one of four types—water, shore, dry emergent, or wet emergent—following the rules found in Table A11. We calculated the area that each type occupied in each dataset within the Preserve, New Parcels, and Outflow Area. For each year, areas mapped as streambed, irrigated agriculture, woody wetland, or uplands by either NWI or the 2021 UGS vegetation map were categorized as "other" and not presented in the results for that respective year.

We found two indicators of potential issues with the mapping comparison. First, none of the area in the Preserve or the New Parcels was mapped as shore or water in the 1997 data. Because 1997 was a wet year around Great Salt Lake, it seems likely that differences in capturing these features may be due to different conventions or interpretations rather than a true lack of water in that year. Second, the amount of area mapped as wetland (instead of not mapped or mapped as upland) increased over time in the Preserve and New Parcels, which could be caused by differences in mapper interpretation. However, many of the areas that had this change from not mapped to mapped as wetland also show an increase in NDVI over a 30-year period, suggesting that the mapped changes may reflect true changes on the ground.

Results

Within the Preserve, both water and shore declined from 1981 to 1997 but are now back to levels slightly higher than in 1981 (Table A11; Figure 15). The size of ponds in the northern part of the Preserve has declined over time, but new ponds in the middle and, in particular, the southern part have more than made up for the difference in area. The amount of dry emergent vegetation has increased approximately linearly over time. Many areas now mapped as dry emergent around Kays Creek and south to the boundary of the Preserve were either mapped as wet emergent or, more commonly, not mapped in older NWI data. By 2020, the amount of wet emergent had declined to be just below the amount of dry emergent in the Preserve.

The greatest amounts of water, shore, dry emergent, and wet emergent in the New Parcels were in 2020 and the lowest amounts were in 1997, except that wet emergent was lowest in 2014. Water more than doubled, shore more than quadrupled, and dry emergent increased by 1.7 times from 1981 to 2020, whereas wet emergent only increased slightly.

The amount of water and shore in the Outflow Area decreased by 3 times and 3.6 times between 1981 and 2020, respectively, and was replaced primarily by wet emergent vegetation, which increased by 2.2 times (Table A11). The decrease in water has primarily been linear, whereas the largest drop in shore occurred between 1997 and 2014, with a small gain in shore from 2014 to 2020. Wet emergent vegetation has almost

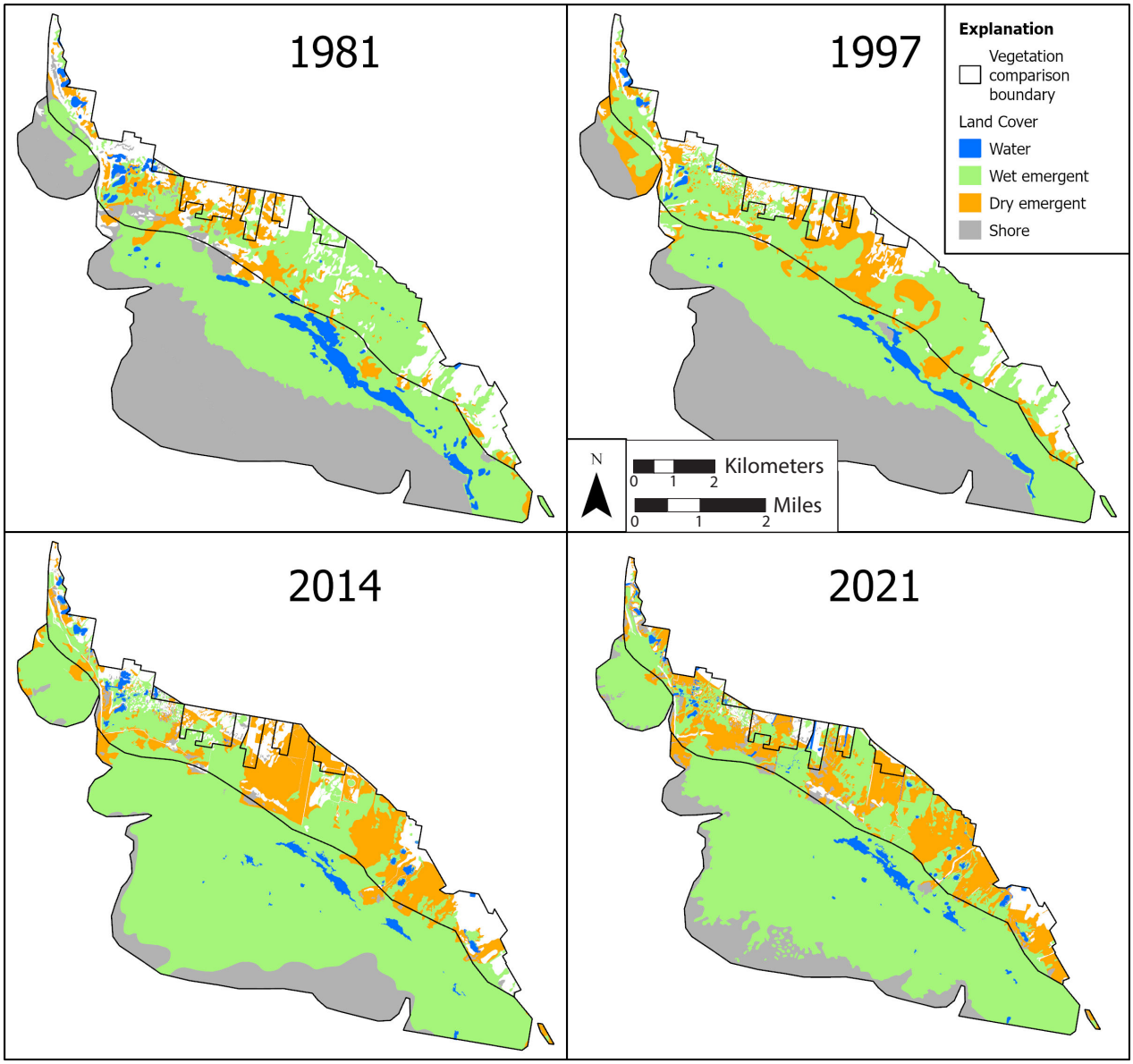

Figure 15. *Changes in the condensed National Wetland Inventory land cover classes over time.*

exactly the same but opposite pattern to the shore, with a large increase between 1997 and 2014 and a minor drop between 2014 and 2020.

NDVI ANALYSIS

Introduction

Normalized Difference Vegetation Index (NDVI) is a commonly used vegetation index derived from multispectral satellite data; values range from -1 to 1 and measure how green a pixel is (Pettorelli et al., 2005). NDVI has been used to identify vegetation types, quantify vegetation health and drought stress, and track vegetation trends over time (Wilson and Norman, 2018). Higher values indicate areas with denser, healthier vegetation, whereas bare areas have values near 0 and areas with standing water have values less than 0. Different vegetation classes also tend to have roughly different NDVI values. Increases in NDVI values over time can occur when bare or wet areas become vegetated, or when vegetation communities shift from those producing a lower NDVI value to those producing a higher NDVI value. Decreases happen when the opposite of the above occurs or when plants within a vegetation community become stressed or lose vigor due to water stress, grazing, or other disturbances.

Methods

Hydrology Units

Based on differences and changes in ownership and management we delineated the study area into hydrology units Preserve, New Parcel, and Outflow. We then subdivided the

components using HUC12 watershed boundaries (Figure 13). We then evaluated water inputs from streams, agricultural drains, storm drains, and flowing wells to further divide the units based on water source. This resulted in 20 hydrology units.

Vegetation Index

We assessed vegetation health and drought stress over time for mapped vegetation classes using a time series from 1992 to 2021 created in Google Earth Engine (Gorelick et al., 2017) with atmospherically corrected Landsat 5, 7, and 8 surface reflectance data. Annual median composites were generated for images taken between July 15th and August 31st, a period optimal for distinguishing vegetation classes and ensuring complete data coverage (Appendix B). We then calculated the median NDVI for each year for each hydrology unit using the following formula:

$$NDVI=(NIR-R)/(NIR+R) \quad (5)$$

where:

NIR = near infrared value

R = infrared value

To focus on vegetation trends, we clipped out areas mapped as the artificial and water classes in the 2021 UGS vegetation map. We also clipped out areas mapped as Woody Riparian because they made up a minute portion of the project area. We used the same data to create slope maps showing the change in NDVI over time in each 30-m pixel. We created a 30-year map depicting slopes for years 1992 to 2021 and a 10-year map depicting slopes for 2012 to 2021.

Model Explanatory Variables

Our analysis aimed to identify drivers of NDVI trends by modeling variables from four data types: climate, hydrology, land cover, and year. For climate, we used the Palmer Drought Severity Index (PDSI) derived from gridMET data (Abatzoglou, 2013), selecting summer mean PDSI due to its strong correlation with NDVI. For hydrology, we evaluated streamflow, groundwater, and lake-level data from USGS records. We modeled peak flow at two sites along the Weber River where records extended back at least 30 years. We chose a site upstream (near Oakley, Utah) and a site downstream (west of Mountain Green, Utah, named Gateway) of the reservoirs that are built along the river to account for human influence on streamflow. We also modeled for spring groundwater levels from a Kaysville well, and maximum annual GSL elevation at Saltair Boat Harbor, looking at their correlation with NDVI.

Land cover data was derived from the LCMAP dataset to calculate impervious surface area within a 5 km buffer of hydrology units, using annual data from Google Earth Engine (Zhu and Woodcock, 2014; Brown et al., 2020). We calculated Pearson correlation coefficients for seven potential explanatory variables (including year) and excluded year and groundwater level from the modeling due to high collinearity among several variables. Our final model included June-August mean PDSI, maximum GSL elevation, day of year (DOY) of the peak flow at Gateway, peak flow at Oakley, impervious surface area, year, and march groundwater level (Table A12), though we acknowledge challenges in interpreting results due to collinearity.

Statistical Analysis

We conducted Mann Kendall trend tests to assess the presence of statistically significant trends in NDVI over 30-year (1992 to 2021) and 10-year (2012 to 2021) time periods, for each hydrology unit.

We created linear regression models to analyze NDVI versus the selected explanatory variables for each hydrologic unit (Table A12), using both a 29-year (1992 to 2020) and a 9-year (2012 to 2020) time period. Impervious surface data was not available for 2021, so this year was not included in our models. Models were compared using corrected Akaike Information Criterion (AICc), with the best models selected based on the lowest AICc and reported alongside alternate models with AICc differences under 6.

For the 30-year and 10-year slope maps, we ran a Mann Kendall trend test on each pixel using code provided on the Google Earth Engine developers community page with minor adjustments to handle slopes between 1 and -1. We considered values of $p < 0.01$ as significant because of the large quantity of pixels in the study area.

Vegetation Community Comparison

We compared 2021 vegetation mapping to 2011 mapping by Long (2014) to understand vegetation changes but found significant methodological differences, such as scale and classification inconsistencies, that made quantifying changes unreliable. Key issues included mismatches in Mesic Grasslands classification, potential misidentification of Marsh versus Phragmites in 2011, and resolution differences likely exaggerating changes. Consequently, the 2011 mapping was used only as supporting information for interpreting remote sensing trends.

The 2011 mapping used UAV-collected high-resolution imagery but excluded some areas, limiting comparison to overlapping regions (96% of the study area). Both datasets were reclassified into six general categories for comparison (Table A13). To align resolutions, the 2011 mapping was downsampled to 20 meters, and the 2021 mapping was rasterized at the same scale. Combined rasters were converted to polygons, with sliver polygons under 400 square meters merged

to produce a dataset showing unique combinations of 2011 and 2021 vegetation mapping.

Evaluation of NDVI Slope Trends

We used the 10-year NDVI slope trend map and the 2011–2021 vegetation comparison to analyze significant trends in vegetation types, focusing on areas where the trends overlapped with the change map (21% of the study area). We examined vegetation change categories comprising at least 5% of the trend area, while considering classification uncertainties for Phragmites/Marsh and Upland/Wet Meadow. Additionally, we calculated the percentage of trend areas mapped as Phragmites in at least one year to better understand how Phragmites treatment or expansion may influence trend results.

To help understand the 30-year trends, we overlaid the 30-year NDVI pixel slope trend map and the UGS 2021 vegetation mapping. We summarized the trends by what is currently mapped as Phragmites and what is not. However, previous Phragmites treatments have occurred and some areas are no longer Phragmites. These areas are not included in the estimates due to the limits of the data.

Full methodology for our NDVI analysis is available in Appendix B.

Results

Mann Kendall Trends

Mann Kendall trends depended on the time period that was examined and on the geographic location in the study area. For the 30-year NDVI trends, seven hydrology units had a significantly increasing NDVI trend and one hydrology unit had a significantly decreasing NDVI trend ($p \leq 0.05$) (Figure 16). Most of the hydrology units in the Outflow Area had significant increasing trends whereas the majority of the hydrology units in the Preserve and New Parcels did not have a significant trend. The eastern and western Preserve units showed significant trends, whereas the center did not. The unit with a decreasing trend was New Middle 1, which contains 88% Mesic Meadow, 9% Wet Meadow, and 2% Phragmites (Table A14).

More than one-half of the study area had an increasing trend in NDVI based on analysis of the 30-year pixel slope map, with the increasing trends heavily concentrated in the Outflow Area (Figure 17). The Preserve, New Parcels, and Outflow Area had 28%, 24%, and 83% of their area with significant increasing trends in NDVI, respectively, whereas 12%, 16%, and 1% of the respective areas had decreasing trends. The rest of the study area did not have a significant trend.

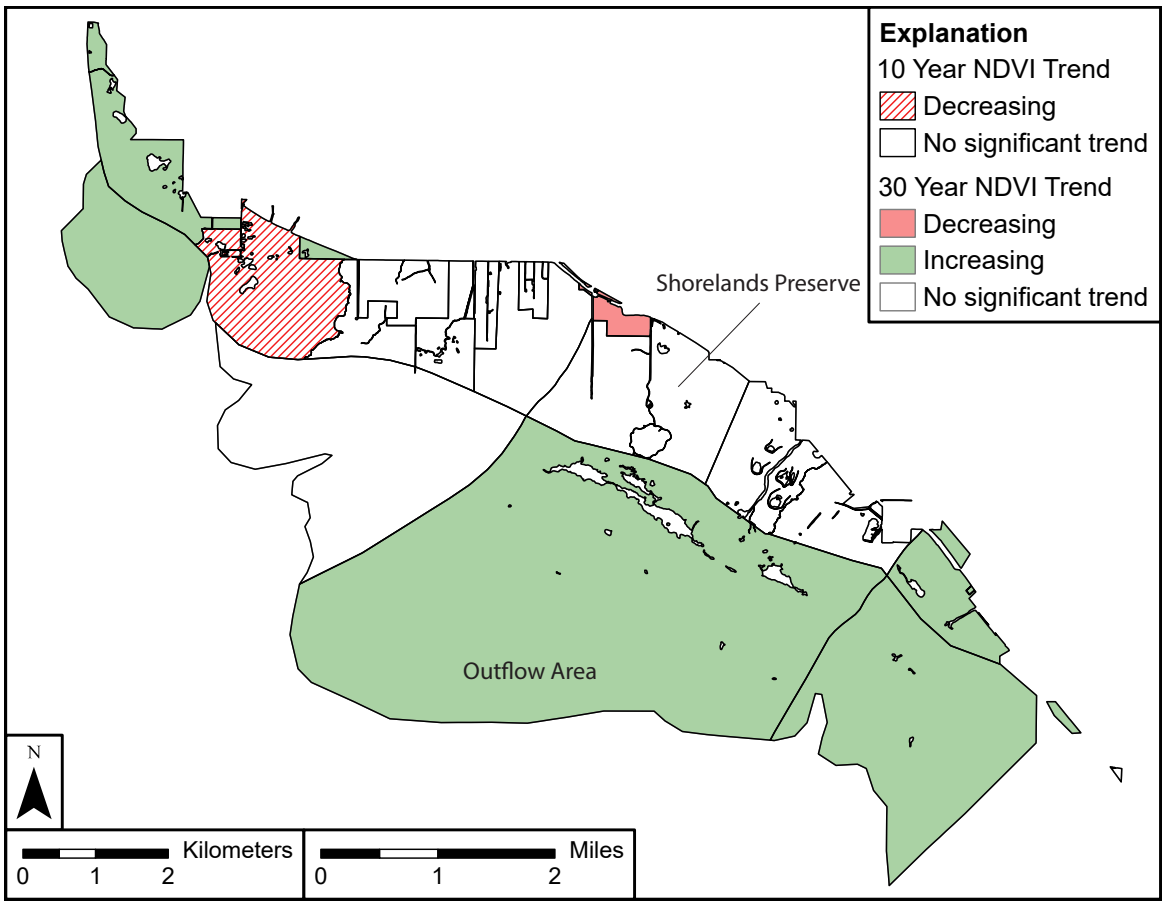

Figure 16. *Mann Kendall trend test results of NDVI by hydrology unit for the 1992–2021 and 2012–2021 time series.*

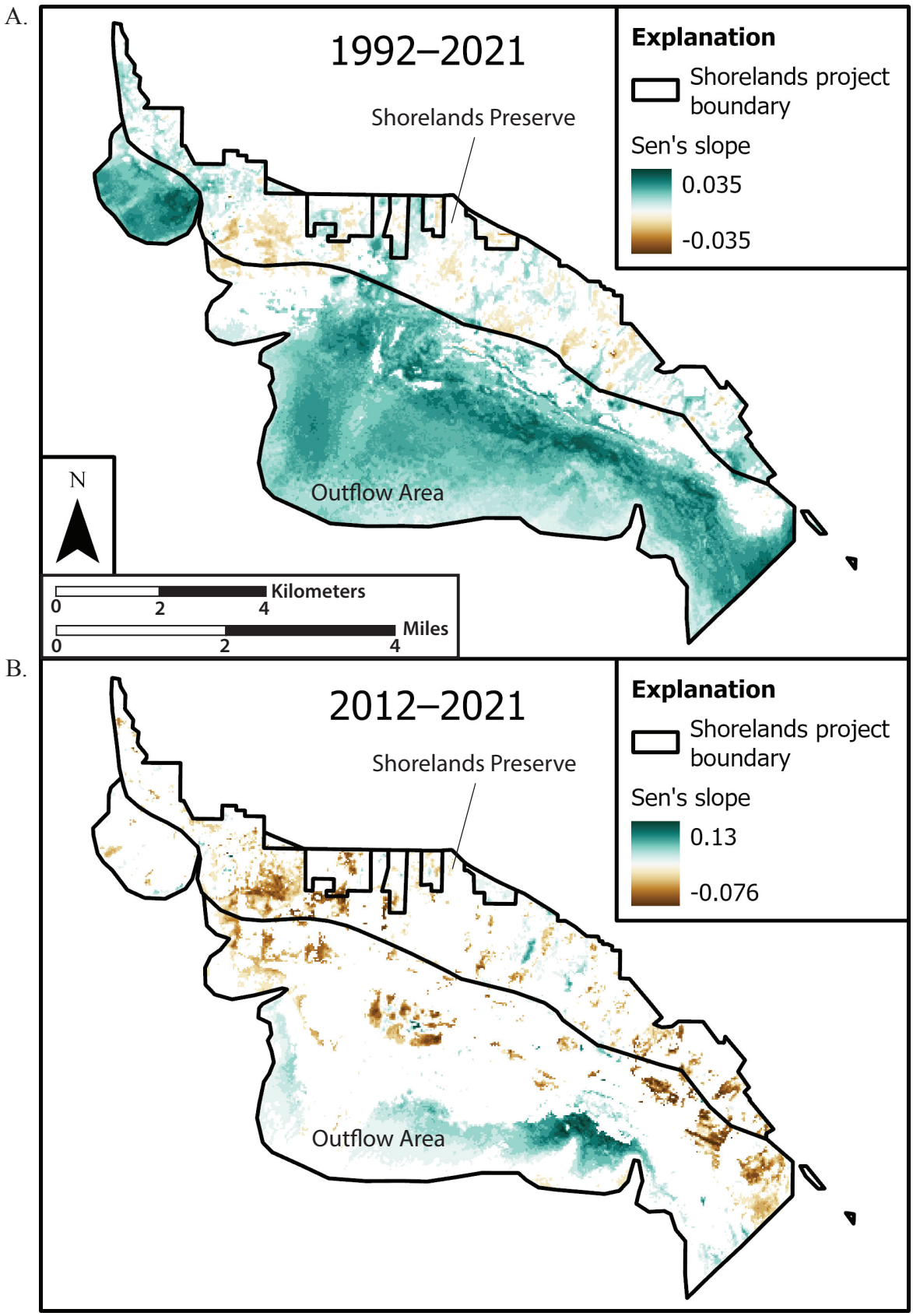

Figure 17. *Sen's slope of NDVI for each pixel in the study area for* ***A)*** *1992–2021 and* ***B)*** *2012–2021.*

One hydrology unit, Preserve West 2, had a decreasing trend in NDVI over the 10-year period (Figure 16). This unit contains approximately 44% Phragmites, 33% Mesic Meadow, 9% Marsh, 6% Playa, 4% Upland, and 3% Wet Meadow (Table A14). The rest of the units showed no significant trend over the 10-year period.

The 10-year pixel NDVI slope map shows that most of the study area pixels did not have a significant trend (Figure 17). The Preserve, New Parcels, and Outflow Area had 3%, 6%, and 14% of their areas with significant increasing trends in NDVI, respectively, whereas 16%, 15%, and 8% of the respective areas had decreasing trends.

Model Results

For the 29-year time period, all explanatory variables were present in models for at least some of the hydrology units (Tables A15 and A16). Summer PDSI was present in 17 of 19 hydrology unit models and always had a positive relationship with NDVI, whereas all other variables had a mix of positive and negative relationships depending on the unit. The next most common explanatory variable was impervious surface area which was present in 13 models. Impervious surface area had a positive relationship with NDVI in all unit models except two where it had a negative relationship. GSL elevation had a negative relationship with NDVI in all units in the Outflow Area, New West 2, New West 4, and Preserve Middle 1 and a positive relationship in the farthest west units in the Preserve and the farthest west New Parcel. Stream flow variables of Peak Flow at Oakley and DOY at Gateway were the least common in the models and were found in 3 and 4 models, respectively, typically in units on the west side of the study area. These two variables had both positive and negative relationships with NDVI.

The variation in NDVI that was explained by the models varied by unit and by the three main geographic components of the study area. Models for units in the Preserve had R^2 ranging from 0.18 to 0.48 except Preserve West 1, which had an R^2 of 0.66. New Parcel unit models had R^2 values ranging from 0.47 to 0.61 except New West 2, which had an R^2 of 0.29. Models for the Outflow Area units had the highest R^2 values ranging between 0.67 and 0.80.

For the 9-year time period, the majority of hydrology units did not have models with explanatory variables that were better than the null model (Tables A17 and A18). Three units had an explanatory variable in their top models, one from each study component area. The best model for New Middle 1 included GSL elevation, which had a negative relationship with NDVI. The best model for Preserve West 3 included impervious surface area which had a negative relationship. The best model for Outflow East 1 included summer PDSI which had a positive relationship. The R^2 values for all three units ranged between 0.41 and 0.50.

NDVI Slope Trends

Within the Preserve, six vegetation change categories were found in 5% or more of the area that had a significant 10-year decreasing NDVI trend, accounting for 57% of the area (Table A19). Four of these categories included Phragmites and the other two were Upland to Upland and Wet Meadow to Upland. Overall, 48% of the area mapped with decreasing trends and 25% of the area mapped with increasing trends had Phragmites in at least one of the two years (Table A20). For the 30-year trends, of increasing areas, 21% are currently mapped as Phragmites and of decreasing areas 27% are currently mapped as Phragmites (Table A20). Mesic Meadow is currently mapped as the vegetation class for 41% of the increasing 30-year trends and 39% of the decreasing 30-year trends.

Within the New Parcels, six vegetation change categories were found in 5% or more of the area that had a significant 10-year trend and account for 76% of the area (Table A21). The one category of increasing trends was Upland to Upland. Top decreasing trends were Upland to Upland, Phragmites to Upland, Wet Meadow to Upland, Wet Meadow to Wet Meadow, and Phragmites to Phragmites. Of the increasing trends, 19% are Phragmites related and of the decreasing trends, 30% are Phragmites related (Table A19). For the 30-year trends, of increasing areas, 20% are currently mapped as Phragmites and of decreasing areas, 8% are currently mapped as Phragmites (Table A19).

Within the Outflow Area, five vegetation change categories were found in 5% or more of the area that had significant 10-year trends, accounting for 75% of the area (Table A21). Top increasing trends include Playa to Wet Meadow, Marsh, or staying Playa and top decreasing trends include Phragmites to Phragmites and Marsh to Phragmites. Overall, 79% of the area having decreasing trends and 11% of the area having increasing trends were mapped as having Phragmites in at least one of the two years (Table A19). For the 30-year trends, 46% of increasing areas are currently mapped as Phragmites and 56% of decreasing areas are currently mapped as Phragmites (Table A20).

DISCUSSION

Water Budget

The combined standard uncertainty of about 12%–24% for the inflow and outflow estimates limits our ability to evaluate the suitability of this approach, the relative merits of outflow options A and B, and hydrologic processes within the Preserve. Inflows and outflows are balanced within uncertainty for both outflow options for water year 2022 and for the average values of water years 2022 and 2023 (Table 6). Inflows

exceed outflows by more than the combined standard uncertainty for water year 2023 for both outflow options (Table 6). During water year 2023, much of the surface water flow was likely taken up by re-filling impoundments and replenishing soil moisture.

Other observations in the water budget are less straightforward to explain. The surface water outflow estimate for water year 2022 using option B is 48% greater than that using option A. The main reason for this large difference is the high value of ET in the Outflow Area used to estimate the surface water outflow. The *Phragmites* may have consumed available soil moisture and groundwater storage to grow to its usual vigor despite the relatively low surface water inflow and precipitation.

Outflow option A underestimates surface water outflow based on observational evidence. In outflow option B, however, total outflows are greater in water year 2022 than in 2023, which does not make sense considering the differences in climate between the two years. One possible interpretation is that ET in the Outflow Area did not increase proportionally to precipitation and surface water outflow during water year 2023, therefore, more surface water than usual flowed through the *Phragmites* toward Farmington Bay. Alternatively, the OpenET ensemble model may not be well calibrated to *Phragmites australis*. A current UGS project in which we have installed an eddy-covariance flux station in a large *Phragmites* stand may result in a refined water use rate, leading to a more accurate water budget and evaluation of hydrologic processes.

Our water budget does not capture some important hydrologic processes that occur within the Preserve boundary, including surface water-groundwater exchange along streams and ditches, groundwater exchange with impoundments, soil moisture and infiltration of precipitation to the shallow unconfined aquifer, and dependence of vegetation on surface water versus shallow groundwater. Characterizing these processes would require a great deal of more focused work at select locations and, like some of the methods we used in this study, would require extrapolation to large areas.

Scope of Vegetation Change

Preserve and New Parcels

Over the 30-year analysis period, more of the Preserve showed an increasing vegetation trend than a decreasing trend, though more than one-half of the Preserve did not change significantly. The NWI analysis confirms this conclusion, showing that some of the wetter wetland types have declined whereas the drier wetland types and mesic areas have expanded. NDVI showed a net decrease of 16% in the study area in the 10-year-trend map, half of which does not seem to be related to *Phragmites* management. Some Wet Meadow and Uplands communities are declining in vigor. *Phragmites* is present in the Preserve, though it is less prominent than in the Outflow Area (Figure 14). The total amount of surface water in the Preserve is similar to that in the 1980s, due to construction of new ponds in its southern half (Table A10). The New Parcels showed similar trends to the Preserve so the two component areas are discussed together hereafter.

Outflow Area

The Outflow Area has changed significantly over time, with expansion of Phragmites, Marsh, and Wet Meadow communities onto the lakebed. Additionally, the amount of visible surface water in ponds in the Outflow Area has declined over time, likely due in part to filling in with sediment and vegetation (Mike Kolendrianos and Chris Brown, Preserve Managers, verbal communications during 2022 and 2023). The NDVI change maps and series of NWI maps all show the expansion of vegetation onto the formerly bare or mostly bare shore, largely within the last 30 years but continuing within the last 10 years as well.

Drivers of the Change

Modeled Variables

Of the variables modeled with NDVI values in the 29-year models, only summer PDSI consistently had an expected relationship with NDVI, with a positive relationship indicating higher NDVI in wetter years. The Outflow Area had a negative relationship between GSL elevation and NDVI with lower lake levels leading to higher NDVI values as water receded and vegetation established. GSL elevation also directly impacted some units in the Outflow Area that were flooded in early years but not later years which resulted in negative NDVI values changing to positive values. Positive relationships between GSL elevation and NDVI in some areas in the Preserve could reflect more overall water availability for both GSL and vegetation, however, this variable should be interpreted with caution because the GSL elevation and NDVI relationship may have a spurious correlation with the "year" effect.

Potential causal explanations for the relationship between other significant model variables were more difficult to parse out and sometimes defied explanation. This difficulty is in large part due to high correlation between the variables and other covariates that were not included in the model. For example, greater adjacent impervious surface area was associated with higher NDVI values in most models and was also highly correlated with GSL elevation and year. Although there are potential mechanisms where conversion of agriculture to development could lead to increased vegetation vigor in surrounding wetlands (i.e., potential decrease in adjacent groundwater extraction, changes in water delivery, more local runoff from pavement to adjacent parts of the Preserve), the strong correlation of impervious surface area with other explanatory

variables leads us to interpret this result with a strong dose of caution. Models for two of the New Parcel units, both directly adjacent to areas with agriculture land converted to development, showed a negative relationship between NDVI and impervious surface, but given the uncertainty of this variable, further work is needed to confirm whether vegetation vigor in the units has truly been affected by the conversion. Variables related to the Weber River primarily affected the western part of the study area, which is logical because irrigation water used in that part of the study area comes from reservoirs in the same watershed (Mike Kolendrianos and Chris Brown, Preserve Managers, verbal communications during 2022 and 2023). However, some units had the expected positive relationship with NDVI while others had unexpected negative relationships that are difficult to interpret.

Neither PDSI nor any of the other explanatory variables performed better than the null model for almost all units in the 9-year model, even though PDSI had such a consistent relationship in the 30-year models. Other factors may influence the amount of water that sites receive besides climate, such as water availability in upgradient reservoirs or movement of water by managers. Also, vegetation vigor may be more influenced by actions such as grazing or *Phragmites* treatment than by water availability.

The areas of change in the pixel NDVI slope maps did not correspond very well with the units we developed based on hydrology and management. Rather, much of the change occurred in more of a patchwork pattern, which may mean that the hydrology units used are an oversimplification of how water moves around the study area or that factors other than water movement are having a large influence on vegetation vigor. These findings could also reflect the fact that managers are able to make decisions about how to best allocate water; managers may choose to dry out one area in favor of increasing water supply for another area, when water supplies are limited. Future work could focus on modeling trends for smaller patches to see if those trends are better explained by the explanatory variables.

Preserve Drivers

Although climate affects the Preserve as shown by the presence of summer PDSI in models for all hydrology units, the lower R^2 values indicate other drivers besides our explanatory variables are influencing the Preserve (Table A17). Other potential drivers of these changes include pond construction, changes in irrigation location or quantity, changes in grazing management with ownership changes, upgradient development that may have removed water or diverted it to another location, *Phragmites* expansion, and *Phragmites* treatment. All of these potential drivers can be visually seen affecting parts of the Preserve in one or more areas in the available Google Earth Imagery. *Phragmites* is less common in the Preserve than in the Outflow Area (Figure 14), which may be due to the existence of fewer hospitable places for *Phragmites* in the Preserve. It is also likely easier to manage the *Phragmites* within the Preserve. Although *Phragmites* treatment or expansion seems to be the cause of some trends, more than half of the trends are not related to *Phragmites* changes (Table A19).

Some specific areas had notable vegetation change trends. For the 10-year trends, Preserve West 2 was the only unit with an overall trend (decreasing) (Figure 16). The 30-year and 10-year NDVI pixel slope maps of Preserve West 2 also showed decreasing trends (Figure 16). This unit had *Phragmites* treatments that largely contributed to that trend but other vegetation classes also showed decreasing trends in the pixel slope maps including Mesic Meadow, Marsh, and Playa. This unit may be receiving less irrigation and therefore drying. The farthest southern and farthest northwest areas of the Preserve show non-wetland to wetland trends in the NWI maps (Figure 15), corroborated by increasing trends on the 30-year pixel NDVI slope map (Figure 17). However, this change to wetland is hard to verify from the available Google Earth Imagery.

More than one-half of the Preserve has no significant trends in either the 30-year or the 10-year vegetation trends despite a pattern of declining GSL levels and declining groundwater levels during these time periods (Figure 17). This lack of change could be for various reasons. Some evidence in Google Earth Imagery shows changes in irrigation which could counterbalance drying trends. In other cases, conflicting changes may balance over time. For example, *Phragmites* may have invaded an area but then was treated, leading to NDVI values similar to pre-invasion values. Additionally, year-to-year climate differences were the largest driver of the explanatory variables in the 29-year models (Table A17). Lastly, wetland vegetation tends to be tolerant of fluctuating water levels (Downard et al., 2017) and that resilience may contribute to the lack of significant trends observed in the units located within the Preserve boundary; vegetation may decline in a drier year and then bounce back to full vigor in the next wet year.

Outflow Area Drivers

The increasing 30-year trends are likely driven mainly by change from no vegetation to vegetation and by change from water in ponds in the Outflow Area to vegetation. The 10-year trends are easier to explain. Looking at the overlap between the 10-year vegetation mapping comparison and areas with significant 10-year trends, 79% of the decreasing trends have a *Phragmites* connection (Table A19) indicating that the predominant cause of decreasing NDVI in the Outflow Area is connected to *Phragmites* decline, most likely because of treatment. Many of these areas of *Phragmites* decline overlap treatment spatial layers and also show visible signs of treatment.

Major 10-year trends not related to *Phragmites* are Playa to Wet Meadow increasing, Playa to Marsh increasing, and Playa to Playa increasing (Table A18). These trends are corroborated

by the NWI comparison (Figure 15) and further emphasize the expansion of multiple vegetation types, not only *Phragmites*, onto the Playa as lake levels have receded. The Playa to Playa with increasing trends are largely areas that were covered by water in 2011, or now have sparse vegetation that was not detected in 2011. GSL water levels and nearby groundwater levels have been steadily decreasing over the time period. Major drivers of this decrease include increased urban development, water diversions, and drought (Meng, 2019). These declining lake levels have allowed vegetation to establish in previously uninhabitable areas. Whereas lake level decline has changed the hydrology of this part of the study area, perennial water from the North Davis Sewer District wastewater treatment plant, stormwater runoff, and irrigation runoff have allowed for vegetation expansion onto the exposed playas (Utah Division of Water Quality, 2014). The high R^2 values for the 29-year time period further indicate that summer PDSI, impervious surface area, GSL elevation, and the Weber River variables may be important drivers in the Outflow Area, but the high values may also be due to the year effect and not the explanatory variables themselves.

Many decreasing NDVI trends in the pixel slope maps in the study area correspond to *Phragmites* treatment, as does the decreasing trend at the Preserve West 2 10-year trend (Figures 16 and 17). *Phragmites* appears to have been successfully removed in parts of the study area although multiple treatments were needed. This trend of removal is confirmed by NDVI slope graphs for individual pixels, Google Earth Imagery, and the 2021 UGS vegetation map (Figure 14).

Implications

Wildlife

Changes documented in this study could impact bird habitat at the Preserve in both positive and negative ways. Decreases in NDVI driven by *Phragmites* treatments may be positive because *Phragmites* is not a high-quality bird habitat (Kettenring et al., 2020), particularly if *Phragmites*-dense stands are replaced by other wetland vegetation. Conversely, decreases in NDVI caused by reduced plant cover could indicate a reduction in nesting habitat available for some species, for example several duck bill species (Bell, 2022). If this occurs due to decreased water inputs, foraging habitat could be reduced for some species. For example, the white-faced ibis, a Utah Species of Greatest Conservation Need commonly observed at the Preserve (The Nature Conservancy, 2023), feeds almost exclusively on shallowly flooded, rather than dry, fields and wetlands (Bray and Klebenow, 1988; Moulton et al., 2013). New impoundments or carefully planned water distribution schedules could increase this habitat at the time of year most advantageous to this species. Our work shows that different inflow source types (stream, storm drain, agricultural drain) peak at different times of the year and quantify the likely ranges of flow, indicating which sources would be most appropriate for timed shallow flooding to benefit the white-faced ibis. These changes could be measured by combining bird counts, NDVI analyses, and on-the-ground vegetation monitoring.

Future Conditions

Land management, rather than climate, hydrology, and land use changes, appears to play a large role in the vegetation patterns over the past ten years at the Preserve. As agricultural water sources have become less reliable or have disappeared in recent years, managers have found new water sources, such as the new Freeport Pond impoundment which is designed to create 40 to 50 acres of open water and wetland habitat. These types of projects, and the ability of managers to move water around where and (sometimes) when it is most beneficial to wildlife and habitat, have likely led to the increased area of ponds and emergent wetlands that we documented in this study. Furthermore, *Phragmites* management is likely easier within the Preserve than in the Outflow Area, both due to the relative accessibility and the importance of water management.

The Outflow Area is subject to less direct management than the Preserve. Some apparent consequences include 2.5 times more *Phragmites* cover in the Outflow Area than in the Preserve and a decreasing amount of ponded water over time. In the future, the Outflow Area may see continued expansion of vegetation onto the sparsely vegetated lakeshore as freshwater leaving the Preserve continues to flush salts out of the soil. Although the vegetation at the leading edge of this change may be the most salt-tolerant species including salt grass and alkali bulrush, *Phragmites* will likely spread to these areas over time. Continued efforts by state agencies and Preserve managers to control *Phragmites* will likely be implemented to reduce its presence along GSL's eastern shore.

SUMMARY AND CONCLUSIONS

Study Overview

The Great Salt Lake Shorelands Preserve provides critical wetland habitat along the eastern margin of Great Salt Lake, an area subject to rapid population growth and urbanization as well as the long-term effects of groundwater pumping and climate change. Changing water levels, flows, and water availability have affected the surface water and vegetation in the Preserve. Management over the past few decades has aimed to conserve the wetlands against these changes. Characterizing water and vegetation trends over time places the current conditions of the study area in a historical context, quantifies water available for future management changes, and identifies areas of concern. In this study we quantified the timing and total amounts of surface water inflows, the scope of vegetation change to date, and identified sensitive and resilient areas to potential future change.

Primary Conclusions

Our data provide detailed documentation of water inflows into one of the most significant wetland complexes along GSL's eastern shore. The data will help technical planning of future water and land management by quantifying the timing, amount, and locations of surface water inflows. This water can be used to benefit specific habitats and species of greatest concern, including providing specific types and timing of water availability (e.g., open water versus shallowly flooded marsh; spring versus fall, etc.). Other Wildlife Management Areas may benefit from our work by anticipating when their source waters peak and the magnitude of likely fluctuations.

Our water budget approach to this study included our direct measurements of surface flow and groundwater levels, and estimates of precipitation and evapotranspiration from remote sources. Each of these measurements has its own characteristic uncertainty, and we represent the overall uncertainty of the water budget using the combined standard uncertainty. The combined standard uncertainties of the individual inflow and outflow estimates for water years 2022 and 2023 and the averages of those two years, including both outflow options (methods of calculating surface water outflow) range from 12% to 24%. The combined standard uncertainties of the total water budgets using outflow option A and option B are 12% and 15%, respectively.

Although the uncertainty limits our ability to evaluate hydrologic processes and the relative merits of our method, we can draw several important conclusions. First, the fact that our water budgets balance within uncertainty (except for water year 2023, for which greater inflows than outflows can be explained by replenishing soil moisture and reservoir volume) suggests that this approach is valid, and can be refined as our understanding of *Phragmites* water use improves and by including additional measurements. A more comprehensive water budget would include soil moisture, impoundment volumes, detailed seepage runs along the major streams paired with piezometers, and better spatial coverage of groundwater level.

Second, the fact that the water budget can be balanced within uncertainty by assuming that the *Phragmites* in the Outflow Area consumes effectively all the surface water and shallow groundwater outflow from the Preserve indicates that this invasive plant consumes a very significant amount of water that could otherwise support more beneficial habitat as well as potentially supporting GSL levels. Our vegetation change, NDVI analyses, and driver variable modeling collectively suggest that *Phragmites* treatment can produce measurable changes in the overall vegetation composition of this area, lending support to current efforts for large-scale treatments.

Statistical analysis and modeling of NDVI trends identifies the most important causes of vegetation changes in the Preserve and Outflow Area, although the presence of multiple correlations among variables prevents definitive interpretations. Summer PDSI, GSL levels, impermeable surface area in adjacent land, and management practices appear to have measurable effects on vegetation over time. Impoundments and *Phragmites* treatments can offset potential drying from drought. Vegetation expanded dramatically onto the GSL playa as lake levels and groundwater levels declined.

Water Budget Summary

This study estimated a water budget to characterize and quantify surface water, groundwater, evapotranspiration, and precipitation contributions, and their interactions with the current vegetation. Through continuous monitoring, discrete data collection, and seasonal flow runs, we attempted to quantify the different components of the water budget equation and assess the implications for water availability, wetland dynamics, and the overall ecological health of the Preserve.

The boundary of the water budget calculation was the Preserve property to a depth of 20 feet. We used our flow run measurements, extrapolated to time periods having characteristic flow regimes, to estimate total annual surface water inflows and outflows. We substituted the results of our continuous monitoring of Kays Creek inflow for the extrapolated flow run result. We estimated annual precipitation using gridmet and annual ET using OpenET. We estimated surface water outflow using two approaches. In outflow option A, we did not attempt to measure dispersed flow observed along the southern boundary of the preserve. In outflow option B, we used ET in the Outflow Area adjacent to and southwest of the Preserve as a proxy for surface water outflow.

Citing the average values of water years 2022 and 2023, inflow of water totaled about 27,450 acre-feet including precipitation (6600 acre-feet, 24% of total inflows), surface flow in streams and drains (17,000 acre-feet, 62%), groundwater flow within and into the shallow unconfined aquifer (3800 acre-feet, 14%) and flow from artesian wells (less than 1%). Outflows totaled about 23,000 acre-feet, including ET within the boundary (12,000 acre-feet, 56%), surface flow through the Preserve's southwestern boundary into the Outflow Area (8900 acre-feet, 42% using outflow option A or 12,600 acre-feet, 51% using outflow option B) and groundwater flow (400 acre-feet, 2%). Significant uncertainties exist in the surface-water outflow estimate, where our manual measurements underestimate outflows due to the presence of non-channelized flow, and the ET of the Outflow Area reflects water inputs from precipitation and shallow groundwater as well as surface flow. Groundwater flow estimates are highly generalized.

Vegetation Analysis

This study provides baseline vegetation mapping data and remote sensing methods that can be used for future comparison

of conditions at the Preserve and to evaluate the effectiveness of future water management practices. Although most of the Preserve appears to have stable vegetation vigor over the past ten years, about 8% of its area showed decreasing NDVI trends that were not associated with *Phragmites* and thus unlikely to be related to intentional *Phragmites* treatment efforts. These decreasing trends were typically associated with areas currently mapped as Upland and were particularly abundant in some small patches. Repeated trend analysis every five to ten years may be helpful for monitoring whether these locations continue to decline or whether new hot spots of change appear. This analysis, if paired with updated vegetation mapping, can be used to differentiate between wetland loss, which may be difficult to reverse, versus areas with declining vegetation vigor, which may be more amenable to management actions.

Implications for Management

Our hydrologic data could be used by the Preserve management to schedule filling and draining of impoundments and routing of water through ditches based on comparing the timing of inflows in different parts of the Preserve with habitat needs such as migratory bird occupation, planning the size of new impoundments, or planning and estimating recharge of the shallow unconfined aquifer. Because The Nature Conservancy owns the water rights to the artesian wells, these rights could be aggregated and new flowing wells installed that sustain local habitat or dilute surface inflows having poor water quality.

We can anticipate more drought years in the future in which the *Phragmites* in the Shorelands Preserve and Outflow Area will consume effectively all the surface water outflow if the present vegetation coverage and water management practices remain in place. Impounding this water before it reaches the Outflow Area *Phragmites*, channelizing it through the *Phragmites* so that it reaches Farmington Bay, and an all-out effort to reduce the *Phragmites* coverage are potential options to put this water to better effect.

The Great Salt Lake Shorelands Preserve and the Public Shooting Grounds Waterfowl Management Area in Bear River Bay (Figure 1) are the least extensively impounded wetlands preserves along Great Salt Lake's eastern margin on public land (B. Downard, verbal communication, 2023). Other preserves have greater volumes of impounded water and, therefore, different water and vegetation coverages and more infrastructure for routing water. Inflows and outflows at other sites are likely better controlled and channelized, but also more numerous. Direct evaporation from open water is likely a significantly greater component of water outflow. Constructing water budgets at these preserves would involve more detailed tracking of water routing, explicitly accounting for both surface water evaporation, and intentional draining and filling of impoundments.

Although management efforts are very important for maintaining conditions at the Preserve, managers may be limited in obtaining water in the face of severe ongoing drought or increased curtailment of irrigation water. Managers will need to continue to find creative solutions to maintain the health and presence of native vegetation communities.

ACKNOWLEDGMENTS

This work was supported by two Utah Division of Forestry, Fire and State Lands Technical Team grants; we are very grateful for their support. We thank Ann Neville (The Nature Conservancy), Stefan Kirby (UGS), Janice Gardner (Sageland Collaborative LLC), and Becka Downard (UGS) for helping us scope, propose, and initiate this project. We thank The Nature Conservancy Shoreland Preserve managers Mike Kolendrianos and Chris Brown for tours and a wealth of information as we started the project, and for constant support throughout. The scope of the project took a very positive unexpected turn when Megan Dovick, Program Director of the University of Utah's Professional Master of Science and Technology program, proposed that we work with their Environmental Sciences class, and we are happy to continue that partnership.

REFERENCES

Abatzoglou, J.T., 2013, Development of gridded surface meteorological data for ecological applications and modeling: International Journal of Climatology, v. 33, no. 1, https://doi.org/10.1002/joc.3413.

Allen, R.G., Pereira, L.S., Raes, D., and Smith, M., 1998, Crop evapotranspiration—guidelines for computing crop water requirements: FAO Irrigation and drainage paper 56, FAO, Rome, p. 300.

Alley, W.M., 1984, The Palmer drought severity index—limitations and assumptions: Journal of Applied Meteorology and Climatology, v. 23, no. 7, p. 1100–1109.

Anderson, P.B., Susong, D.D., Wold, S.R., Heilweil, V.M., and Baskin, R.L., 1994, Hydrogeology of recharge areas and water quality of the principal aquifers along the Wasatch Front and adjacent areas, Utah: U.S. Geological Survey Water-Resources Investigation Report 93-4221, 74 p.

Barton, K., and Barton, M.K., 2015, Package 'mumin', v. 1, no. 18, p. 439.

Bell, M.E., 2022, Nest-site selection, success, and response to predation by cinnamon teal and other ground-nesting ducks in the wetlands of Great Salt Lake, Utah: Logan, Utah State University, Ph.D. dissertation, 186 p.

Bowen, G., 2023, Water isotopes data products: Waterisotopes.org, https://wateriso.utah.edu/waterisotopes/index.html, accessed September 2023.

Bray, M.P., and Klebenow, D.A., 1988, Feeding ecology of white-faced ibises in a Great Basin Valley, USA: Colonial Waterbirds, v. 11, no. 1, p. 24–31.

Bright, B.J., Welch, A.H., and Knochenmus, L.A., 2007, Water resources of the Basin and Range carbonate-rock aquifer system, White Pine County, Nevada, and adjacent areas in Nevada and Utah: U.S. Geological Survey Scientific Investigations Report 2007-5261, 96 p., 4 plates, 1 appendix, https://pubs.usgs.gov/sir/2007/5261/.

Brown, J.F., Tollerud, H.J., Barber, C.P., Zhou, Q., Dwyer, J.L., Vogelmann, J.E., Loveland, T.R., Woodcock, C.E., Stehman, S.V., Zhu, Z., Pengra, B.W., Smith, K., Horton, J.A., Xian, G., Auch, R.F., Sohl, T.L., Sayler, K.L., Gallant, A.L., Zelenak, D., Reker, R.R., and Rover, J., 2020, Lessons learned implementing an operational continuous United States national land change monitoring capability—The Land Change Monitoring, Assessment, and Projection (LCMAP) approach: Remote Sensing of Environment, v. 238, no. 111356, https://doi.org/10.1016/j.rse.2019.111356.

Clark, I.D., and Fritz, P.F., 1997, Environmental isotopes in hydrogeology: Boca Raton, CRC Press, 342 p.

Clyde, C.G., Duffy, C.J., Fisk, E.P., Hoggan, D.H., and Hansen, D.E., 1984, Management of groundwater recharge areas in the mouth of Weber Canyon: Utah Water Research Laboratory Hydraulics and Hydrology Series UWRL/H-84/01, 101 p.

Dahl, T.E., Dick, J., Swords, J., and Wilen, B., 2020, Data collection requirements and procedures for mapping wetland, deepwater and related habitats of the United States (version 3): Madison, Wisconsin, U.S. Fish and Wildlife Service Division of Habitat and Resource Conservation, National Standards and Support Team, 91 p.

Desert Research Institute, 2024, West wide drought tracker: https://wrcc.dri.edu/wwdt/time/, accessed October 2024.

Downard, R., Frank, M., Perkins, J., Kettenring, K. and Larese-Casanova, M., 2017, Wetland plants of Great Salt Lake—a guide to identification, communities, & bird habitat: Logan, Utah State University Extension, 221 p.

Downard, B., 2024, Great Salt Lake wetland vegetation and what it tells us about environmental gradients and disturbance, *in* Vanden Berg, M., editor, Great Salt Lake and the Bonneville Basin—Geologic history and Anthropocene issues: Utah Geological Association Publication 51, 25 p., https://doi.org/10.31711/ugap.v51i.140.

De Cicco, L.A., Lorenz D., Hirsch R.M., Watkins W., Johnson M., 2022, dataRetrieval—R packages for discovering and retrieving water data available from U.S. federal hydrologic web services, v.2.7.11 https://code.usgs.gov/water/dataRetrieval.Duffield, D.M., 2023, Representative properties of hydraulic values: Online, http://www.aqtesolv.com/aquifer-tests/aquifer_properties.htm, accessed September 2023.

Ducks Unlimited, 2007, Great Salt Lake wetlands assessment project—vegetation classification and mapping: Online, https://www.ducks.org/utah/utah-conservation-projects/ut-great-salt-lake-wetlands-assessment-project, accessed March 2021.

Feth, J.H., Barker, D.A., Moore, L.G., Brown, R.J., and Veirs, C.E., 1966, Lake Bonneville—geology and hydrology of the Weber Delta district, including Ogden, Utah: U.S. Geological Survey Professional Paper 518, 76 p.

Fetter, C.H., 2001, Applied hydrogeology 4th edition: Upper Saddle River, New Jersey, Prentice Hall, 612 p.

Fox J., and Weisberg S., 2019, An R companion to applied regression, 3rd edition: Thousand Oaks, California, Sage, https://us.sagepub.com/en-us/nam/an-r-companion-to-applied-regression/book246125.

Friedman, I., Smith, G.I., Johnson, C.A., and Moscti, R.J., 2002, Stable isotope compositions of waters in the Great Basin, United States: Journal of Geophysical Research, v. 107, no. D19, 22 p., https://doi.org/10.1029/2001JD000566.

Gates, J.S., 1995, Description and quantification of the ground-water basins of the Wasatch Front, Utah, 1904–1994, *in* Lund, W.R., editor, Environmental and engineering geology of the Wasatch Front Region: Utah Geological Association Publication 24, p. 221–248.

Goodwin, P., and Molinari, R., 2022, Cache Valley wetland mapping—supplemental report: Utah Geological Survey Open File Report 744, 28 p., 2 appendices, https://doi.org/10.34191/OFR-744.

Gorelick, N., Hancher, M., Dixon, M., Ilyushchenko, S., Thau, D., and Moore, R., 2017, Google Earth Engine—Planetary-scale geospatial analysis for everyone: Remote Sensing of Environment, v. 202, p. 18–27.

Great Salt Lake Strike Team, 2023: Policy assessment—Data and insights summary: Online, https://gardner.utah.edu/wp-content/uploads/GSL-Assessment-Feb2023.pdf?x71849, accessed July 2023.

gridMET, 2023, Online: https://www.climatologylab.org/gridmet.html, accessed multiple times during 2023.

HDR Engineering, 2021, Annual hydrology monitoring report—2020: Unpublished report for Utah Department of Transportation, Project No. S-0067(14)0.

HDR Engineering, 2022, Annual Hydrology Monitoring Report—2021: Unpublished report for Utah Department of Transportation Project No. S-0067(14)0.

HDR Engineering, 2023, Annual Hydrology Monitoring Report—2022: Unpublished report for Utah Department of Transportation Project No. S-0067(14)0.

HDR Engineering, 2024, Annual Hydrology Monitoring Report—2023: Unpublished report for Utah Department of Transportation Project No. S-0067(14)0.

JCGM (Joint Committee for Guides in Meteorology), 2008, Evaluation of measurement data—Guide to the

expression of uncertainty in measurement: Online, https://www.bipm.org/documents/20126/2071204/JCGM_100_2008_E.pdf/cb0ef43f-baa5-11cf-3f85-4dcd86f77bd6.

Jensen, M.E., Burman, R.D., and Allen, R.G., 1990, Evapotranspiration and irrigation water requirements—ASCE manuals and reports on engineering practice No. 70: American Society of Civil Engineers, Reston, Virginia, pages 332 p.

Kettenring, K.M., Cranney, C.R., Downard, R., Hambrecht, K.R., Tarsa, E.E., Menuz, D.R. and Rohal, C.B., 2020, Invasive plants of Great Salt Lake wetlands—What, where, when, how, and why?, *in* Baxter, B.K., and Butler, J.K., editors, Great Salt Lake Biology—A terminal lake in a time of change: Cham, Switzerland, Springer Nature, p. 397–434.

Long, A.L., 2014, Distribution and drivers of a widespread, invasive wetland grass, *Phragmites australis*, in Great Salt Lake wetlands: Logan, Utah State University, M.S. thesis, 42 p.

McKean, A., and Hylland, M.D., 2019, Geologic map of the Baileys Lake quadrangle, Salt Lake and Davis Counties, Utah: Utah Geological Survey Map 281, 28 p., 2 plates, scale 1:24,000, https://doi.org/10.34191/M-281DM.

Melton, F.S., Huntington, J., Grimm, R., Herring, J., Hall, M., Rollison, D., Erickson, T., Allen, R., Anderson, M., Fisher, J.B., and Kilic, A., 2022, OpenET—Filling a critical data gap in water management for the western United States: Journal of the American Water Resources Association, v. 58, no. 6, p. 971–994.

Meng, Q., 2019, Climate change and extreme weather drive the declines of saline lakes—a showcase of the Great Salt Lake: Climate, v. 7, no. 2, p. 19.

Monteith, J.L., and Unsworth, M.H., 2013, Principles of environmental physics: Waltham, Massachusetts, Academic Press, 401 p.

Moulton, C., Carlisle, J., Brennar, K., and Cavallaro, R., 2013, Assessment of foraging habitats of white-faced ibis near two important breeding colonies in eastern Idaho: Idaho Department of Fish and Game and Idaho Bird Observatory, 30 p.

Natural Resources Conservation Service, 2021, Web soil survey, interactive soil and ecological site description maps: Online, https://websoilsurvey.sc.egov.usda.gov/App/WebSoilSurvey.aspx, accessed March 2021.

Oviatt, C.G., 2014, The Gilbert episode in the Great Salt Lake basin, Utah: Utah Geological Survey Miscellaneous Publication 14-3, 20 p., https://doi.org/10.34191/MP-14-3.

Oviatt, C.G., Young, D.C., and Duke, D., 2024, The Currey cycle of Great Salt Lake: an early Younger Dryas lake in the Bonneville basin, Utah, USA: Journal of Quaternary Science, p. 1-14, DOI: 10.1002/jqs.3644

Patakamuri, S.K., O'Brien, N., and Patakamuri, M.S.K., 2020, Package 'modifiedmk': Cran. R-project, https://cran.r-project.org/web/packages/modifiedmk/index.html.

Pettorelli, N., Vik, J.O., Mysterud, A., Gaillard, J.M., Tucker, C.J., and Stenseth, N.C., 2005, Using the satellite-derived NDVI to assess ecological responses to environmental change: Trends in Ecology & Evolution, v. 20, no. 9, p. 503–510.

Roberts, A.J., 2013, Avian diets in a saline ecosystem—Great Salt Lake, Utah, USA: Human-Wildlife Interactions, v. 7, no. 1, p. 158–168.

Roderick, M.L., Farquhar, G.D., and Hobbins, M.T., 2019, Maximizing agricultural water use efficiency entails trade-offs: Trends in Plant Science, v. 24, no. 11, p. 975–987.

Sack, D., 2005, Geologic map of the Clearfield 7.5′ quadrangle, Davis County, Utah: Utah Geological Survey Miscellaneous Publication 05-4, 14 p., 2 plates, scale 1:24,000, https://doi.org/10.34191/MP-05-4.

Solomon, B.J., 2007, Surficial geologic map of part of the Kaysville quadrangle, Davis County, Utah: Utah Geological Survey Map M-224, 2 plates, scale 1:24,00, https://doi.org/10.34191/M-224.

Smith, J., Laczniak, R., Moreo, M., and Welborn, T., 2007, Mapping evapotranspiration units in the Basin and Range carbonate-rock aquifer system, White Pine County, Nevada, and adjacent areas in Nevada and Utah: U.S. Geological Survey Scientific Investigations Report 2007-5087, 20 p., https://doi.org/10.3133/sir20075087.

Taylor, C.J., and Alley, W.M., 2013, Ground-water-level monitoring and the importance of long-term water-level data: U.S. Geological Survey Circular 1217, 68 p., https://doi.org/10.3133/cir1217.

The Nature Conservancy, 2023, Great Salt Lake Shorelands Preserve: Online, www.nature.org/en-us/get-involved/how-to-help/places-we-protect/the-great-salt-lake-shorelands-preserve/, accessed many times during summer 2023.

Thiros, S.A., 1995, Chemical composition of ground water, hydrologic properties of basin-fill material, and ground-water movement in Salt Lake Valley, Utah: Utah Department of Natural Resources Technical Publication No. 110-A, 59 p.

Utah Climate Center, 2024, Surface weather and climate observations, GSOD network, station ID 725755: Online, https://climate.usu.edu/, accessed October 2024.

Utah Division of Forestry, Fire and State Lands, 2013, Final Great Salt Lake comprehensive management plan and record of decision: Online, https://ffsl.utah.gov/wp-content/uploads/OnlineGSL-CMPandROD-March2013.pdf.

Utah Division of Water Quality, 2014, 2013 Great Salt Lake fringe wetland survey: Online, https://lf-public.deq.utah.gov/WebLink/Electronic-File.aspx?docid=15307&eqdocs=DWQ-2014-019440&dbid=0&repo=Public.

U.S. Census Bureau, 2023, Quickfacts—Davis County, Utah, www.census.gov/quickfacts/fact/table/daviscountyutah, accessed October 2023.

U.S. Geological Survey, 2024, National water information system: Online, https://maps.waterdata.usgs.gov/mapper/, accessed October 2024.

Wilson, N.R., and Norman, L.M., 2018, Analysis of vegetation recovery surrounding a restored wetland using the normalized difference infrared index (NDII) and normalized difference vegetation index (NDVI): International Journal of Remote Sensing, v. 39, no. 10, p. 3243–3274.

Zamora, H.A., and Inkenbrandt, P.C., 2024, Estimate of groundwater flow and salinity contribution to Great Salt Lake using groundwater levels and spatial analysis, *in* Vanden Berg, M., editor, Great Salt Lake and the Bonneville Basin—Geologic history and Anthropocene issues: Utah Geological Association Publication 51, 24 p.

Zhu, Z., and Woodcock, C.E., 2014, Continuous change detection and classification of land cover using all available Landsat data: Remote Sensing of Environment, v. 144, p. 152–171, https://doi.org/10.1016/j.rse.2014.01.011.

APPENDICES

APPENDIX A: DATA TABLES

Table A1. *Flow rate data from flowing wells.*

Date	Site ID	Flow (gpm)	Flow (cfs)	Error	Mean Flow (cfs)	Standard Deviation	Total Annual Volume (cf)	Total Annual Volume (acre-feet)
11/15/22	FW-1	0.00	0.000	0%				
7/21/21	FW-10	2.08	0.005				18,977.59	
9/7/21	FW-10	2.08	0.005				2372.20	
9/13/21	FW-10	2.08	0.005				17,396.12	
10/27/21	FW-10	2.08	0.005				77,664.79	
4/27/22	FW-10	2.41	0.005	2%			46,653.24	
8/23/22	FW-10	1.75	0.004	3%			30,576.27	
11/15/22	FW-10	2.08	0.005		0.0046	0.001		4.45
7/21/21	FW-11	5.14	0.011				46,926.95	
9/7/21	FW-11	5.14	0.011				5865.87	
9/13/21	FW-11	5.14	0.011				43,016.37	
10/27/21	FW-11	5.14	0.011				176,316.94	
4/27/22	FW-11	5.05	0.011	4%			117,193.82	
8/23/22	FW-11	5.40	0.012	8%			82,867.28	
11/15/22	FW-11	4.98	0.011	3%	0.0113	0.0005		10.84
7/21/21	FW-2	2.70	0.006	7%			24,360.65	
9/7/21	FW-2	2.64	0.006	4%			3010.87	
9/13/21	FW-2	2.64	0.006	2%			22,079.69	
10/27/21	FW-2	2.64	0.006	1%			56,389.13	
4/27/22	FW-2	0.62	0.001	1%			13,457.66	
8/23/22	FW-2	0.58	0.001	1%			8781.70	2.94
11/15/22	FW-2	0.52	0.001	2%	0.0039	0.0024		
7/21/21	FW-3	1.78	0.004	6%			28,813.28	
9/30/21	FW-3	2.49	0.006	6%			11,803.97	
10/27/21	FW-3	2.11	0.005	2%			81,124.24	
4/27/22	FW-3	2.58	0.006	2%			48,335.44	
8/23/22	FW-3	1.73	0.004	1%			26,584.59	4.51
11/15/22	FW-3	1.60	0.004	5%	0.0045	0.0009		
7/21/21	FW-4	3.54	0.008				32,958.73	
9/13/21	FW-4	2.88	0.006	2%			23,961.48	
10/27/21	FW-4	2.85	0.006	2%			120,389.07	
4/27/22	FW-4	4.11	0.009	2%			90,614.94	
8/23/22	FW-4	3.97	0.009	3%			63,577.01	
11/16/22	FW-4	3.90	0.009	1%	0.0078	0.0014		7.61
7/21/21	FW-6	9.40	0.021				85,764.10	
9/7/21	FW-6	9.40	0.021				10,720.51	
9/13/21	FW-6	9.40	0.021				78,617.09	
10/27/21	FW-6	9.40	0.021				343,005.06	
4/27/22	FW-6	10.43	0.023	4%			217,453.42	
8/23/22	FW-6	8.96	0.020	9%			141,864.31	
11/15/22	FW-6	8.81	0.019	5%	0.0207	0.002		20.14
7/21/21	FW-7	0.25	0.001				2235.34	
9/7/21	FW-7	0.25	0.001				279.42	
9/13/21	FW-7	0.25	0.001				2049.06	
10/27/21	FW-7	0.25	0.001				12,713.50	
4/27/22	FW-7	0.49	0.001	1%			9407.06	
11/15/22	FW-7	0.00	0.000	0%	0.0005	0.0008		0.61
7/21/21	FW-8	2.72	0.006				32,238.09	
9/30/21	FW-8	2.06	0.005	5%			10,592.66	
10/27/21	FW-8	2.07	0.005	3%			88,389.10	
4/27/22	FW-8	3.04	0.007	3%			69,531.26	
8/23/22	FW-8	3.16	0.007	2%			51,333.00	
11/15/22	FW-8	3.27	0.007	2%	0.0060	0.0013		5.79
7/21/21	FW-9	12.79	0.028				195,808.82	
9/30/21	FW-9	16.23	0.036	5%			69,643.41	
10/27/21	FW-9	10.91	0.024	6%			442,118.48	
4/27/22	FW-9	14.65	0.032	4%			337,338.78	
8/23/22	FW-9	15.43	0.034	6%			176,831.42	
11/15/22	FW-9	6.72	0.015	6%	0.0281	0.0087		28.05

Table A2. *Summary records of wells measured for water levels during flow runs and for groundwater flow estimates.*

Site ID	Latitude	Longitude	Land Surface Elevation (m)	Land Surface Elevation (ft)	Type	Water Right Number	WIN	Well Depth (ft)
FP-W1	41.050680	-112.035150	1288.96	4228.88	Shallow Monitoring Well	n/a	n/a	4
FP-W2D	41.050860	-112.033980	1289.36	4230.19	Shallow Monitoring Well	n/a	n/a	11
FP-W2S	41.050860	-112.033990	1289.38	4230.24	Shallow Monitoring Well	n/a	n/a	5
FP-W3	41.050010	-112.034350	1288.35	4226.86	Shallow Monitoring Well	n/a	n/a	3
FW-1	41.058840	-112.059300	1287.91	4225.43	Flowing Well	31-4536	30780	400
FW-3	41.051030	-112.052600	1285.07	4216.12	Flowing Well	n/a	n/a	n/a
FW-4	41.058790	-112.050170	1290.80	4234.91	Flowing Well	31-3991	33987	232
FW-6	41.052280	-112.032420	1291.33	4236.64	Flowing Well	31-3421	n/a	215
FW-7	41.050890	-112.033880	1289.96	4232.14	Flowing Well	31-3422	n/a	327
FW-8	41.049530	-112.032720	1288.88	4228.60	Flowing Well	31-3423	n/a	247
FW-9	41.052930	-112.026640	1292.29	4239.80	Flowing Well	31-3420	n/a	125
FW-10	41.049370	-112.017710	1292.37	4240.07	Flowing Well	31-3371	n/a	400
FW-11	41.034790	-112.000100	1288.34	4226.85	Flowing Well	31-3511	n/a	114
GW-3	41.060692	-112.043810	1297.70	4238.00	WDCP Monitoring Well	n/a	n/a	15
MW-03	41.041891	-112.052697	1264.78	4149.53	Shallow Monitoring Well	n/a	n/a	12
MW-04	41.044071	-112.031652	1268.21	4160.78	Shallow Monitoring Well	n/a	n/a	12

n/a - Data not available.

Table A3. *Groundwater levels and shut-in pressures collected during flow runs. Well data are in Table A2.*

Date	Well	PSI (atmospheres)	DTW[1] (ft below measuring point)	Stickup (ft)	Reference Elevation of Measuring Point (ft)	Water Level Elevation (ft)	Aquifer[2]
9/30/21	FW-8	6.5	-15.02	0.00	4228.60	4243.61	C
9/30/21	FW-9	2.8	-6.47	0.00	4239.80	4246.27	C
9/30/21	FW-3	5.3	-12.24	-0.27	4216.12	4228.63	C
9/30/21	FW-2	3.4	-7.85	0.00			C
9/30/21	DW-2		1.61	0.00			C
4/27/22	FW-1		-2.30	0.17	4225.43	4227.56	C
4/27/22	FW-3	7.3	-16.86	-0.27	4216.12	4233.25	C
4/27/22	FW-2			0.00			C
4/27/22	FW-4	5.2	-12.01	-0.35	4234.91	4247.28	C
4/27/22	FW-5		1.00	0.00			C
4/27/22	FW-7		2.39	0.00	4232.14	4229.75	C
4/27/22	FP-W2D		3.26	2.04	4230.24	4228.20	U
4/27/22	FP-W1		3.86	1.15	4228.88	4223.87	U
4/27/22	FP-W2S		3.81	1.30	4230.19	4225.08	U
4/27/22	FP-W3		2.95	1.63	4226.86	4222.28	U
4/27/22	FW-11	10.2	-23.56	0.00	4226.85	4250.41	C
4/27/22	FW-10	3.2	-7.39	0.00	4240.07	4247.46	C
4/27/22	FW-8	7.0	-16.17	0.00	4228.60	4244.77	C
4/27/22	FW-9	2.6	-6.01	0.00	4239.80	4245.81	C
4/27/22	FW-6	4.6	-10.63	0.00	4236.64	4247.27	C
4/28/22	FW-10		-7.39	0.00	4240.07	4247.46	C
6/17/22	FP-W1		dry	1.15	4228.88		U
6/17/22	FP-W2S		4.47	1.30	4230.19	4224.42	U
6/17/22	FP-W2D		5.53	2.04	4230.24	4222.67	U
6/17/22	FP-W3		dry	1.63	4226.86		U
8/24/22	FW-1	0.0	0.00	0.17	4225.43	4225.26	C
8/24/22	FW-3	5.1	-11.78	-0.27	4216.12	4228.17	C
8/24/22	FW-4	4.8	-11.09	-0.35	4234.91	4246.35	C
8/24/22	FW-8	6.7	-15.48	0.00	4228.60	4244.07	C
8/24/22	FW-7		0.81	0.00	4232.14	4231.33	C
8/24/22	FW-9	2.0	-4.62	0.00	4239.80	4244.42	C
8/24/22	FW-11	9.8	-22.64	0.00	4226.85	4249.49	C
8/24/22	FW-10	1.6	-3.70	0.00	4240.07	4243.77	C
8/24/22	FW-9	2.0	-4.62	0.00	4239.80	4244.42	C
4/27/22	FP-W1		3.86	1.15	4228.88	4223.87	U
4/27/22	FP-W3		2.93	1.63	4226.86	4222.30	U
4/27/22	FP-W2S		3.81	1.30	4230.19	4225.08	U
4/27/22	FP-W2D		3.26	2.04	4230.24	4224.94	U
11/15/22	FW-1	0.0	0.00	0.17	4225.43	4225.26	C
11/16/22	FW-4	4.9	-11.32	-0.35	4234.91	4246.58	C
11/15/22	FW-3	4.0	-9.24	-0.27	4216.12	4225.63	C
11/15/22	FW-2	1.8	-4.16	0.00	0.00	4.16	C
11/15/22	FW-8	5.6	-12.94	0.00	4228.60	4241.53	C
11/15/22	FW-7			0.00	4232.14	4232.14	C
11/15/22	FW-6	3.4	-7.85	0.00	4236.64	4244.50	C
11/15/22	FW-9		0.00	0.00	4239.80	4239.80	C
11/15/22	FW-11	7.5	-17.33	0.00	4226.85	4244.17	C
11/15/22	FP-W1		dry	1.15	4228.88		U
11/15/22	FP-W2S		dry	1.30	4230.19		U
11/15/22	FP-W2D		7.62	2.04	4230.24	4220.58	U
11/15/22	FP-W3		dry	1.63	4226.86		U
6/17/22	FP-W3		dry				U
6/17/22	FP-W1		dry				U
6/17/22	FP-W2S		4.47	1.30	4230.19	4224.42	U
6/17/22	FP-W2D		5.53	2.04	4230.24	4222.67	U
8/24/22	FW-7		0.81	0.00	4232.14	4231.33	C
8/24/22	FW-6	3.5	-8.09	0.00	4236.64	4244.73	C
10/13/22	FP-W2D		8.09	2.04	4230.24	4220.11	U
10/13/22	FP-W2S		dry	1.30	4230.19		U
10/13/22	FP-W3		dry	1.63	4226.86		U
10/13/22	FP-W1		dry	1.15	4228.88		U
2/9/23	FP-W2D		3.54	2.04	4230.24	4224.66	U
2/9/23	FP-W2S		3.08	1.30	4230.19	4225.81	U
2/9/23	FP-W3		1.71	1.63	4226.86	4223.52	U
2/9/23	FP-W1		2.87	1.15	4228.88	4224.86	U
5/14/23	FP-W2D		2.49	2.04	4230.24	4225.71	U
5/14/23	FP-W2S		1.82	1.30	4230.19	4227.07	U
5/14/22	FP-W3		1.61	1.63	4226.86	4223.62	U
5/14/23	FP-W1		1.70	1.15	4228.88	4226.03	C
5/17/23	FW-1	0.0	0.00	0.17	4225.43	4225.26	C
5/17/23	FW-4	4.5	-10.40	-0.35	4234.91	4245.66	C
5/17/23	FW-3	5.8	-13.40	-0.27	4216.12	4229.78	C
5/17/23	FW-8	6.8	-15.59	0.00	4228.60	4244.19	C
5/17/23	FW-6	3.8	-8.78	0.00	4236.64	4245.42	C
5/17/23	FW-9	2.0	-4.62	0.00	4239.80	4244.42	C
5/17/23	FW-11	9.2	-21.25	0.00	4226.85	4248.10	C

[1] Negative depths to water indicate a water level above land surface.
[2] C = confined aquifer, U = shallow unconfined aquifer.

Table A4. *Chemistry data from wells in the Great Salt Lake Shorelands Preserve.*

Site	Date	Ca (mg/L)	Mg (mg/L)	Na (mg/L)	K (mg/L)	HCO_3 (mg/L)	SO_4 (mg/L)	Cl (mg/L)	CO_2 (mg/L)	TDS (mg/L)	Water Type
WL-GW03-210907	9/7/21	52.9	29.6	102	13.3	276	77.5	131	730	550	Na-HCO_3
WL-GW04-210907	9/7/21	25.1	59.6	102	19.4	480	19	111	6.49	578	Mg-HCO_3
WL-GW05-210907	9/7/21	63.6	34.7	63.6	13.4	371	24.6	96.7	829	480	Ca-HCO_3
WL-H2-210913	9/13/21	108	93.6	198	60	575	98.2	431	189	1380	Na-Cl
WL-SPD1-210913	9/13/21	1.81	1.11	191	7.09	441	19	33.9	1.92	513	Na-HCO_3
WL-SPD6-210913	9/13/21	2.38	1.77	205	7.6	535	19	39	8.75	561	Na-HCO_3

Table A5. *Summary of water budget uncertainty analysis.*

Quantity	Value (acre-feet/year)	Uncertainty (%)	Absolute Uncertainty (acre-feet/year)	Squared Uncertainty	Contribution (%)
Combined Uncertainty - Outflow Option A					
Evapotranspiration	12,120	33	4000	15,997,163	51
Stream Flow	25,633	10	2563	6,570,478	21
Precipitation	6591	12	791	625,585	2
Groundwater Flow	4279	67	2867	8,220,556	26
Total	48,624		10,221	31,413,782	100
Combined Standard Uncertainty[1]		**5605**	**Percent of Total Water Budget**		**12%**

Combined Uncertainty - Outflow Option B					
Evapotranspiration	39,205	33	12,938	167,383,159	89
Stream Flow	25,633	10	2563	6,570,478	3
Precipitation	21,077	12	2529	6,396,883	3
Groundwater Flow	4279	67	2867	8,220,556	4
Total	90,194			188,571,075	100
Combined Standard Uncertainty[1]		**13,732**	**Percent of Total Water Budget**		**15%**

[1]Combined standard uncrtainty is the square root of the sum of the squared uncertainty.

Table A6. *Estimates of within-year and year-to-year changes in groundwater storage from groundwater levels in wells in the unconfined shallow aquifer.*

Within-Year

Well	Dates	DTWmin	DTWmax	WL Change	S	A (ft^2)	Depth (ft)	Width (ft)	Volume (ft^3)	Volume (ac-ft)	V_{all} (ac-ft)
GW-3	2020	-0.6	2.1	-2.7	0.22	1	15	1	-8.91	-0.0002	-1.02
GW-3	2021	0.1	1.9	-1.8	0.22	1	15	1	-5.94	-0.0001	-0.68
FP-W2S	6/17 to 10/13/2022	4.47	7	-2.53	0.22	1	5	1	-2.78	-0.0001	-0.32
FP-W2D	6/17 to 10/13/2022	5.53	8.09	-2.56	0.22	1	11	1	-6.2	-0.0001	-0.71
											-0.68 Average

Year-to-Year

Well	Dates	2022 DTW	2023 DTW	WL Change	S	A	D	W	V ft^3	V ac-ft	V_{all} (ac-ft)
FP-W2S	4/27/22 to 5/14/23	1.82	3.81	-1.99	0.22	1	12	1	-5.2536	-0.000120833	-0.6
FP-W2D	4/27/22 to 5/14/23	2.49	3.26	-0.77	0.22	1	12	1	-2.0328	-4.68E-05	-0.23
											-0.42 Average

Well	Dates	2020 DTW	2021 DTW	WL Change	S	A	D	W	V ft^3	V ac-ft	V_{all} (ac-ft)
GW-3	2020 mimimum DTW	-0.6	-	-	0.22	1	15	1	-2.31	-0.00005313	-0.26
GW-3	2021 mimimum DTW	-	0.1	-0.7							
GW-3	2020 maximum DTW	1.9	-	-	0.22	1	15	1	-0.66	-0.00001518	-0.08
GW-3	2021 maximum DTW	-	2.1	-0.2							-0.17 Average

DTWmin: Minimum depth to water in well.
DTWmax: Maximum depth to water in well.
WL Change: Change in water levels in well.
S: Storativity
A: Area
V_{all}: Storage volume change estaimted from well, extrpolatd to entire Shorelands Preserve.

Table A7. *Vegetation classes and subclasses mapped at the Shorelands Preserve and associated evapotranspiration units.*

UGS Broad Class	UGS subclass	Evapotranspiration Units[1]	Description
Water	Permanent	Open Water	Reasonably permanent waterbodies with open water or aquatic vegetation like duckweed (Lemna sp.), pondweed (Zanichellia sp.), or algae.
Phragmites	Dense	Marshland	Dense patches of invasive phragmites (Phragmites australis) typically existing as a dense monocultre with greater than 50% cover.
	Mixed	Meadowland	Sparse patches of invasive Phragmites typically growing amongst other species.
Playa	Barren	Dry Playa	Barren depressions, salt flats, or playas with occasional salt tolerant plants like seepweed (Suaeda sp.), pickleweed (Salicornia rubra), or iodine bush (Allenrolfea occidentalis). Vegetation cover typically less than 30%.
	Vegetated	Dry Playa	Depressions, salt flats, or playas with greater than 30% cover of salt-tolerant species.
Marsh	Cattail	Marshland	Basins, pond fringes, and other wet areas with permanent or near permanent flooding and saturation supporing dense cattail (Typa sp.) stands. Other emergent species may present but not dominant.
	Bulrush	Marshland	Basins, pond fringes, and other wet areas supporting dense bulrush, typically Schoenoplectus americanus or S. acutus but S. maritimus may be present closer to Great Salt Lake. Cattails and other emergent species may be present but not dominant.
	--	Marshland	Basins, pond fringes, and other visibly flooded or saturated areas where the dominant vegetation was unidentifiable based on treatment history or variable imagery signatures. Assumed to be a mix of phragmites, bulrush, and cattails.
Wet meadow	Dense saltgrass	Meadowland	Low terraces, saline basins, and colonized mudflats along Great Salt Lake supporting dense, near monocultures of salt grass (Distichlis spicata).
	Saline	Meadowland	Low terraces, basins, and other seasonally wet areas supporting dense cover of salt-tolerant graminoids like salt grass, wire rush (Juncus arcticus), and foxtail barley (Hordeum jubatum) with salt grass present as a dominant species in the community.
	Fresh	Meadowland	Low terraces, basins, and other seasonally wet areas supporting dense cover of salt-tolerant graminoids like spike rush (Eleocharis sp), wire rush, and foxtail barley with salt grass present but never as a dominant species in the community.
Mesic meadow	Mesic grasses	Grassland	Widely varied landscapes and positions receiving occasional irrigation or flooding typically dominated by perennial upland grasses like tall wheat grass (Thinopyrum ponticum) and alkalai sacaton (Sporobolus airoides) with occasional annual grasses or forbs. Salt grass may be also be present. Patches of bare ground present.
	Irrigated pasture	Recently irrigated cropland	Level, irrigated fields supporting common pasture grasses and forbs like tall wheatgrass, foxtail barley, or clover.
	Ruderal annuals	Grassland	Dry to occasionaly wet areas near roads, corrals, and other disturbance supporitng invasive and weedy annuals like like forage kochia (Bassia scoparia), prickly lettuce (Lactua serriola), or curlycup gumweed (Grindelia squarrosa).
Woody riparian	Woody riparian	Meadowland	Cottonwoods (Populus sp.), crack willows (Salix fragilis), and Russian olives (Eleagnus angustifolia) along creeks and irrigation ditches.
Upland	Shrubby	Dense Desert Shrubland	Dry or rarely flooded upper terraces and mounds supporting greasewood (Sarcobatus vermiculata) and a sparse of grasses or annual forbs.
	Annual grasses	Sparse Desert Shrubland	Dry areas suporting a near monoculture of annual grasses like cheatgrass (Bromus tectorum) or Mediterranean barley (Hordeum marinum).
Artificial	Artificial crop	Recently irrigated cropland	Irrigated fields dedicated to row crops or alfalfa.
	Impervious surface	Xerophytic	Roads, buildings, etc. typically lacking vegetation.

Notes
[1] as defined by Smith et. Al., 2007

Table A8. *Description of hydropattern classes assigned to wetland mapping data.*

Hydropattern Category	Cowardin Water Regime	Description
Permanent water	F, G, H	Near permanent standing water
Flooding and saturation	E	Frequent standing water, saturated when water absent
Semi-permanent saturation	D	Very little standing water, near constant saturation
Seasonal flooding	C	Frequent standing water, no saturation when dry
Temporary flooding	A, J	Infrequent or occasional surface water, or applied surface water
Seasonal saturation	B	Seasonal saturation, generally from groundwater or being in relative low area
Irrigation	A	Actively irrigated areas
Dry	J or none	No hydrology

Table A9. *Water sources assigned to wetland mapping data.*

Water Source	Description
Applied irrigation	Water is directly applied to field or vegetation. Limited to just irrigated pastures and croplands.
Managed	Water is managed to stay at certain levels or flows. Typically applied to ditches and impounded ponds.
Overbank flooding	Overbank flooding from creeks and large ditches. Typically only occurs during runoff and flood events.
Irrigation returns and shallow flows	Tail water coming off of irrigated fields and pastures or as shallow sheetflows without clear origin. The most common water source in the mapping.
Great Salt Lake	Flooded or dry depending on Great Salt Lake water levels.
Groundwater	Groundwater or located near artesian well.
Direct outflow from canals	Water flowing out of the end of canals, ditches or channelized streams. Distinct from applied irrigation in that it does not apply to croplands or irrigated pastures and distinct from irrigation returns in that it has a clear, relatively permanent surface water connection to a major ditch or canal.

Table A10. *Summary of mapped vegetation classes by study component area. The percent area is calculated as the percent of the vegetation class within each study component area.*

		Preserve		New		Outflow		Overall	
		Acre	**% of area**	**Acre**	**% of area**	**Acre**	**% of area**	**Acre**	**% of area**
Water	Permanent	86.8	2	5.6	1	108.4	1	200.7	1
	Total	86.8	2	5.6	1	108.4	1	200.7	1
Phragmites	Dense	640.4	14	47.7	9	4576.4	47	5264.5	36
	Mixed	210.4	5	12.1	2	324.2	3	546.8	4
	Total	850.9	19	59.8	11	4900.6	50	5811.3	39
Playa	Barren	26.6	1	0.0	0	480.6	5	507.2	3
	Vegetated	175.4	4	18.5	4	1123.1	11	1317.0	9
	Total	201.9	5	18.5	4	1603.8	16	1824.2	12
Marsh	Cattail	298.4	7	1.3	0	83.1	1	382.8	3
	Bulrush	248.0	6	27.7	5	513.0	5	788.6	5
	Unclassified	67.9	2	4.8	1	383.2	4	455.8	3
	Total	614.3	14	33.8	6	979.2	10	1627.3	11
Wet meadow	Dense saltgrass	83.3	2	0.0	0	2126.9	22	2210.1	15
	Saline	397.5	9	30.1	6	15.5	0	443.1	3
	Fresh	204.9	5	11.9	2	0.0	0	216.8	1
	Total	685.7	16	42.0	8	2142.4	22	2870.1	19
Mesic meadow	Mesic grasses	1528.0	35	276.9	53	92.1	1	1896.9	13
	Irrigated pasture	101.1	2	5.6	1	0.0	0	106.7	1
	Ruderal annuals	79.9	2	26.1	5	0.0	0	106.0	1
	Total	1709.0	39	308.6	59	92.1	1	2109.6	14
Woody riparian	Woody riparian	26.4	1	2.0	0	0.3	0	28.7	0
	Total	26.4	1	2.0	0	0.3	0	28.7	0
Upland	Shrubby	58.5	1	12.3	2	0.0	0	70.9	0
	Annual grasses	40.6	1	20.4	4	0.0	0	61.0	0
	Total	99.1	2	32.7	6	0.0	0	131.9	1
Artificial	Artificial crop	91.4	2	0.0	0	0.0	0	91.4	1
	Impervious surface	52.7	1	23.4	4	0.0	0	76.1	1
	Total	144.1	3	23.4	4	0.0	0	167.5	1

Note: rounding errors may exist

Table A11. *Area of each condensed land cover category (derived from the National Wetland Inventory) by the study component areas.*

Analysis Class	NWI Codes	Vegetation Map Codes	Preserve (ha)				Outflow (ha)				New Parcels (ha)			
			1981	1997	2014	2021	1981	1997	2014	2021	1981	1997	2014	2021
Water	Unconsolidated bottom and aquatic bed classes (all with F and G water regimes)	Water class (all with F or wetter water regimes)	30.0	18.0	33.2	35.1	135.4	88.8	51.5	43.9	1.0	0.8	1.2	2.2
Shore	Unconsolidated shore classes (all with A or C water regimes)	Playa class (all with A or C water regimes)	81.0	0.0	44.8	81.7	2155.9	1995.1	534.4	592.9	1.6	0.0	4.2	7.5
Dry emergent	Emergent class with A water regime	Mesic Meadow, Phragmites and Wet Meadow classes with A or B water regimes	279.8	422.1	681.4	783.1	63.9	135.5	86.9	41.4	55.7	49.0	83.2	94.0
Wet emergent	Emergent class with C or F water regimes	Marsh, Phragmites, and Wet Meadow classes with C, D, E, or F water regimes	832.5	871.0	627.1	701.7	1374.0	1529.5	3087.1	3084.5	42.7	40.3	38.4	46.9

Table A12. *Explanatory variables considered for the NDVI global models.*

Variable	Site Number	Unit	Range 30 Year	Range 10 Year	Type	Hypothesized Relationship	Actual Relationship	Data Source
June-August Mean PDSI (Summer PDSI)	Preserve area	Preserve	-4.96 to 4.77	-4.96 to 2.79	climate	+	+	University of Idaho-GRIDMET (Abatzoglou, 2013)
Max GSL Elevation at Saltair	10010000	ft	4190.93 top 4203.29	4192.81 to 4198.68	climate, human influence, and hydrology influences	+/-	+/-	U.S. Geological Survey
Day of Year Peak Flow at Gateway (DOY Gateway)	10136500	day	42 to 253	54 to 234	winter and spring climate, human influence	+	+/-	U.S. Geological Survey
Peak Flow at Oakley (Peak Oakley)	10128500	csf	604 to 3530	604 to 2810	winter and spring climate	+	+/-	U.S. Geological Survey
Impervious Surface Area	example East HUC12 5km buffer	ha	2375.09 to 33055.51	3183.92 to 33055.51	human influence	-	+/-	U.S. Geological Survey LCMAP (Zhu and Woodcock, 2014)
Year	NA	year	1992 to 2021	2012 to 2021	linear annual increase	NA	NA	
March Groundwater Level	410204111565401	ft	-40.35 to -23.14	-40.35 to -31.92	climate, human influence, and hydrology influences	NA	NA	U.S. Geological Survey

Table A13. *Reclassification of the 2011 vegetation mapping and the 2021 vegetation mapping.*

Broad Comparison	2011 Mapping	2021 Mapping	
		Broad Class	Subclass
Water	Open water	Water	Permanent
Marsh	Typha	Marsh	Cattail
	Schoenoplectus acutus		Bulrush
			Mixed
Phragmites	Pragmites	Phragmites	Dense
			Mixed
Wet Meadow	Saltgrass	Wet Meadow	Dense saltgrass
	Other emergent wetland		Saline
			Fresh
Playa	Pickleweed	Playa	Vegetated
	Playa		Barren
Upland	Upland	Mesic Meadow	Mesic grasses
			Irrigated pasture
			Ruderal annuals
		Woody Riparian	Woody riparian
		Upland	Shrubby
			Annual grasses
		Artificial	Artificial crop
			Impervious surface

Table A14. *Area in acres of vegetation classes by hydrology unit.*

Shorelands Zones		**Preserve**										**New Parcels**					**Outflow Area**			
Hydrology Unit		**West 1**	**West 2**	**West 3**	**West 4**	**Middle 1**	**Middle 2**	**Middle 3**	**East 1**	**East 2**	**East 3**	**West 1**	**West 2**	**West 3**	**West 4**	**Middle 1**	**West 1**	**West 2**	**Middle 1**	**East 1**
Water	Permanent	19.5	23.6	6.8	0.0	5.0	14.8	10.6	6.4	0.0	0.0	1.1	1.9	2.1	0.5	0.0	0.0	0.1	105.9	2.4
	Total	19.5	23.6	6.8	0.0	5.0	14.8	10.6	6.4	0.0	0.0	1.1	1.9	2.1	0.5	0.0	0.0	0.1	105.9	2.4
Phragmites	Dense	105.2	185.3	249.9	5.8	42.2	13.9	0.4	34.8	2.3	0.7	0.0	39.5	6.7	0.0	1.4	218.1	1084.2	2135.6	1138.5
	Mixed	46.0	118.0	16.5	1.3	23.3	4.3	0.0	0.0	1.0	0.0	0.8	7.6	3.7	0.0	0.0	86.5	56.2	179.9	1.7
	Total	151.3	303.3	266.4	7.1	65.5	18.1	0.4	34.8	3.3	0.7	0.8	47.1	10.4	0.0	1.4	304.6	1140.3	2315.5	1140.2
Playa	Barren	7.8	12.0	3.7	0.0	0.0	0.0	0.0	0.9	2.1	0.0	0.0	0.0	0.0	0.0	0.0	27.7	88.4	279.1	85.4
	Vegetated	34.0	29.8	31.1	50.6	14.4	0.0	2.8	12.3	0.4	0.0	1.6	12.3	3.2	1.5	0.0	29.2	189.6	747.7	156.7
	Total	41.8	41.9	34.7	50.6	14.4	0.0	2.8	13.2	2.5	0.0	1.6	12.3	3.2	1.5	0.0	56.9	278.0	1026.8	242.1
Marsh	Cattail	28.8	26.5	0.0	0.0	115.1	52.6	56.9	18.6	0.0	0.0	0.3	0.0	0.0	0.6	0.5	0.0	0.0	69.3	13.8
	Bulrush	0.0	36.5	7.7	7.6	104.9	51.1	23.7	15.4	1.0	0.0	6.0	21.7	0.0	0.0	0.0	0.0	28.9	332.9	151.2
	Unclassified	0.0	1.2	0.0	1.7	53.6	11.2	0.2	0.0	0.0	0.0	0.0	0.0	4.8	0.0	0.0	0.0	0.4	372.7	10.1
	Total	28.8	64.2	7.7	9.4	273.6	114.8	80.8	34.0	1.0	0.0	6.3	21.7	4.8	0.6	0.5	0.0	29.2	775.0	175.0
Wet Meadow	Dense saltgrass	27.3	12.4	3.1	7.2	22.2	5.6	0.8	4.5	0.2	0.0	0.0	0.0	0.0	0.0	0.0	280.8	357.2	1286.2	202.6
	Saline	7.1	6.5	7.6	46.8	246.5	44.2	31.5	7.1	0.0	0.0	2.8	2.7	16.2	3.7	4.7	6.4	0.0	7.5	1.6
	Fresh	0.0	3.1	6.3	159.2	31.6	0.0	4.8	0.0	0.0	0.0	0.0	2.0	0.0	8.1	1.8	0.0	0.0	0.0	0.0
	Total	34.4	22.0	17.1	213.1	300.3	49.9	37.1	11.6	0.2	0.0	2.8	4.7	16.2	11.8	6.6	287.2	357.2	1293.8	204.2
Mesic Meadow	Mesic grasses	106.7	222.0	105.0	210.0	309.5	231.3	182.7	149.3	8.7	2.7	9.8	137.7	39.6	46.6	43.2	15.5	57.1	19.4	0.0
	Irrigated pasture	49.3	0.3	0.0	0.0	0.0	0.0	13.1	38.4	0.0	0.0	0.0	0.0	0.0	5.6	0.0	0.0	0.0	0.0	0.0
	Ruderal annuals	5.4	0.0	0.3	1.9	7.2	24.0	8.3	32.8	0.0	0.1	0.2	1.5	2.8	2.6	19.0	0.0	0.0	0.0	0.0
	Total	161.5	222.4	105.2	211.9	316.8	255.3	204.0	220.4	8.7	2.7	10.0	139.2	42.3	54.8	62.2	15.5	57.1	19.4	0.0
Woody Riparian	Woody riparian	0.3	0.2	0.0	1.5	5.3	12.0	2.2	5.0	0.0	0.0	0.0	0.0	0.5	0.0	1.5	0.0	0.0	0.3	0.0
	Total	0.3	0.2	0.0	1.5	5.3	12.0	2.2	5.0	0.0	0.0	0.0	0.0	0.5	0.0	1.5	0.0	0.0	0.3	0.0
Upland	Shrubby	11.8	27.7	8.3	0.0	2.3	0.0	0.1	8.3	0.0	0.0	6.3	6.0	0.0	0.0	0.0	0.0	0.0	0.0	0.0
	Annual grasses	7.2	1.5	0.0	2.5	8.2	0.9	0.5	19.9	0.0	0.0	0.0	0.0	20.4	0.0	0.0	0.0	0.0	0.0	0.0
	Total	19.0	29.2	8.3	2.5	10.5	0.9	0.6	28.1	0.0	0.0	6.3	6.0	20.4	0.0	0.0	0.0	0.0	0.0	0.0
Artificial	Artificial crop	0.2	34.1	0.0	0.0	0.0	0.0	56.1	1.1	0.0	0.0	0.0	0.0	0.0	0.0	0.0	0.0	0.0	0.0	0.0
	Impervious surface	2.3	1.9	0.2	5.8	5.8	6.5	16.3	13.7	0.0	0.2	0.1	1.4	5.0	2.1	14.8	0.0	0.0	0.0	0.0
	Total	2.5	35.9	0.2	5.8	5.8	6.5	72.4	14.7	0.0	0.2	0.1	1.4	5.0	2.1	14.8	0.0	0.0	0.0	0.0

Table A15. *Results of the model selection with a difference in AICc of less than 6 for each hydrology unit for 1992-2020. Potential uninformative parameters have not been removed. The response variable is the median July 15- Aug 31st NDVI value for each year. Model coefficients are the mean summer PDSI, max elevation of the Great Salt Lake, impervious surface area, day of year of peak flow at Gateway, and peak flow at Oakley respectively.*

Hydrology Unit	Intercept	Summer PDSI	Max GSL Level Saltair	Impervious Surface	DOY Gateway	Peak Oakley	df	AICc	Delta	Model Weights	uninformative	List Variables
New Middle 1	0.7331	0.0136	NA	0.0000	3.75E-04	NA	5	-93.3512	0.0000	0.5647		DOYGateway+LCMAP+SummerPDSIMean
New Middle 1	0.8132	0.0126	NA	0.0000	NA	NA	4	-91.3819	1.9693	0.2110		LCMAP+SummerPDSIMean
New Middle 1	17.0233	0.0127	-0.0038	0.0000	NA	NA	5	-89.0298	4.3214	0.0651	1	LCMAP+MaxGSLLevelSaltair+SummerPDSIMean
New Middle 1	-28.5008	0.0145	0.0069	NA	4.82E-04	NA	5	-88.8475	4.5037	0.0594		DOYGateway+MaxGSLLevelSaltair+SummerPDSIMean
New Middle 1	0.8178	0.0135	NA	0.0000	NA	0.0000	5	-88.5659	4.7853	0.0516	1	peakOakley+LCMAP+SummerPDSIMean
New West 1	-25.4352	0.0085	0.0061	0.0000	NA	NA	5	-114.7935	0.0000	0.4203		LCMAP+MaxGSLLevelSaltair+SummerPDSIMean
New West 1	0.2723	0.0086	NA	0.0000	NA	NA	4	-114.2413	0.5522	0.3189		LCMAP+SummerPDSIMean
New West 1	0.2911	0.0083	NA	0.0000	-0.0001	NA	5	-112.0508	2.7427	0.1067	1	DOYGateway+LCMAP+SummerPDSIMean
New West 1	0.2640	0.0074	NA	0.0000	NA	6.43E-06	5	-111.8220	2.9715	0.0951	1	peakOakley+LCMAP+SummerPDSIMean
New West 2	0.3226	0.0110	NA	0.0000	NA	NA	4	-88.5484	0.0000	0.3102		LCMAP+SummerPDSIMean
New West 2	34.0576	0.0105	-0.0080	NA	NA	NA	4	-86.8990	1.6494	0.1360		MaxGSLLevelSaltair+SummerPDSIMean
New West 2	0.3496	0.0106	NA	0.0000	-0.0001	NA	5	-86.2047	2.3436	0.0961	1	DOYGateway+LCMAP+SummerPDSIMean
New West 2	9.0337	0.0110	-0.0021	0.0000	NA	NA	5	-85.7611	2.7873	0.0770	1	LCMAP+MaxGSLLevelSaltair+SummerPDSIMean
New West 2	0.3205	0.0107	NA	0.0000	NA	1.76E-06	5	-85.6223	2.9261	0.0718	1	peakOakley+LCMAP+SummerPDSIMean
New West 2	31.7383	0.0101	-0.0075	NA	-0.0002	NA	5	-85.4773	3.0711	0.0668	1	DOYGateway+MaxGSLLevelSaltair+SummerPDSIMean
New West 2	33.2555	0.0096	-0.0078	NA	NA	4.51E-06	5	-84.0585	4.4898	0.0329	1	peakOakley+MaxGSLLevelSaltair+SummerPDSIMean
New West 2	0.4283	0.0082	NA	NA	NA	NA	3	-83.3659	5.1825	0.0232		SummerPDSIMean
New West 2	0.3111	NA	NA	0.0000	NA	2.22E-05	4	-83.1849	5.3635	0.0212		peakOakley+LCMAP
New West 2	0.4658	0.0079	NA	NA	-0.0003	NA	4	-82.7959	5.7524	0.0175	1	DOYGateway+SummerPDSIMean
New West 2	0.3487	NA	NA	0.0000	NA	NA	3	-82.7396	5.8088	0.0170		LCMAP
New West 2	24.7034	NA	-0.0058	NA	NA	2.28E-05	4	-82.6145	5.9339	0.0160		peakOakley+MaxGSLLevelSaltair
New West 3	0.3320	0.0151	NA	0.0000	NA	NA	4	-100.0407	0.0000	0.4660		LCMAP+SummerPDSIMean
New West 3	-7.1530	0.0151	0.0018	0.0000	NA	NA	5	-97.2651	2.7757	0.1163	1	LCMAP+MaxGSLLevelSaltair+SummerPDSIMean
New West 3	0.3400	0.0150	NA	0.0000	0.0000	NA	5	-97.1731	2.8676	0.1111	1	DOYGateway+LCMAP+SummerPDSIMean
New West 3	0.3303	0.0148	NA	0.0000	NA	1.44E-06	5	-97.1146	2.9262	0.1079	1	peakOakley+LCMAP+SummerPDSIMean
New West 3	23.2975	0.0144	-0.0054	NA	NA	NA	4	-96.4804	3.5603	0.0786		MaxGSLLevelSaltair+SummerPDSIMean
New West 3	0.4253	0.0129	NA	NA	NA	NA	3	-95.0201	5.0207	0.0379		SummerPDSIMean
New West 3	22.0346	0.0142	-0.0051	NA	-0.0001	NA	5	-94.1560	5.8847	0.0246	1	DOYGateway+MaxGSLLevelSaltair+SummerPDSIMean
New West 4	31.0851	0.0152	-0.0073	0.0000	NA	NA	5	-102.3676	0.0000	0.2367		LCMAP+MaxGSLLevelSaltair+SummerPDSIMean
New West 4	0.5496	0.0151	NA	0.0000	NA	NA	4	-102.1149	0.2527	0.2086		LCMAP+SummerPDSIMean
New West 4	0.4834	0.0164	NA	NA	NA	NA	3	-101.4128	0.9549	0.1468		SummerPDSIMean
New West 4	0.4571	0.0166	NA	NA	2.03E-04	NA	4	-100.6557	1.7120	0.1006	1	DOYGateway+SummerPDSIMean
New West 4	0.5219	0.0154	NA	0.0000	1.36E-04	NA	5	-100.0419	2.3257	0.0740	1	DOYGateway+LCMAP+SummerPDSIMean
New West 4	0.5022	0.0182	NA	NA	NA	0.0000	4	-99.5113	2.8563	0.0567	1	peakOakley+SummerPDSIMean
New West 4	0.5556	0.0161	NA	0.0000	NA	0.0000	5	-99.4262	2.9414	0.0544	1	peakOakley+LCMAP+SummerPDSIMean
New West 4	-5.4135	0.0160	0.0014	NA	NA	NA	4	-99.0295	3.3381	0.0446	1	MaxGSLLevelSaltair+SummerPDSIMean
New West 4	0.4766	0.0186	NA	NA	2.11E-04	0.0000	5	-98.7322	3.6355	0.0384	1	DOYGateway+peakOakley+SummerPDSIMean
New West 4	-3.3878	0.0164	9.16E-04	NA	1.95E-04	NA	5	-97.8570	4.5106	0.0248	1	DOYGateway+MaxGSLLevelSaltair+SummerPDSIMean
New West 4	-3.7751	0.0177	0.0010	NA	NA	0.0000	5	-96.7372	5.6304	0.0142	1	peakOakley+MaxGSLLevelSaltair+SummerPDSIMean
Outflow East 1	119.6438	0.0216	-0.0287	0.0000	NA	NA	5	-45.5850	0.0000	0.6151		LCMAP+MaxGSLLevelSaltair+SummerPDSIMean
Outflow East 1	-1.5067	0.0197	NA	0.0000	NA	NA	4	-42.3895	3.1955	0.1245		LCMAP+SummerPDSIMean
Outflow East 1	110.9548	NA	-0.0266	0.0000	NA	4.69E-05	5	-40.7726	4.8125	0.0554		peakOakley+LCMAP+MaxGSLLevelSaltair
Outflow East 1	104.9351	NA	-0.0252	0.0000	NA	NA	4	-40.1516	5.4334	0.0406		LCMAP+MaxGSLLevelSaltair
Outflow East 1	-1.4642	0.0193	NA	0.0000	-0.0002	NA	5	-39.5941	5.9910	0.0308	1	DOYGateway+LCMAP+SummerPDSIMean
Outflow Middle 1	117.6020	0.0131	-0.0281	0.0000	NA	NA	5	-57.3259	0.0000	0.4945		LCMAP+MaxGSLLevelSaltair+SummerPDSIMean
Outflow Middle 1	108.5563	NA	-0.0260	0.0000	NA	NA	4	-55.3572	1.9687	0.1848		LCMAP+MaxGSLLevelSaltair
Outflow Middle 1	111.6918	NA	-0.0267	0.0000	NA	2.23E-05	5	-53.7204	3.6056	0.0815	1	peakOakley+LCMAP+MaxGSLLevelSaltair
Outflow Middle 1	113.5823	NA	-0.0272	0.0000	-0.0003	NA	5	-53.1430	4.1829	0.0611	1	DOYGateway+LCMAP+MaxGSLLevelSaltair
Outflow Middle 1	207.8210	0.0125	-0.0495	NA	NA	NA	4	-51.9090	5.4170	0.0330		MaxGSLLevelSaltair+SummerPDSIMean

Table A15 Continued. *Results of the model selection with a difference in AICc of less than 6 for each hydrology unit for 1992-2020. Potential uninformative parameters have not been removed. The response variable is the median July 15- Aug 31st NDVI value for each year. Model coefficients are the mean summer PDSI, max elevation of the Great Salt Lake, impervious surface area, day of year of peak flow at Gateway, and peak flow at Oakley respectively.*

Hydrology Unit	Intercept	Summer PDSI	Max GSL Level Saltair	Impervious Surface	DOY Gateway	Peak Oakley	df	AICc	Delta	Model Weights	uninformative	List Variables
Outflow West 1	129.6221	NA	-0.0309	0.0000	-0.0007	NA	5	-47.6800	0.0000	0.2523		DOYGateway+LCMAP+MaxGSLLevelSaltair
Outflow West 1	113.7004	NA	-0.0271	0.0000	NA	NA	4	-47.2441	0.4360	0.2029		LCMAP+MaxGSLLevelSaltair
Outflow West 1	115.8404	0.0102	-0.0276	0.0000	NA	NA	5	-46.4043	1.2757	0.1333	1	LCMAP+MaxGSLLevelSaltair+SummerPDSIMean
Outflow West 1	115.3851	NA	-0.0275	0.0000	NA	2.74E-05	5	-45.8016	1.8785	0.0986	1	peakOakley+LCMAP+MaxGSLLevelSaltair
Outflow West 1	216.9251	NA	-0.0516	NA	-0.0009	NA	4	-45.3537	2.3263	0.0788		DOYGateway+MaxGSLLevelSaltair
Outflow West 1	216.2321	NA	-0.0514	NA	-0.0010	3.15E-05	5	-44.2859	3.3941	0.0462	1	DOYGateway+peakOakley+MaxGSLLevelSaltair
Outflow West 1	-0.5002	NA	NA	0.0000	NA	NA	3	-44.1074	3.5727	0.0423		LCMAP
Outflow West 1	222.1266	0.0058	-0.0528	NA	-0.0009	NA	5	-43.0515	4.6285	0.0249	1	DOYGateway+MaxGSLLevelSaltair+SummerPDSIMean
Outflow West 1	-0.5261	0.0095	NA	0.0000	NA	NA	4	-42.9001	4.7799	0.0231	1	LCMAP+SummerPDSIMean
Outflow West 1	-0.4103	NA	NA	0.0000	-0.0005	NA	4	-42.7288	4.9512	0.0212	1	DOYGateway+LCMAP
Outflow West 1	-0.5428	NA	NA	0.0000	NA	2.55E-05	4	-42.4584	5.2216	0.0185	1	peakOakley+LCMAP
Outflow West 1	225.3467	NA	-0.0536	NA	NA	NA	3	-42.2492	5.4308	0.0167		MaxGSLLevelSaltair
Outflow West 2	183.3876	NA	-0.0436	NA	-0.0012	5.18E-05	5	-40.2085	0.0000	0.3306		DOYGateway+peakOakley+MaxGSLLevelSaltair
Outflow West 2	198.0564	0.0152	-0.0471	NA	-0.0011	NA	5	-39.6227	0.5858	0.2467		DOYGateway+MaxGSLLevelSaltair+SummerPDSIMean
Outflow West 2	184.5284	NA	-0.0438	NA	-0.0012	NA	4	-38.9163	1.2922	0.1733		DOYGateway+MaxGSLLevelSaltair
Outflow West 2	150.9555	NA	-0.0359	0.0000	-0.0011	NA	5	-36.5506	3.6579	0.0531	1	DOYGateway+LCMAP+MaxGSLLevelSaltair
Outflow West 2	129.7663	0.0190	-0.0309	0.0000	NA	NA	5	-35.8851	4.3234	0.0381		LCMAP+MaxGSLLevelSaltair+SummerPDSIMean
Outflow West 2	209.5742	0.0172	-0.0498	NA	NA	NA	4	-35.5633	4.6453	0.0324		MaxGSLLevelSaltair+SummerPDSIMean
Outflow West 2	193.9891	NA	-0.0461	NA	NA	5.07E-05	4	-35.0013	5.2072	0.0245		peakOakley+MaxGSLLevelSaltair
Outflow West 2	194.9993	NA	-0.0464	NA	NA	NA	3	-34.5841	5.6244	0.0199		MaxGSLLevelSaltair
Preserve East 1	-0.1075	0.0141	NA	0.0000	NA	NA	4	-66.3157	0.0000	0.3803		LCMAP+SummerPDSIMean
Preserve East 1	31.8990	0.0146	-0.0076	0.0000	NA	NA	5	-64.2683	2.0473	0.1366	1	LCMAP+MaxGSLLevelSaltair+SummerPDSIMean
Preserve East 1	-0.0966	0.0176	NA	0.0000	NA	0.0000	5	-64.2305	2.0851	0.1341	1	peakOakley+LCMAP+SummerPDSIMean
Preserve East 1	-0.0851	0.0139	NA	0.0000	-0.0001	NA	5	-63.4783	2.8373	0.0920	1	DOYGateway+LCMAP+SummerPDSIMean
Preserve East 1	92.5177	0.0143	-0.0219	NA	NA	NA	4	-62.9815	3.3342	0.0718		MaxGSLLevelSaltair+SummerPDSIMean
Preserve East 1	-0.0440	NA	NA	0.0000	NA	NA	3	-62.1666	4.1491	0.0478		LCMAP
Preserve East 1	89.3802	0.0138	-0.0212	NA	-0.0003	NA	5	-61.2526	5.0631	0.0302	1	DOYGateway+MaxGSLLevelSaltair+SummerPDSIMean
Preserve East 1	94.8630	0.0167	-0.0225	NA	NA	0.0000	5	-60.4218	5.8938	0.0200	1	peakOakley+MaxGSLLevelSaltair+SummerPDSIMean
Preserve East 2	64.6752	0.0148	-0.0153	NA	NA	0.0000	5	-66.2074	0.0000	0.1570		peakOakley+MaxGSLLevelSaltair+SummerPDSIMean
Preserve East 2	51.3962	NA	-0.0121	NA	NA	NA	3	-66.1915	0.0159	0.1558		MaxGSLLevelSaltair
Preserve East 2	58.3918	0.0082	-0.0138	NA	NA	NA	4	-65.9588	0.2486	0.1387	1	MaxGSLLevelSaltair+SummerPDSIMean
Preserve East 2	0.2137	NA	NA	0.0000	NA	NA	3	-64.9317	1.2757	0.0830		LCMAP
Preserve East 2	0.2183	0.0143	NA	0.0000	NA	0.0000	5	-64.3969	1.8104	0.0635		peakOakley+LCMAP+SummerPDSIMean
Preserve East 2	0.1872	0.0075	NA	0.0000	NA	NA	4	-64.1970	2.0103	0.0575	1	LCMAP+SummerPDSIMean
Preserve East 2	51.5415	NA	-0.0122	NA	NA	0.0000	4	-63.6675	2.5399	0.0441	1	peakOakley+MaxGSLLevelSaltair
Preserve East 2	42.8108	NA	-0.0101	0.0000	NA	NA	4	-63.5595	2.6479	0.0418	1	LCMAP+MaxGSLLevelSaltair
Preserve East 2	51.9485	NA	-0.0123	NA	6.22E-05	NA	4	-63.5366	2.6708	0.0413	1	DOYGateway+MaxGSLLevelSaltair
Preserve East 2	59.4445	0.0084	-0.0141	NA	1.01E-04	NA	5	-63.1654	3.0420	0.0343	1	DOYGateway+MaxGSLLevelSaltair+SummerPDSIMean
Preserve East 2	48.8841	0.0083	-0.0116	0.0000	NA	NA	5	-63.1171	3.0903	0.0335	1	LCMAP+MaxGSLLevelSaltair+SummerPDSIMean
Preserve East 2	0.1770	NA	NA	0.0000	1.64E-04	NA	4	-62.5485	3.6588	0.0252	1	DOYGateway+LCMAP
Preserve East 2	0.2272	NA	NA	0.0000	NA	0.0000	4	-62.4848	3.7226	0.0244	1	peakOakley+LCMAP
Preserve East 2	0.4452	NA	NA	NA	NA	NA	2	-61.9751	4.2323	0.0189		
Preserve East 2	0.1370	0.0080	NA	0.0000	2.16E-04	NA	5	-61.8518	4.3555	0.0178	1	DOYGateway+LCMAP+SummerPDSIMean
Preserve East 2	41.8285	NA	-0.0099	0.0000	NA	0.0000	5	-60.8212	5.3862	0.0106	1	peakOakley+LCMAP+MaxGSLLevelSaltair
Preserve East 2	52.1103	NA	-0.0123	NA	6.40E-05	0.0000	5	-60.7805	5.4269	0.0104	1	DOYGateway+peakOakley+MaxGSLLevelSaltair
Preserve East 2	40.0743	NA	-0.0095	0.0000	9.66E-05	NA	5	-60.7294	5.4780	0.0101	1	DOYGateway+LCMAP+MaxGSLLevelSaltair
Preserve East 3	0.5526	0.0216	NA	NA	NA	0.0000	4	-62.2464	0.0000	0.2634		peakOakley+SummerPDSIMean
Preserve East 3	0.4272	0.0244	NA	0.0000	NA	-0.0001	5	-61.3148	0.9315	0.1653	1	peakOakley+LCMAP+SummerPDSIMean
Preserve East 3	27.3887	0.0244	-0.0064	NA	NA	-0.0001	5	-61.1877	1.0587	0.1551	1	peakOakley+MaxGSLLevelSaltair+SummerPDSIMean

Table A15 Continued. *Results of the model selection with a difference in AICc of less than 6 for each hydrology unit for 1992-2020. Potential uninformative parameters have not been removed. The response variable is the median July 15- Aug 31st NDVI value for each year. Model coefficients are the mean summer PDSI, max elevation of the Great Salt Lake, impervious surface area, day of year of peak flow at Gateway, and peak flow at Oakley respectively.*

Hydrology Unit	Intercept	Summer PDSI	Max GSL Level Saltair	Impervious Surface	DOY Gateway	Peak Oakley	df	AICc	Delta	Model Weights	uninformative	List Variables
Preserve East 3	0.4671	0.0136	NA	NA	NA	NA	3	-60.6345	1.6119	0.1176		SummerPDSIMean
Preserve East 3	0.5401	0.0218	NA	NA	1.02E-04	0.0000	5	-59.4404	2.8060	0.0648	1	DOYGateway+peakOakley+SummerPDSIMean
Preserve East 3	18.2279	0.0148	-0.0042	NA	NA	NA	4	-58.6518	3.5945	0.0437	1	MaxGSLLevelSaltair+SummerPDSIMean
Preserve East 3	0.3813	0.0146	NA	0.0000	NA	NA	4	-58.6193	3.6271	0.0429	1	LCMAP+SummerPDSIMean
Preserve East 3	0.4581	0.0137	NA	NA	6.95E-05	NA	4	-57.9819	4.2645	0.0312	1	DOYGateway+SummerPDSIMean
Preserve East 3	0.4633	NA	NA	NA	NA	NA	2	-57.9580	4.2884	0.0309		
Preserve Middle 1	17.3564	0.0115	-0.0040	NA	NA	NA	4	-110.6611	0.0000	0.2791		MaxGSLLevelSaltair+SummerPDSIMean
Preserve Middle 1	0.5973	0.0104	NA	NA	NA	NA	3	-109.6881	0.9730	0.1716		SummerPDSIMean
Preserve Middle 1	0.5470	0.0112	NA	0.0000	NA	NA	4	-108.6884	1.9726	0.1041	1	LCMAP+SummerPDSIMean
Preserve Middle 1	18.7526	0.0129	-0.0043	NA	NA	0.0000	5	-108.4243	2.2367	0.0912	1	peakOakley+MaxGSLLevelSaltair+SummerPDSIMean
Preserve Middle 1	16.4559	0.0113	-0.0038	NA	-0.0001	NA	5	-108.2301	2.4309	0.0828	1	DOYGateway+MaxGSLLevelSaltair+SummerPDSIMean
Preserve Middle 1	23.9009	0.0114	-0.0055	0.0000	NA	NA	5	-107.9789	2.6821	0.0730	1	LCMAP+MaxGSLLevelSaltair+SummerPDSIMean
Preserve Middle 1	0.6129	0.0102	NA	NA	-0.0001	NA	4	-107.8763	2.7847	0.0693	1	DOYGateway+SummerPDSIMean
Preserve Middle 1	0.6049	0.0111	NA	NA	NA	0.0000	4	-107.1517	3.5094	0.0483	1	peakOakley+SummerPDSIMean
Preserve Middle 1	0.5538	0.0126	NA	0.0000	NA	0.0000	5	-106.3401	4.3210	0.0322	1	peakOakley+LCMAP+SummerPDSIMean
Preserve Middle 1	0.5642	0.0110	NA	0.0000	-0.0001	NA	5	-106.0991	4.5620	0.0285	1	DOYGateway+LCMAP+SummerPDSIMean
Preserve Middle 1	0.6192	0.0109	NA	NA	-0.0001	0.0000	5	-105.0693	5.5917	0.0170	1	DOYGateway+peakOakley+SummerPDSIMean
Preserve Middle 2	0.6435	0.0123	NA	NA	NA	NA	3	-86.0056	0.0000	0.3192		SummerPDSIMean
Preserve Middle 2	-14.0742	0.0113	0.0035	NA	NA	NA	4	-84.5013	1.5043	0.1505	1	MaxGSLLevelSaltair+SummerPDSIMean
Preserve Middle 2	0.6861	0.0117	NA	0.0000	NA	NA	4	-83.7580	2.2475	0.1038	1	LCMAP+SummerPDSIMean
Preserve Middle 2	0.6549	0.0133	NA	NA	NA	0.0000	4	-83.4693	2.5363	0.0898	1	peakOakley+SummerPDSIMean
Preserve Middle 2	0.6498	0.0122	NA	NA	0.0000	NA	4	-83.3615	2.6441	0.0851	1	DOYGateway+SummerPDSIMean
Preserve Middle 2	-23.6247	0.0114	0.0058	0.0000	NA	NA	5	-81.7679	4.2377	0.0384	1	LCMAP+MaxGSLLevelSaltair+SummerPDSIMean
Preserve Middle 2	-14.9203	0.0111	0.0037	NA	-0.0001	NA	5	-81.7413	4.2643	0.0379	1	DOYGateway+MaxGSLLevelSaltair+SummerPDSIMean
Preserve Middle 2	-13.5174	0.0119	0.0034	NA	NA	0.0000	5	-81.6042	4.4013	0.0353	1	peakOakley+MaxGSLLevelSaltair+SummerPDSIMean
Preserve Middle 2	0.7078	0.0114	NA	0.0000	-0.0001	NA	5	-81.0432	4.9624	0.0267	1	DOYGateway+LCMAP+SummerPDSIMean
Preserve Middle 2	0.6895	0.0124	NA	0.0000	NA	0.0000	5	-80.8846	5.1210	0.0247	1	peakOakley+LCMAP+SummerPDSIMean
Preserve Middle 2	0.6603	0.0133	NA	NA	0.0000	0.0000	5	-80.5796	5.4260	0.0212	1	DOYGateway+peakOakley+SummerPDSIMean
Preserve Middle 3	0.4741	0.0080	NA	0.0000	NA	NA	4	-109.7475	0.0000	0.4464		LCMAP+SummerPDSIMean
Preserve Middle 3	0.4763	0.0086	NA	0.0000	NA	0.0000	5	-106.9302	2.8173	0.1091	1	peakOakley+LCMAP+SummerPDSIMean
Preserve Middle 3	3.2332	0.0080	-0.0007	0.0000	NA	NA	5	-106.8355	2.9119	0.1041	1	LCMAP+MaxGSLLevelSaltair+SummerPDSIMean
Preserve Middle 3	0.4759	0.0080	NA	0.0000	0.0000	NA	5	-106.8086	2.9388	0.1027	1	DOYGateway+LCMAP+SummerPDSIMean
Preserve Middle 3	27.0060	0.0079	-0.0063	NA	NA	NA	4	-106.7827	2.9648	0.1014		MaxGSLLevelSaltair+SummerPDSIMean
Preserve Middle 3	26.1904	0.0078	-0.0061	NA	-0.0001	NA	5	-104.2065	5.5410	0.0280	1	DOYGateway+MaxGSLLevelSaltair+SummerPDSIMean
Preserve Middle 3	27.1835	0.0081	-0.0063	NA	NA	0.0000	5	-103.8505	5.8970	0.0234	1	peakOakley+MaxGSLLevelSaltair+SummerPDSIMean
Preserve West 1	-37.7910	0.0118	0.0090	0.0000	NA	NA	5	-92.3068	0.0000	0.4563		LCMAP+MaxGSLLevelSaltair+SummerPDSIMean
Preserve West 1	0.2243	0.0120	NA	0.0000	NA	NA	4	-91.7278	0.5790	0.3416		LCMAP+SummerPDSIMean
Preserve West 1	0.2363	0.0138	NA	0.0000	NA	0.0000	5	-89.2766	3.0302	0.1003	1	peakOakley+LCMAP+SummerPDSIMean
Preserve West 1	0.2256	0.0120	NA	0.0000	0.0000	NA	5	-88.7874	3.5194	0.0785	1	DOYGateway+LCMAP+SummerPDSIMean
Preserve West 2	-63.5309	0.0092	0.0152	0.0000	NA	NA	5	-92.9077	0.0000	0.2886		LCMAP+MaxGSLLevelSaltair+SummerPDSIMean
Preserve West 2	-64.0174	NA	0.0153	0.0000	NA	2.68E-05	5	-91.5902	1.3174	0.1493		peakOakley+LCMAP+MaxGSLLevelSaltair
Preserve West 2	0.4853	NA	NA	NA	-0.0004	2.81E-05	4	-90.7454	2.1622	0.0979		DOYGateway+peakOakley
Preserve West 2	-18.0069	NA	0.0044	NA	-0.0004	2.84E-05	5	-90.4222	2.4854	0.0833	1	DOYGateway+peakOakley+MaxGSLLevelSaltair
Preserve West 2	0.5348	0.0079	NA	NA	-0.0004	NA	4	-89.7660	3.1417	0.0600		DOYGateway+SummerPDSIMean
Preserve West 2	0.5000	0.0045	NA	NA	-0.0004	1.97E-05	5	-89.1115	3.7962	0.0432	1	DOYGateway+peakOakley+SummerPDSIMean
Preserve West 2	-58.1536	NA	0.0139	0.0000	-0.0003	NA	5	-88.1972	4.7105	0.0274		DOYGateway+LCMAP+MaxGSLLevelSaltair
Preserve West 2	-65.4083	NA	0.0157	0.0000	NA	NA	4	-88.1508	4.7569	0.0267		LCMAP+MaxGSLLevelSaltair
Preserve West 2	0.4328	NA	NA	NA	NA	2.78E-05	3	-88.1381	4.7696	0.0266		peakOakley
Preserve West 2	0.4856	0.0083	NA	NA	NA	NA	3	-87.9811	4.9266	0.0246		SummerPDSIMean

Table A15 Continued. *Results of the model selection with a difference in AICc of less than 6 for each hydrology unit for 1992-2020. Potential uninformative parameters have not been removed. The response variable is the median July 15- Aug 31st NDVI value for each year. Model coefficients are the mean summer PDSI, max elevation of the Great Salt Lake, impervious surface area, day of year of peak flow at Gateway, and peak flow at Oakley respectively.*

Hydrology Unit	Intercept	Summer PDSI	Max GSL Level Saltair	Impervious Surface	DOY Gateway	Peak Oakley	df	AICc	Delta	Model Weights	uninformative	List Variables
Preserve West 2	0.4924	NA	NA	0.0000	-0.0004	2.82E-05	5	-87.8421	5.0656	0.0229		DOYGateway+peakOakley+LCMAP
Preserve West 2	-11.0286	0.0071	0.0028	NA	-0.0004	NA	5	-87.7267	5.1810	0.0216	1	DOYGateway+MaxGSLLevelSaltair+SummerPDSIMean
Preserve West 2	0.5097	0.0086	NA	0.0000	-0.0003	NA	5	-87.2377	5.6700	0.0169	1	DOYGateway+LCMAP+SummerPDSIMean
Preserve West 2	0.5356	NA	NA	NA	-0.0004	NA	3	-87.2281	5.6796	0.0169		DOYGateway
Preserve West 3	0.3785	0.0121	NA	0.0000	-0.0005	NA	5	-58.9141	0.0000	0.1446		DOYGateway+LCMAP+SummerPDSIMean
Preserve West 3	-62.2953	0.0131	0.0149	0.0000	NA	NA	5	-58.8336	0.0805	0.1389		LCMAP+MaxGSLLevelSaltair+SummerPDSIMean
Preserve West 3	0.2789	0.0134	NA	0.0000	NA	NA	4	-58.8186	0.0955	0.1378		LCMAP+SummerPDSIMean
Preserve West 3	0.3645	NA	NA	0.0000	-0.0006	3.64E-05	5	-58.5354	0.3787	0.1196		DOYGateway+peakOakley+LCMAP
Preserve West 3	0.4232	NA	NA	0.0000	-0.0006	NA	4	-57.5272	1.3870	0.0723		DOYGateway+LCMAP
Preserve West 3	0.2511	NA	NA	0.0000	NA	3.55E-05	4	-57.2157	1.6985	0.0618		peakOakley+LCMAP
Preserve West 3	-63.2033	NA	0.0151	0.0000	NA	3.45E-05	5	-57.1480	1.7662	0.0598	1	peakOakley+LCMAP+MaxGSLLevelSaltair
Preserve West 3	-65.3806	NA	0.0156	0.0000	NA	NA	4	-56.6850	2.2291	0.0474		LCMAP+MaxGSLLevelSaltair
Preserve West 3	0.3109	NA	NA	0.0000	NA	NA	3	-56.6436	2.2705	0.0465		LCMAP
Preserve West 3	-52.9227	NA	0.0127	0.0000	-0.0005	NA	5	-56.5326	2.3816	0.0439	1	DOYGateway+LCMAP+MaxGSLLevelSaltair
Preserve West 3	0.2601	0.0105	NA	0.0000	NA	1.52E-05	5	-56.3097	2.6045	0.0393	1	peakOakley+LCMAP+SummerPDSIMean
Preserve West 3	0.5430	NA	NA	NA	-0.0008	3.86E-05	4	-55.0160	3.8981	0.0206		DOYGateway+peakOakley
Preserve West 3	0.6119	NA	NA	NA	-0.0008	NA	3	-54.1419	4.7723	0.0133		DOYGateway
Preserve West 3	30.1618	NA	-0.0071	NA	-0.0008	3.81E-05	5	-54.0110	4.9031	0.0125	1	DOYGateway+peakOakley+MaxGSLLevelSaltair
Preserve West 3	31.0007	NA	-0.0072	NA	-0.0008	NA	4	-53.2339	5.6802	0.0084	1	DOYGateway+MaxGSLLevelSaltair
Preserve West 4	0.5060	0.0110	NA	NA	NA	NA	3	-82.6455	0.0000	0.2172		SummerPDSIMean
Preserve West 4	0.4445	0.0123	NA	0.0000	NA	NA	4	-81.4031	1.2424	0.1167	1	LCMAP+SummerPDSIMean
Preserve West 4	15.6294	0.0121	-0.0036	NA	NA	NA	4	-81.0681	1.5774	0.0987	1	MaxGSLLevelSaltair+SummerPDSIMean
Preserve West 4	0.4787	0.0085	NA	NA	NA	1.47E-05	4	-80.8272	1.8184	0.0875	1	peakOakley+SummerPDSIMean
Preserve West 4	0.5288	0.0109	NA	NA	-0.0002	NA	4	-80.6898	1.9557	0.0817	1	DOYGateway+SummerPDSIMean
Preserve West 4	0.4474	NA	NA	NA	NA	3.06E-05	3	-80.4421	2.2034	0.0722		peakOakley
Preserve West 4	0.4330	0.0102	NA	0.0000	NA	1.08E-05	5	-78.9340	3.7116	0.0340	1	peakOakley+LCMAP+SummerPDSIMean
Preserve West 4	0.4748	NA	NA	NA	-0.0002	3.08E-05	4	-78.7714	3.8742	0.0313	1	DOYGateway+peakOakley
Preserve West 4	0.5015	0.0082	NA	NA	-0.0002	1.55E-05	5	-78.7582	3.8874	0.0311	1	DOYGateway+peakOakley+SummerPDSIMean
Preserve West 4	0.4677	0.0120	NA	0.0000	-0.0001	NA	5	-78.7552	3.8903	0.0311	1	DOYGateway+LCMAP+SummerPDSIMean
Preserve West 4	13.5069	0.0098	-0.0031	NA	NA	1.19E-05	5	-78.7124	3.9331	0.0304	1	peakOakley+MaxGSLLevelSaltair+SummerPDSIMean
Preserve West 4	14.1007	0.0118	-0.0032	NA	-0.0001	NA	5	-78.6572	3.9883	0.0296	1	DOYGateway+MaxGSLLevelSaltair+SummerPDSIMean
Preserve West 4	3.2270	0.0123	-0.0007	0.0000	NA	NA	5	-78.4733	4.1723	0.0270	1	LCMAP+MaxGSLLevelSaltair+SummerPDSIMean
Preserve West 4	0.5029	NA	NA	NA	NA	NA	2	-78.1070	4.5385	0.0225		
Preserve West 4	0.4312	NA	NA	0.0000	NA	3.05E-05	4	-77.8366	4.8090	0.0196	1	peakOakley+LCMAP
Preserve West 4	4.7874	NA	-0.0010	NA	NA	3.06E-05	4	-77.8252	4.8204	0.0195	1	peakOakley+MaxGSLLevelSaltair

Table A16. *Hydrology unit summaries including top models for the 1992–2020 year time series. Model coefficients are the mean summer PDSI, max elevation of the Great Salt Lake, impervious surface area, day of year of peak flow at Gateway, and peak flow at Oakley respectively.*

Hydrology Unit	Area (ac)	Sen's Slope	P-Value	Trend Direction	Intercept	Summer PDSI	Max GSL Elevation	Impervious Surface	DOY Gateway	Peak Oakley	df	Model Weights	Covariates	R^2
New Middle 1	70.6388	-0.0039	0.0075	decreasing	0.7331	0.0136	NA	-1.31E-08	3.75E-04	NA	5	0.5647	DOYGateway+imperviousSurface+SummerPDSIMean	0.6063
New West 1	27.8316	0.0019	0.0224	increasing	-25.4352	0.0085	0.0061	2.45E-08	NA	NA	5	0.4203	imperviousSurface+MaxGSLLevelSaltair+SummerPDSIMean	0.5434
New West 2	230.9216	0.0013	0.3535	no sig trend	0.3226	0.0110	NA	1.29E-08	NA	NA	4	0.3102	imperviousSurface+SummerPDSIMean	0.2907
New West 3	97.3213	0.0011	0.3177	no sig trend	0.3320	0.0151	NA	1.06E-08	NA	NA	4	0.4660	imperviousSurface+SummerPDSIMean	0.4760
New West 4	68.6675	-0.0023	0.2712	no sig trend	31.0851	0.0152	-0.0073	-1.54E-08	NA	NA	5	0.2367	imperviousSurface+MaxGSLLevelSaltair+SummerPDSIMean	0.5872
Outflow East 1	1761.4781	0.0203	0.0006	increasing	119.6438	0.0216	-0.0287	1.01E-07	NA	NA	5	0.6151	imperviousSurface+MaxGSLLevelSaltair+SummerPDSIMean	0.8093
Outflow Middle 1	5430.4553	0.0167	0.0008	increasing	117.6020	0.0131	-0.0281	1.03E-07	NA	NA	5	0.4945	imperviousSurface+MaxGSLLevelSaltair+SummerPDSIMean	0.7755
Outflow West 1	664.2518	0.0168	0.0150	increasing	129.6221	NA	-0.0309	3.54E-08	-6.81E-04	NA	5	0.2523	DOYGateway+imperviousSurface+MaxGSLLevelSaltair	0.7632
Outflow West 2	1861.8813	0.0126	0.0977	no sig trend	183.3876	NA	-0.0436	NA	-0.0012	5.18E-05	5	0.3306	DOYGateway+peakOakley+MaxGSLLevelSaltair	0.6668
Preserve East 1	342.1912	0.0056	0.0000	increasing	-0.1075	0.0141	NA	4.18E-08	NA	NA	4	0.3803	imperviousSurface+SummerPDSIMean	0.4871
Preserve East 2	15.7243	0.0041	0.0001	increasing	64.6752	0.0148	-0.0153	NA	NA	-3.54E-05	5	0.1570	peakOakley+MaxGSLLevelSaltair+SummerPDSIMean	0.2692
Preserve East 3	3.4288	-0.0001	0.9822	no sig trend	0.5526	0.0216	NA	NA	NA	-4.59E-05	4	0.2634	peakOakley+SummerPDSIMean	0.2237
Preserve Middle 1	981.0920	0.0003	0.7753	no sig trend	17.3564	0.0115	-0.0040	NA	NA	NA	4	0.2791	MaxGSLLevelSaltair+SummerPDSIMean	0.4125
Preserve Middle 2	438.9954	-0.0013	0.3008	no sig trend	0.6435	0.0123	NA	NA	NA	NA	3	0.3192	SummerPDSIMean	0.2489
Preserve Middle 3	325.7098	0.0014	0.1340	no sig trend	0.4741	0.0080	NA	1.32E-08	NA	NA	4	0.4464	imperviousSurface+SummerPDSIMean	0.3547
Preserve West 1	436.7490	0.0059	0.0016	increasing	-37.7910	0.0118	0.0090	4.56E-08	NA	NA	5	0.4563	imperviousSurface+MaxGSLLevelSaltair+SummerPDSIMean	0.6590
Preserve West 2	682.8791	-0.0012	0.2117	no sig trend	-63.5309	0.0092	0.0152	2.61E-08	NA	NA	5	0.2886	imperviousSurface+MaxGSLLevelSaltair+SummerPDSIMean	0.3455
Preserve West 3	439.5118	0.0042	0.4262	no sig trend	0.3785	0.0121	NA	2.23E-08	-5.24E-04	NA	5	0.1446	DOYGateway+imperviousSurface+SummerPDSIMean	0.3569
Preserve West 4	494.6204	-0.0003	0.8865	no sig trend	0.5060	0.0110	NA	NA	NA	NA	3	0.2172	SummerPDSIMean	0.1864

Table A17. *Results of the model selection with a difference in AICc of less than 6 for each hydrology unit for 2012-2020. Potential uninformative parameters have not been removed. The response variable is the median July 15- Aug 31st NDVI value for each year. Model coefficients are the mean summer PDSI, max elevation of the Great Salt Lake, impervious surface area, day of year of peak flow at Gateway, and peak flow at Oakley respectively.*

Hydrology Unit	Intercept	Summer PDSI	Max GSL Elevation	Impervious Surface	DOY Gateway	Peak Oakley	df	AICc	Delta	Model Weights	Uninformative	List Variables	R^2
New Middle 1	121.7624	NA	-0.0289	NA	NA	NA	3	-22.4771	0	0.5894		MaxGSLLevelSaltair	0.4513
New Middle 1	0.5847	NA	NA	NA	NA	NA	2	-20.6727	1.8043	0.2391		1	0
New Middle 1	0.5274	NA	NA	NA	NA	3.65E-05	3	-17.8503	4.6268	0.0583	1	peakOakley	0.0826
New Middle 1	0.5971	0.0121	NA	NA	NA	NA	3	-17.4764	5.0006	0.0484	1	SummerPDSIMean	0.0437
New Middle 1	-0.4600	NA	NA	0.0000	NA	NA	3	-17.0699	5.4071	0.0395	1	LCMAP	-0.0005
New West 1	0.3840	NA	NA	NA	NA	NA	2	-30.4052	0	0.4651		1	0
New West 1	0.3938	0.0095	NA	NA	NA	NA	3	-28.7774	1.6278	0.2061	1	SummerPDSIMean	0.1966
New West 1	0.4234	NA	NA	NA	-0.0003	NA	3	-28.3354	2.0698	0.1652	1	DOYGateway	0.1562
New West 1	0.3620	NA	NA	NA	NA	1.40E-05	3	-26.4105	3.9947	0.0631	1	peakOakley	-0.045
New West 1	0.7691	NA	NA	0.0000	NA	NA	3	-26.25	4.1551	0.0582	1	LCMAP	-0.0638
New West 1	-0.0628	NA	1.07E-04	NA	NA	NA	3	-25.6054	4.7998	0.0422	1	MaxGSLLevelSaltair	-0.1428
New West 2	0.4356	NA	NA	NA	NA	NA	2	-20.8553	0	0.445		1	0
New West 2	2.0341	NA	NA	0.0000	NA	NA	3	-20.1382	0.7171	0.3109	1	LCMAP	0.2739
New West 2	0.4948	NA	NA	NA	-0.0005	NA	3	-18.1151	2.7401	0.1131	1	DOYGateway	0.0909
New West 2	0.4406	0.0049	NA	NA	NA	NA	3	-16.3026	4.5526	0.0457	1	SummerPDSIMean	-0.1119
New West 2	-24.6170	NA	0.0060	NA	NA	NA	3	-16.2617	4.5935	0.0448	1	MaxGSLLevelSaltair	-0.1169
New West 2	0.4309	NA	NA	NA	NA	2.97E-06	3	-16.0672	4.788	0.0406	1	peakOakley	-0.1413
New West 3	0.4420	NA	NA	NA	NA	NA	2	-31.1088	0	0.5817		1	0
New West 3	0.4690	NA	NA	NA	-0.0002	NA	3	-27.5865	3.5223	0.1	1	DOYGateway	0.0084
New West 3	33.8673	NA	-0.0080	NA	NA	NA	3	-27.5223	3.5865	0.0968	1	MaxGSLLevelSaltair	0.0013
New West 3	0.4199	NA	NA	NA	NA	1.41E-05	3	-27.1916	3.9172	0.082	1	peakOakley	-0.0361
New West 3	0.4467	0.0045	NA	NA	NA	NA	3	-26.9965	4.1123	0.0744	1	SummerPDSIMean	-0.0588
New West 3	0.7562	NA	NA	0.0000	NA	NA	3	-26.7298	4.379	0.0651	1	LCMAP	-0.0906
New West 4	0.4725	NA	NA	NA	NA	NA	2	-30.1307	0	0.5471		1	0
New West 4	0.4809	0.0081	NA	NA	NA	NA	3	-27.4586	2.6721	0.1438	1	SummerPDSIMean	0.0978
New West 4	0.5019	NA	NA	NA	-0.0002	NA	3	-26.6928	3.4378	0.0981	1	DOYGateway	0.0177
New West 4	0.4449	NA	NA	NA	NA	1.76E-05	3	-26.5947	3.536	0.0934	1	peakOakley	0.0069
New West 4	22.4350	NA	-0.0052	NA	NA	NA	3	-25.7814	4.3493	0.0622	1	MaxGSLLevelSaltair	-0.087
New West 4	0.7436	NA	NA	0.0000	NA	NA	3	-25.5556	4.575	0.0555	1	LCMAP	-0.1146
Outflow East 1	0.5966	0.0417	NA	NA	NA	NA	3	-12.3718	0	0.6847		SummerPDSIMean	0.5074
Outflow East 1	0.5538	NA	NA	NA	NA	NA	2	-9.5966	2.7751	0.171		1	0
Outflow East 1	0.4231	NA	NA	NA	NA	8.32E-05	3	-7.9955	4.3763	0.0768	1	peakOakley	0.199
Outflow Middle 1	0.3763	NA	NA	NA	NA	NA	2	-17.7051	0	0.2953		1	0
Outflow Middle 1	0.3984	0.0214	NA	NA	NA	NA	3	-17.0623	0.6428	0.2141	1	SummerPDSIMean	0.2799
Outflow Middle 1	0.2885	NA	NA	NA	NA	5.60E-05	3	-16.5514	1.1537	0.1658	1	peakOakley	0.2378
Outflow Middle 1	-1.2355	NA	NA	0.0000	NA	NA	3	-16.4934	1.2117	0.1611	1	LCMAP	0.2329
Outflow Middle 1	109.5936	NA	-0.0260	NA	NA	NA	3	-16.1632	1.5419	0.1366	1	MaxGSLLevelSaltair	0.2043
Outflow Middle 1	0.3690	NA	NA	NA	6.18E-05	NA	3	-12.925	4.7801	0.0271	1	DOYGateway	-0.1403
Outflow West 1	0.4104	NA	NA	NA	NA	NA	2	-18.1576	0	0.375		1	0
Outflow West 1	2.7374	NA	NA	0.0000	NA	NA	3	-17.4518	0.7059	0.2635	1	LCMAP	0.2748
Outflow West 1	0.4996	NA	NA	NA	-0.0008	NA	3	-17.148	1.0097	0.2263	1	DOYGateway	0.2499
Outflow West 1	-70.0015	NA	0.0168	NA	NA	NA	3	-14.6395	3.5182	0.0646	1	MaxGSLLevelSaltair	0.0089
Outflow West 1	0.4059	-0.0044	NA	NA	NA	NA	3	-13.5075	4.6502	0.0367	1	SummerPDSIMean	-0.124
Outflow West 1	0.4097	NA	NA	NA	NA	4.58E-07	3	-13.3579	4.7998	0.034	1	peakOakley	-0.1428
Outflow West 2	0.4672	NA	NA	NA	NA	NA	2	-12.8583	0	0.3676		1	0
Outflow West 2	0.5935	NA	NA	NA	-0.0011	NA	3	-12.4004	0.4579	0.2924	1	DOYGateway	0.2946
Outflow West 2	3.4570	NA	NA	0.0000	NA	NA	3	-11.7282	1.13	0.2089	1	LCMAP	0.2399
Outflow West 2	-90.4683	NA	0.0217	NA	NA	NA	3	-9.2383	3.62	0.0602	1	MaxGSLLevelSaltair	-0.0024
Outflow West 2	0.4744	0.0071	NA	NA	NA	NA	3	-8.271	4.5873	0.0371	1	SummerPDSIMean	-0.1162
Outflow West 2	0.4565	NA	NA	NA	NA	6.82E-06	3	-8.0843	4.774	0.0338	1	peakOakley	-0.1396
Preserve East 1	0.5859	NA	NA	NA	NA	NA	2	-13.8573	0	0.5779		1	0
Preserve East 1	0.6076	0.0212	NA	NA	NA	NA	3	-11.4667	2.3906	0.1749	1	SummerPDSIMean	0.1256
Preserve East 1	0.5398	NA	NA	NA	NA	2.93E-05	3	-9.6104	4.2469	0.0691	1	peakOakley	-0.0747
Preserve East 1	58.8664	NA	-0.0139	NA	NA	NA	3	-9.5798	4.2775	0.0681	1	MaxGSLLevelSaltair	-0.0784
Preserve East 1	0.6114	NA	NA	NA	-0.0002	NA	3	-9.2162	4.6411	0.0568	1	DOYGateway	-0.1229
Preserve East 1	0.8513	NA	NA	0.0000	NA	NA	3	-9.0887	4.7686	0.0533	1	LCMAP	-0.1389
Preserve East 2	0.5104	NA	NA	NA	NA	NA	2	-18.4773	0	0.4676		1	0
Preserve East 2	111.8195	NA	-0.0265	NA	NA	NA	3	-17.468	1.0093	0.2823	1	MaxGSLLevelSaltair	0.25
Preserve East 2	0.5246	0.0138	NA	NA	NA	NA	3	-15.3333	3.144	0.0971	1	SummerPDSIMean	0.0492
Preserve East 2	0.4723	NA	NA	NA	NA	2.42E-05	3	-14.3116	4.1657	0.0583	1	peakOakley	-0.0651
Preserve East 2	-0.2128	NA	NA	0.0000	NA	NA	3	-14.0657	4.4116	0.0515	1	LCMAP	-0.0946
Preserve East 2	0.5010	NA	NA	NA	7.95E-05	NA	3	-13.7133	4.764	0.0432	1	DOYGateway	-0.1383
Preserve East 3	0.5156	NA	NA	NA	NA	NA	2	-18.7279	0	0.6049		1	0
Preserve East 3	1.8205	NA	NA	0.0000	NA	NA	3	-15.6216	3.1063	0.128	1	LCMAP	0.0532
Preserve East 3	0.5613	NA	NA	NA	NA	0.0000	3	-14.8871	3.8409	0.0886	1	peakOakley	-0.0273
Preserve East 3	0.5082	-0.0072	NA	NA	NA	NA	3	-14.3609	4.367	0.0681	1	SummerPDSIMean	-0.0892
Preserve East 3	-6.4737	NA	0.0017	NA	NA	NA	3	-13.9405	4.7874	0.0552	1	MaxGSLLevelSaltair	-0.1413
Preserve East 3	0.5199	NA	NA	NA	0.0000	NA	3	-13.9354	4.7925	0.0551	1	DOYGateway	-0.1419
Preserve Middle 1	0.6084	NA	NA	NA	NA	NA	2	-30.6871	0	0.5439		1	0
Preserve Middle 1	0.5745	NA	NA	NA	NA	2.16E-05	3	-28.0031	2.684	0.1421	1	peakOakley	0.0966
Preserve Middle 1	38.3770	NA	-0.0090	NA	NA	NA	3	-27.3887	3.2983	0.1045	1	MaxGSLLevelSaltair	0.0328
Preserve Middle 1	0.6150	0.0064	NA	NA	NA	NA	3	-27.2489	3.4381	0.0975	1	SummerPDSIMean	0.0176
Preserve Middle 1	0.6251	NA	NA	NA	-0.0001	NA	3	-26.3347	4.3524	0.0617	1	DOYGateway	-0.0874
Preserve Middle 1	0.7292	NA	NA	0.0000	NA	NA	3	-25.9258	4.7613	0.0503	1	LCMAP	-0.1379
Preserve Middle 2	0.6452	NA	NA	NA	NA	NA	2	-27.0967	0	0.464		1	0
Preserve Middle 2	0.6566	0.0111	NA	NA	NA	NA	3	-25.277	1.8197	0.1868	1	SummerPDSIMean	0.1793
Preserve Middle 2	0.6030	NA	NA	NA	NA	2.69E-05	3	-24.5123	2.5844	0.1275	1	peakOakley	0.1065
Preserve Middle 2	53.7672	NA	-0.0127	NA	NA	NA	3	-24.3501	2.7466	0.1175	1	MaxGSLLevelSaltair	0.0903

Table A17. *Results of the model selection with a difference in AICc of less than 6 for each hydrology unit for 2012-2020. Potential uninformative parameters have not been removed. The response variable is the median July 15- Aug 31st NDVI value for each year. Model coefficients are the mean summer PDSI, max elevation of the Great Salt Lake, impervious surface area, day of year of peak flow at Gateway, and peak flow at Oakley respectively.*

Hydrology Unit	Intercept	Summer PDSI	Max GSL Elevation	Impervious Surface	DOY Gateway	Peak Oakley	df	AICc	Delta	Model Weights	Uninformative	List Variables	R^2
Preserve Middle 2	0.6718	NA	NA	NA	-0.0002	NA	3	-23.0705	4.0262	0.062	1	DOYGateway	-0.0487
Preserve Middle 2	0.6074	NA	NA	0.0000	NA	NA	3	-22.3	4.7967	0.0422	1	LCMAP	-0.1424
Preserve Middle 3	0.6780	NA	NA	NA	NA	NA	2	-25.2945	0	0.4679		1	0
Preserve Middle 3	0.6921	0.0137	NA	NA	NA	NA	3	-24.3763	0.9182	0.2956	1	SummerPDSIMean	0.2575
Preserve Middle 3	0.6434	NA	NA	NA	NA	2.21E-05	3	-21.6501	3.6444	0.0756	1	peakOakley	-0.0051
Preserve Middle 3	0.7098	NA	NA	NA	-0.0003	NA	3	-21.4085	3.8861	0.067	1	DOYGateway	-0.0325
Preserve Middle 3	23.8675	NA	-0.0055	NA	NA	NA	3	-20.7856	4.509	0.0491	1	MaxGSLLevelSaltair	-0.1065
Preserve Middle 3	0.9153	NA	NA	0.0000	NA	NA	3	-20.6012	4.6933	0.0448	1	LCMAP	-0.1294
Preserve West 1	0.5114	NA	NA	NA	NA	NA	2	-26.0304	0	0.5237		1	0
Preserve West 1	0.5235	0.0118	NA	NA	NA	NA	3	-24.2227	1.8077	0.2121	1	SummerPDSIMean	0.1804
Preserve West 1	0.4787	NA	NA	NA	NA	2.09E-05	3	-22.347	3.6834	0.083	1	peakOakley	-0.0095
Preserve West 1	0.5394	NA	NA	NA	-0.0002	NA	3	-21.9892	4.0412	0.0694	1	DOYGateway	-0.0504
Preserve West 1	0.9356	NA	NA	0.0000	NA	NA	3	-21.7323	4.2981	0.0611	1	LCMAP	-0.0809
Preserve West 1	-14.5574	NA	0.0036	NA	NA	NA	3	-21.3626	4.6678	0.0508	1	MaxGSLLevelSaltair	-0.1262
Preserve West 2	0.4653	NA	NA	NA	NA	NA	2	-23.3944	0	0.4486		1	0
Preserve West 2	0.5262	NA	NA	NA	-0.0005	NA	3	-21.6393	1.7551	0.1865	1	DOYGateway	0.1852
Preserve West 2	1.5355	NA	NA	0.0000	NA	NA	3	-21.3465	2.0479	0.1611	1	LCMAP	0.1582
Preserve West 2	-60.4299	NA	0.0145	NA	NA	NA	3	-20.3549	3.0396	0.0981	1	MaxGSLLevelSaltair	0.0602
Preserve West 2	0.4735	0.0081	NA	NA	NA	NA	3	-19.5255	3.8689	0.0648	1	SummerPDSIMean	-0.0305
Preserve West 2	0.4665	NA	NA	NA	NA	0.0000	3	-18.5955	4.799	0.0407	1	peakOakley	-0.1427
Preserve West 3	3.1319	NA	NA	0.0000	NA	NA	3	-13.9483	0	0.4657		LCMAP	0.4134
Preserve West 3	0.5085	NA	NA	NA	NA	NA	2	-12.7453	1.203	0.2552		1	0
Preserve West 3	-155.5472	NA	0.0372	NA	NA	NA	3	-11.925	2.0233	0.1693	1	MaxGSLLevelSaltair	0.2656
Preserve West 3	0.5984	NA	NA	NA	-0.0008	NA	3	-9.8594	4.0889	0.0603	1	DOYGateway	0.0761
Preserve West 3	0.5418	NA	NA	NA	NA	0.0000	3	-8.1965	5.7518	0.0263	1	peakOakley	-0.1114
Preserve West 4	0.4954	NA	NA	NA	NA	NA	2	-24.2391	0	0.591		1	0
Preserve West 4	61.2184	NA	-0.0145	NA	NA	NA	3	-21.3806	2.8585	0.1415	1	MaxGSLLevelSaltair	0.0789
Preserve West 4	0.5238	NA	NA	NA	-0.0002	NA	3	-20.0789	4.1602	0.0738	1	DOYGateway	-0.0644
Preserve West 4	0.5012	0.0056	NA	NA	NA	NA	3	-19.9221	4.317	0.0683	1	SummerPDSIMean	-0.0831
Preserve West 4	0.8967	NA	NA	0.0000	NA	NA	3	-19.7602	4.4789	0.0629	1	LCMAP	-0.1028
Preserve West 4	0.4761	NA	NA	NA	NA	1.23E-05	3	-19.7444	4.4947	0.0625	1	peakOakley	-0.1047

Table A18. *Hydrology unit summaries including top models for the 2012–2020 year time series. parameters have not been removed. The response variable is the median July 15- Aug 31st NDVI value for each year. Model coefficients are the mean summer PDSI, max elevation of the potential uninformative Great Salt Lake, impervious surface area, day of year of peak flow at Gateway, and peak flow at Oakley respectively.*

Hydrology Units	Area (ac)	Sen's Slope	P-value	Trend Direction	Intercept	Summer PDSI	Max GSL Elevation	Impervious Surface	DOY Gateway	Peak Oakley	df	Model Weights	Covariates	R^2
New Middle 1	70.6388	0.0079	0.2105	no sig trend	121.7624	NA	-0.0289	NA	NA	NA	3	0.5894	MaxGSLLevelSaltair	0.4513
New West 1	27.8316	-0.0060	0.4743	no sig trend	0.3840	NA	NA	NA	NA	NA	2	0.4651	1	0.0000
New West 2	230.9216	-0.0171	0.0736	no sig trend	0.4356	NA	NA	NA	NA	NA	2	0.4450	1	0.0000
New West 3	97.3213	-0.0048	0.5915	no sig trend	0.4420	NA	NA	NA	NA	NA	2	0.5817	1	0.0000
New West 4	68.6675	-0.0062	0.1074	no sig trend	0.4725	NA	NA	NA	NA	NA	2	0.5471	1	0.0000
Outflow East 1	1761.4781	-0.0032	0.8580	no sig trend	0.5966	0.0417	NA	NA	NA	NA	3	0.6847	SummerPDSI	0.5074
Outflow Middle 1	5430.4553	0.0110	0.1074	no sig trend	0.3763	NA	NA	NA	NA	NA	2	0.2953	1	0.0000
Outflow West 1	664.2518	-0.0110	0.3711	no sig trend	0.4104	NA	NA	NA	NA	NA	2	0.3750	1	0.0000
Outflow West 2	1861.8813	-0.0140	0.1524	no sig trend	0.4672	NA	NA	NA	NA	NA	2	0.3676	1	0.0000
Preserve East 1	342.1912	-0.0196	0.1524	no sig trend	0.5859	NA	NA	NA	NA	NA	2	0.5779	1	0.0000
Preserve East 2	15.7243	-0.0073	0.4743	no sig trend	0.5104	NA	NA	NA	NA	NA	2	0.4676	1	0.0000
Preserve East 3	3.4288	-0.0153	0.2105	no sig trend	0.5156	NA	NA	NA	NA	NA	2	0.6049	1	0.0000
Preserve Middle 1	981.0920	-0.0041	0.5915	no sig trend	0.6084	NA	NA	NA	NA	NA	2	0.5439	1	0.0000
Preserve Middle 2	438.9954	-0.0034	0.4743	no sig trend	0.6452	NA	NA	NA	NA	NA	2	0.4640	1	0.0000
Preserve Middle 3	325.7098	-0.0130	0.1524	no sig trend	0.6780	NA	NA	NA	NA	NA	2	0.4679	1	0.0000
Preserve West 1	436.7490	-0.0113	0.2105	no sig trend	0.5114	NA	NA	NA	NA	NA	2	0.5237	1	0.0000
Preserve West 2	682.8791	-0.0170	0.0318	decreasing	0.4653	NA	NA	NA	NA	NA	2	0.4486	1	0.0000
Preserve West 3	439.5118	-0.0240	0.1524	no sig trend	3.1319	NA	NA	-2.41E-07	NA	NA	3	0.4657	imperviousSurface	0.4134
Preserve West 4	494.6204	-0.0050	0.3711	no sig trend	0.4954	NA	NA	NA	NA	NA	2	0.5910	1	0.0000

Table A19. *Phragmites- and non-Phragmites-related increasing and decreasing 10-year trends.*

Component Area	Phragmites Related	Area increasing (ac)	% of increasing trends	Area decreasing (ac)	% of decreasing trends
New	yes	6	19	23	30
New	no	25	81	55	70
Outflow	yes	153	11	651	79
Outflow	no	1209	89	177	21
Preserve	yes	33	25	331	48
Preserve	no	102	75	357	52

Table A20. *Phragmites- and non-Phragmites-related increasing and decreasing 30-year trends.* .

Component Area	Currently Phragmites	% of increasing trends	% of decreasing trends
New	yes	20	8
New	no	80	92
Outflow	yes	46	56
Outflow	no	54	44
Preserve	yes	21	27
Preserve	no	79	73

Table A21. *The 2011–2021 vegetation change categories that make up more than 5% of each study component area.*

Location	Trend	Type of Change	Area (acres)	% of Component Area with Trend	Overall % of Component Area
Preserve	decreasing	Upland to Upland	109.2	13.3	2.7
Preserve	decreasing	Phragmites to Phragmites	95.8	11.6	2.4
Preserve	decreasing	Wet Meadow to Upland	87.6	10.6	2.2
Preserve	decreasing	Marsh to Phragmites	81.0	9.8	2.0
Preserve	decreasing	Phragmites to Upland	50.7	6.2	1.2
Preserve	decreasing	Phragmites to Marsh	48.6	5.9	1.2
New	decreasing	Upland to Upland	27.4	25.2	5.6
New	increasing	Upland to Upland	18.4	16.9	3.7
New	decreasing	Phragmites to Upland	13.0	12.0	2.7
New	decreasing	Wet Meadow to Upland	12.3	11.3	2.5
New	decreasing	Wet Meadow to Wet Meadow	6.0	5.6	1.2
New	decreasing	Phragmites to Phragmites	5.5	5.0	1.1
Outflow	increasing	Playa to Wet Meadow	684.2	31.2	7.8
Outflow	decreasing	Phragmites to Phragmites	281.8	12.9	3.2
Outflow	increasing	Playa to Marsh	261.7	12.0	3.0
Outflow	decreasing	Marsh to Phragmites	248.4	11.3	2.8
Outflow	increasing	Playa to Playa	176.1	8.0	2.0

APPENDIX B: DETAILED METHODS OF NDVI ANALYSIS

Hydrology Units

We split the study area into hydrology units to represent areas that receive similar water inputs and management. We first delineated hydrology units—Preserve, New Parcel, and Outflow Area geographic components based on differences in how each area is managed. We then subdivided the components using HUC12 watershed boundaries (Figure 13), and then evaluated water inputs from streams, agricultural drains, storm drains, and flowing wells to further divide the units based on water source. The result is 19 hydrology units. Unit labels are a combination of the study unit component name, HUC12 affiliation (as west, middle or east), and a unique number (e.g., New West 4).

Vegetation Index

We evaluated and mapped changes in vegetation health/drought stress over time for the vegetation classes established by our mapping. We used Google Earth Engine (Gorelick, et al., 2017) to create a time series from 1992 to 2021 using the Landsat 5, 7, and 8 Surface Reflectance data which have already been atmospherically corrected. We masked out clouds, cloud shadows, and snow using Landsat's QA band. For each year, we created a median composite of all images between July 15th and August 31st. This time of year was easiest to generally distinguish the vegetation classes and allowed for a complete data set with no missing data due to cloud cover. August was generally peak greenness for the Mesic Meadow, Wet Meadow, Marsh, and Phragmites classes, but not for the Upland and Playa classes. We then calculated the median NDVI for each year for each hydrology unit using the following formula:

$$NDVI = (NIR - R)/(NIR + R)$$

where:

NIR = near infrared value

R = infrared value

In our study, vegetation classes varied in NDVI in the July to August timeframe in the following order from lower to higher index values: Water, Playa, Upland, Mesic Meadow/Wet Meadow (similar values), Phragmites/Marsh (similar values), and Woody Vegetation.

To focus on vegetation trends, we clipped out areas mapped as the artificial and water classes in the 2021 UGS vegetation map. We also clipped out areas mapped as Woody Riparian because they made up a minute portion of the project area. We used the same data to create slope maps showing the change in NDVI over time in each 30-m pixel. We created a 30-year map depicting slopes for years 1992 to 2021 and a 10-year map depicting slopes for 2012 to 2021.

Model Explanatory Variables

Our next analysis sought to identify likely drivers of the NDVI trends. We chose to model specific data sets from each of four data types—climate, hydrologic, land cover, and year—giving priority to time span of the available data, proximity to the study area, and preliminary correlation with NDVI trends in the study area.

For the climate data, we used the Palmer Drought Severity Index (PDSI) calculated using the gridMET dataset hosted on Google Earth Engine (Abatzoglou, 2013) because it incorporates both precipitation and temperature and is commonly used as a metric for drought (Alley, 1984). We chose to model summer (June through August) mean PDSI value for the study area ("summer PDSI") because it was the most strongly correlated with the NDVI values of the hydrology units.

For the hydrologic explanatory variables, we evaluated data for nearby streams, groundwater, and lake-level monitoring stations from the USGS database using the dataRetrieval package in R (De Cicco et al., 2022). The only stream monitoring stations upgradient of the study area having data for the entire 30-year time period were on the Weber River. The Weber River flows into Great Salt Lake about 10 kilometers north of the northern edge of the study area, and water from the Weber River

is diverted in canals to agricultural areas to the north and east of the study area. We chose a site upstream (near Oakley, Utah) and a site downstream (west of Mountain Green, Utah, named Gateway) of the reservoirs that are built along the river to account for human influence on streamflow. We calculated both peak flow and day of year (DOY) of peak flow for both reservoir sites and selected for modeling the variable that was most strongly correlated to NDVI values in the study area for each station (peak flow at Oakley and DOY at Gateway).

Two groundwater wells near the study area had data for the full 30-year time period, represented as groundwater level measurements taken once per year in the spring. We selected a well in Kaysville because its water levels were correlated with NDVI values in the study area.

For Great Salt Lake elevation, we used measurements from Saltair Boat Harbor site because of the period of record of data available, higher correlations to NDVI at the study area, and proximity to the study area. We modeled the maximum annual values of Great Salt Lake elevation.

We used the Land Change Monitoring, Assessment, and Projection (LCMAP) dataset to calculate the amount of impervious surface in the area surrounding the study area (Zhu and Woodcock, 2014; Brown et al., 2020). The LCMAP dataset shows the likely annual land cover class based on Landsat imagery that has been modeled using the Continuous Change Detection and Classification (CCDC) algorithm (Zhu and Woodcock, 2014). For the Preserve and New Parcels, we calculated impervious surface area within a 5-kilometer buffer upgradient of each hydrology unit. For the Outflow Area, we calculated impervious surface area within a 5-kilometer buffer upgradient of the study area boundary split by each corresponding HUC12 boundary. Annual impervious surface area was retrieved from the LCMAP dataset curated by Samapriya Roy on Google Earth Engine.

We next examined the Pearson correlation coefficients for the pool of seven potential explanatory variables (the six variables described above plus year) to decide which variables to include in our statistical analysis. Year, impervious surface area, GSL elevation, and groundwater level were all highly correlated to each other ($r \geq 0.8$). We examined variance inflation factors (VIF) using the car package in R (Fox and Weisberg, 2019) and found that we could only include two of these variables in our models without exceeding a VIF of 4. Of those four variables, we selected GSL elevation and impervious surface for analysis. We hypothesized that GSL elevation is influenced by changes in stream flow and groundwater levels, as well as other hydrologic factors, and thus would integrate more information in one measure compared to groundwater levels. We also were interested in how changes in land development patterns might affect the study area and thus included impervious surface rather than year. However, we acknowledge that the strong collinearity between variables makes it difficult to interpret model results. None of the other variables had a VIF greater than 4. The final variables chosen for the models were summer PDSI, peak flow at Oakley, DOY at Gateway, GSL elevation, and impervious surface area (Table A12).

Statistical Analysis

We conducted Mann Kendall trend tests to assess the presence of statistically significant trends in NDVI over 30-year (1992 to 2021) and 10-year (2012 to 2021) time periods, for each hydrology unit. We accounted for temporal autocorrelation with the "modifiedmk" package when applicable (Patakamuri et al., 2020). The Mann Kendall test is a nonparametric trend test that evaluates whether there is a consistent increasing or decreasing trend in a time series.

We created linear regression models to analyze NDVI versus the selected explanatory variables discussed above for each hydrologic unit (Table A12), using both a 29-year (1992 to 2020) and a 9-year (2012 to 2020) time period because impervious surface data from 2021 was not available. We compared linear models that included combinations of zero to three variables for the 29-year time period and zero or one variable for the 9-year time period. Our preferred model had the lowest corrected Akaike Information Criterion (AICc) from the model selection function in the MuMIn package in R (Barton and Barton, 2015). Models with a difference in AICc of less than six could also be considered as good models for each unit while excluding models with uninformative parameters. Overall, patterns for each explanatory variable (sign of relationship and geographic area of importance) were similar when comparing the preferred model and the models with an AICc of less than six, so for this report we focus on the preferred model but we report the alternate models in Tables A15 and A16. Our selection of July 15th to August 31st median may impact the trends we see and which explanatory variables are the most important for each unit. For instance, peak greenness of upland vegetation is earlier in the spring and the study area can experience a spike in water in fall when upstream users stop irrigating depending on the year (Mike Kolendrianos and Chris Brown, Preserve Managers, verbal communications during 2022 and 2023).

For the 30-year and 10-year slope maps, we ran a Mann Kendall trend test on each pixel using code provided on the Google Earth Engine developers community page with minor adjustments to handle slopes between 1 and -1. We considered values of $p < 0.01$ as significant because of the large quantity of pixels in the study area.

Vegetation Community Comparison

To obtain a more detailed understanding of changes in vegetation over time, we compared our 2021 vegetation mapping to existing vegetation community mapping from 2011 by Long (2014). However, due to large methodological differences between data products, including significant differences in mapping scale and mapped classes, we concluded it was not appropriate to use this data to quantify overall change in the vegetation communities in the study area over time. The main concerns with the direct comparison of the two layers were threefold. First, areas mapped as Mesic Grasslands by the UGS did not easily fall into any of the categories mapped by Long, and likely some of these areas should be considered Upland and some Wet Meadow. Second, based on examination of aerial imagery from 2011, there may have been misidentification of Marsh versus Phragmites in the 2011 data, particularly in the outflow area. Third, differences in resolution between the layers is likely to overestimate the amount of change that occurred over time. Due to these issues, we used the comparison layer only as supporting information to help us interpret trends detected in the remote sensing analysis.

The 2011 vegetation mapping was conducted via supervised classification of high-resolution, multi-spectral imagery collected in summer 2011 using an UAV (unmanned aerial vehicle) system (Long, 2014). Some parts of the study area were not mapped by Long (2014) and thus the vegetation community comparison considers only the overlap area between the two datasets, which covers 96% of the study area.

The vegetation communities in the 2011 mapping differed slightly from the nine broad classes identified in the 2021 UGS mapping and both mapping datasets were reclassified into six general categories for the mapping comparison (Table A13). We matched resolution and data type between the two mapping datasets by (1) downsampling the 2011 vegetation mapping to 20 meters (the approximate resolution of the 0.1-acre threshold used in the 2021 mapping) using majority sampling techniques, and (2) converting the 2021 vegetation mapping to a 20-meter resolution raster with cell values assigned using maximum combined area. We combined these rasters into a single raster with each cell containing a value representing the vegetation community mapped in 2011 and the vegetation community mapped in 2021. We converted the resulting raster to polygonal data and eliminated sliver polygons less than 400 square meters in area by merging them with neighboring polygons having the greatest shared border length. This resulted in a polygonal dataset with discrete areas depicting all unique combinations of 2011 and 2021 mapping.

Evaluation of NDVI Slope Trends

We overlaid the 10-year NDVI pixel slope trend map with the data from the 2011 to 2021 vegetation community comparison to help us understand what types of vegetation communities had significant trends and to see if the trends were corroborated by the mapping comparison, keeping in mind the major caveats listed above (potential 2011 Phragmites and Marsh confusion and potential overlap in definitions of Upland and Wet Meadow communities). We focused only on those areas having a significant 10-year slope trend that overlapped the change map, which accounted for 21% of the study area. We looked at the vegetation change map categories that composed 5% or more of the trend area, keeping in mind the issues with Phragmites/Marsh and Upland/Wet Meadow classification when interpreting results. We also calculated what percent of areas that showed change were mapped as Phragmites in at least one year, to better understand how *Phragmites* treatment or expansion may influence trend results.

To help understand the 30-year trends, we overlaid the 30-year NDVI pixel slope trend map and the UGS 2021 vegetation mapping. We summarized the trends by what is currently mapped as Phragmites and what is not. However, previous *Phragmites* treatments have occurred and some areas are no longer *Phragmites*. These areas would not be included in the estimates due to the limits of the data.

APPENDIX C: VEGETATION CLASSES AND SUBCLASSES MAPPED AT THE SHORELANDS PRESERVE

Figure C1. *Vegetation classes and subclasses mapped at the Shorelands Preserve. From 1 to 6: Water-Permanent, Phragmites-Dense, Phragmites-Mixed, Playa-Barren, Playa-Vegetated, Woody Riparian.*

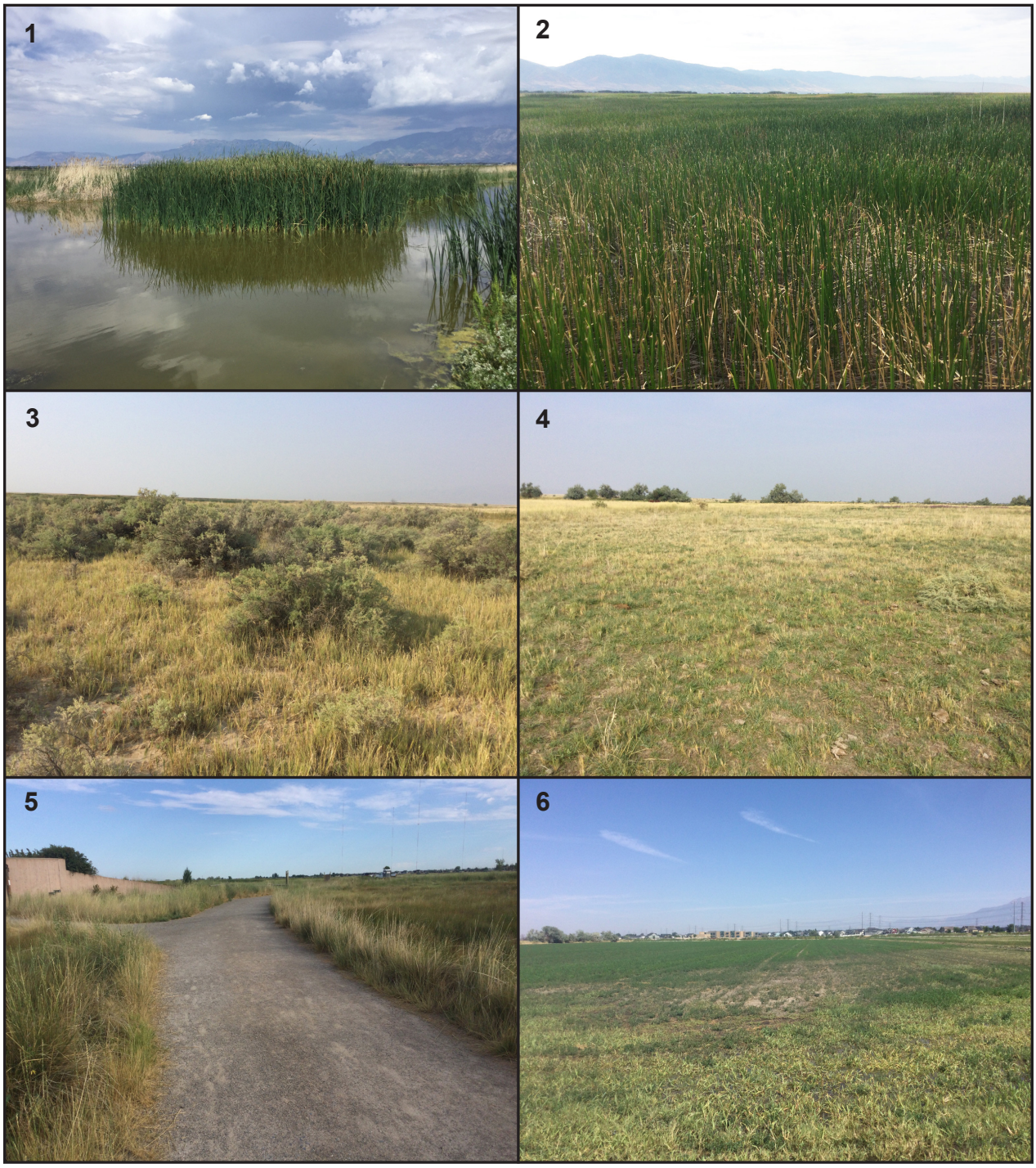

Figure C1 continued. *Vegetation classes and subclasses mapped at the Shorelands Preserve. From 1 to 6: Marsh-Cattail, Marsh-Bulrush, Upland-Shrubby, Upland-Annual grasses, Artificial-Impervious, Artificial-Crops.*

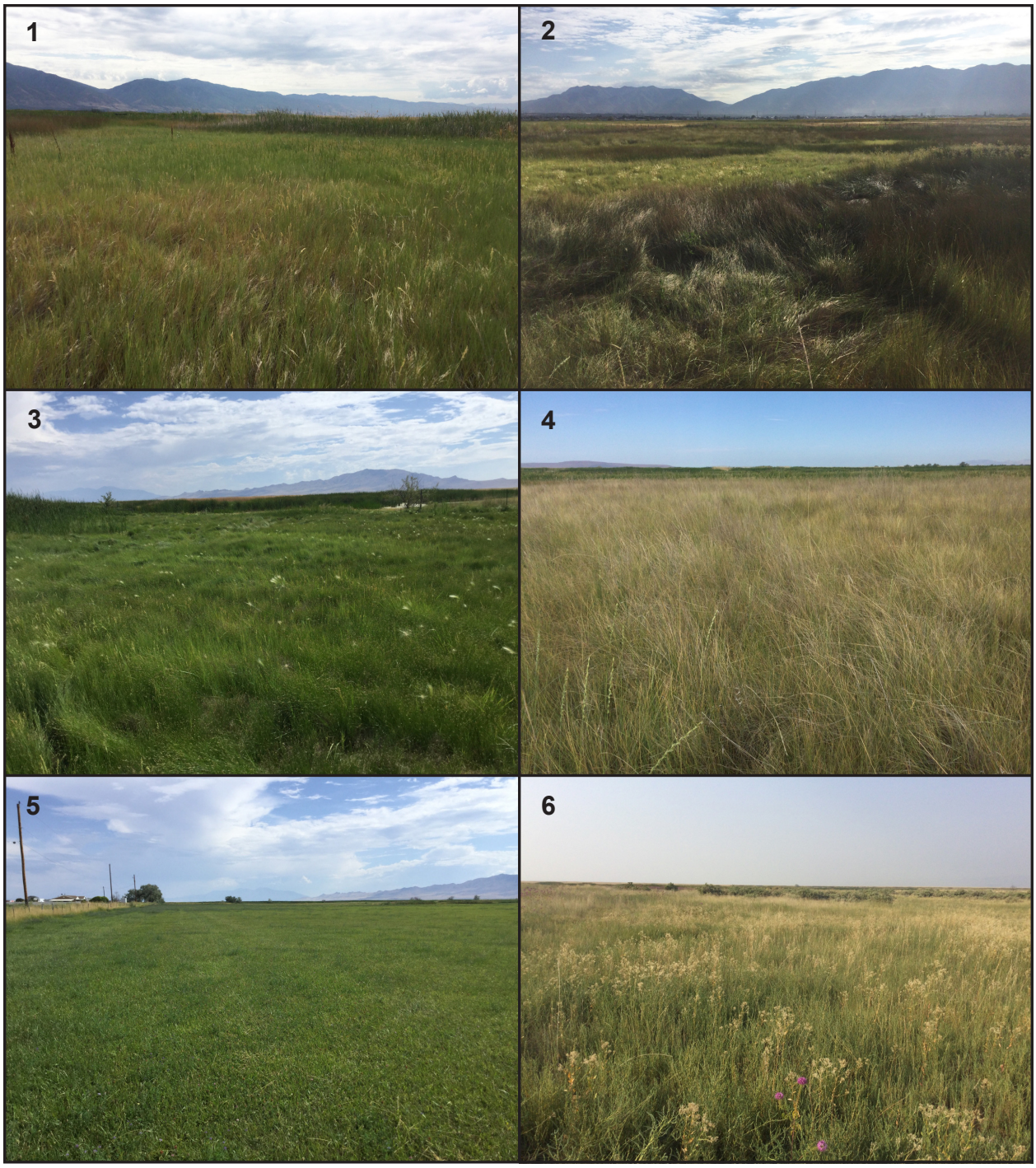

Figure C1 continued. *Vegetation classes and subclasses mapped at the Shorelands Preserve. From 1 to 6: Wet meadow-Dense saltgrass, Wet meadow-Saline, Wet meadow-Fresh, Mesic meadow-Mesic grasses, Mesic meadow-Irrigated pasture, Mesic meadow-Ruderal annuals.*